UNIVERSITÉ DU QUÉBEC À MONTRÉAL

DÉVELOPPEMENT DE MÉTHODES ANALYTIQUES POUR L'IDENTIFICATION ET LA CARACTÉRISATION DE MÉTABOLITES RÉACTIFS ET LEURS ADDUITS PROTÉIQUES PAR SPECTROMÉTRIE DE MASSE

THÈSE

PRÉSENTÉE

COMME EXIGENCE PARTIELLE

DU DOCTORAT EN CHIMIE

PAR

ANDRÉ LEBLANC

MARS 2015

REMERCIEMENTS

De prime abord, je voudrais remercier le professeur René Roy et Tze Chieh Shiao car leur collaboration fut cruciale au succès de plusieurs des projets présentés dans cette thèse.

Je remercie également les professeurs Isabelle Marcotte, Huu van Traa et Steve Bourgault qui ont fait partie de mon comité de thèse, qui m'ont donné d'excellents conseils et qui ont toujours été généreux avec leur temps.

Je remercie le professeur Klaus Klarskov pour avoir généreusement accepté de siéger comme membre externe de mon jury.

Je remercie l'université, tout le personnel de soutien et surtout toutes mes paires aux études graduées, ils ont tous été plus important qu'ils ne le pensent.

À tous mes collègues de laboratoire, qui ont tous été indispensables à mon cheminement, chacun et chacune de leur propre façon.

Je tiens à remercier ma mère, mon père, ma sœur, et toute ma famille ainsi que tous mes amis. Ils m'ont toujours soutenu et encouragé dans tous les aspects de ma vie.

Finalement, j'aimerais particulièrement souligner ma reconnaissance envers ma directrice de recherche, professeure Lekha Sleno sans qui tout ceci ne serait pas possible. Je ne pourrai jamais suffisamment la remercier, mais je ferai mon mieux.

TABLE DES MATIÈRES

LISTE DES FIGURES

LISTE DES TABLEAUX

LISTE DES ABRÉVIATIONS, SIGLES ET ACRONYMES

ABC	tampon de bicarbonate d'ammonium
ACN	acétonitrile
AP	atom percent
APAP	acetaminophen
APCI	ionisation chimique à pression atmosphérique (atmospheric-pressure chemical ionization)
AQC	6-aminoquinolyl *N*-hydroxysuccinimidyl carbamate
ATZ	atrazine
BSA	albumine de sérum de bovin (bovine serum albumin)
cc	centimètre cube
CE	énergie de collision (collision energy)
CES	intervalle d'énergie de collision (collision energy spread)
CID	dissociation induite par collision (collision-induced dissociation)
CuAAC	copper catalyzed azide-alkyne cycloaddition
CV	coefficient de variation
CXP	collision potentiel de sortie (collision exit potential)
CYA	cyanazine
CYP	cytochrome P450

DBS	soustraction dynamique du bruit de fond (dynamic background)
DBS	fond dynamique soustraction (dynamic background substraction)
DDM	*n*-dodécyl-β-D-maltopyranoside
DMSO	diméthylsulfoxyde
DNA	acide désoxyribonucléique (deoxyribonucleic acid)
DP	différence de potentiel
DTT	dithiothréitol
ECC	extrait chromatogramme composé (extracted compound chromatogram)
EI	ionisation par impact électronique (electron ionization)
EIC	chromatogrammes d'ions extraits (extracted ion chromatogram)
ESI	ionisation par électro-nébulisation (electrospray ionisation)
EtOAc	acétate d'éthyle
EtOH	éthanol
FDR	taux de fausses découvertes (false discovery rate)
FT-ICR	résonance cyclotronique ionique à transformée de Fourrier (Fourier transform ion cyclotron resonance)
GC	chromatographie gazeuse (gas chromatography)
GC-MS	chromatographie gazeuse couplée à la spectrométrie de masse (gas chromatography-mass spectrometry)

GSH	glutathion (réduit)
GSSG	glutathion (oxydé)
HEPES	acide 4-(2-hydroxyéthyl)-1-pipérazine éthane sulfonique
HILIC	chromatographie à interaction hydrophile (hydrophilic interaction chromatography)
HLM	microsomes de foie humain (human liver microsomes)
HPLC	chromatographie liquide à haute performance (high-performance liquid chromatography)
HRMS	spectrométrie de masse en haute résolution (high resolution mass spectrometry)
IAM	iodoacétamide
IDA	acquisition dynamique indépendante (independent dynamic acquisition)
IP	intrapéritonéale
IRMS	isotope ratio mass spectrometry
IS	standard interne
ISWS	solution standard d'étalon interne (internal standard working solution)
KE	énergie cinétique
l	longueur du tube à temps de vol
LC	chromatographie liquide (liquid chromatography)

LC-ESI-MS	chromatographie liquide par électro-nébulisation couplée à la spectrométrie de masse (liquid chromatography–electrospray ionization mass spectrometry)
LIT	piège à ions linéaire (linear ion trap)
MDF	filtrage par défaut de masse (mass defect filtering)
MeOH	méthanol
MFE	molecular feature extraction
MRM	suivi de réactions multiples (multiple reaction monitoring)
MS	spectrométrie de masse (mass spectrometry)
MS/MS	spectrométrie de masse en tandem (tandem mass spectrometry)
NADPH	nicotinamide adénine dinucléotide phosphate
NAPQI	*N*-acétyl-p-benzoquinone imine
NEM	*N*-éthylmaléimide
NLS	balayage de perte neutre (neutral loss scan)
NMR	résonance magnétique nucléaire (nuclear magnetic resonance)
PROP	propazine
PTM	modification post-traductionnel (post translational modification)
Q	quadripôle
QqLIT	triple quadripôles piège à ions linéaire
QqQ	triple quadripôles

QqTOF	spectre de masse hybride quadripôles associé à un temps de vol (hybrid quadrupole time of flight mass spectrometer)
Rcf	force centrifuge relative (relative centrifugal force)
RLM	microsomes de foie de rat (rat liver microsomes)
RPLC	chromatographie en phase inverse (reversed-phase liquid chromatography)
rpm	tour par minute (revolutions per minute)
RSA	albumine de sérum de rat (rat serum albumin)
S9	fractions subcellulaires hépatiques (cytosolic liver fractions)
SA	albumine de sérum (serum albumin)
SCX	échange de cations fort (strong cation exchange)
SIM	sélection d'ion (single ion monitoring)
SIM	simazine
SPE	extraction en phase solide (solid phase extraction)
SS-NMR	résonance magnétique nucléaire à phase solide (solid-state nuclear magnetic resonance)
THPTA	tris(3-hydroxypropyltriazolylmethyl)amine
TIC	chromatogramme de courant ionique total (total ion chromatogram)
TLC	chromatographie sur couche mince (thin layer chromatography)
TMP	triméthoprime

TOF	temps de vol (time of-flight)
UHPLC-MS	chromatographie liquide à ultra performance couplée à la spectrométrie de masse (ultra high performance liquid chromatography mass spectrometry)
UV	ultra-violet

LISTE DES SYMBOLES ET DES UNITÉS

Å	angstrom
amu	unité de masse atomique (*atomic mass units*)
°C	degrés Celsius
Micro (μ)	10^{-6}
Nano (n)	10^{-9}
Counts	Nombre d'ions qui frappent le détecteur par secondes
Da	Dalton
g	gramme
h	heure
I	intensité du courant
kilo (k)	10^{3}
L	litre
M	moles/litres
milli (m)	10^{-3}
m/z	rapport masse (m) sur charge (z) d'une molécule ionisée
min	minutes
mol	mole
pico (p)	10^{-12}
ppm	parties par millions
psi	unité de pression (*pound per square inch)*
V	Volt
%	pourcentage

RÉSUMÉ

Le thème central qui relie tous les projets présentés dans cette thèse est le développement de méthodes analytiques de fine pointe en spectrométrie de masse appliquées à l'analyse de molécules biologiques. La plupart des projets abordés ont pour but d'étudier des métabolites réactifs de médicaments. Ces espèces ont longtemps été associées à des effets toxiques de médicaments par le biais de leur habileté à se lier aux protéines présentes dans les cellules. L'étude des métabolites réactifs passe par, entre autres, l'étude des transformations métaboliques que subissent les médicaments, par la caractérisation de ses liaisons avec des protéines et par l'identification des protéines ciblées par ces espèces réactives. Dans cette thèse, quatre nouvelles méthodes analytiques sont présentées qui ont pour but d'identifier, caractériser et quantifier des métabolites réactifs et leurs adduits protéiques.

Le premier projet en question utilise la spectrométrie de masse à haute résolution pour étudier le métabolisme de l'atrazine et trois de ses analogues. L'atrazine est un pesticide controversé qui pourrait avoir des effets toxiques chez les humains et les animaux aquatiques. Même si ce composé a été étudié d'une manière exhaustive, notre nouvelle méthode de dépistage a réussi à trouver plusieurs nouveaux métabolites, y compris certains métabolites réactifs. Nous avons donc contribué à l'avancement des connaissances vis-à-vis du métabolisme de ce composé.

Le deuxième projet présenté démontre une autre méthode de dépistage mais cette fois-ci, une méthode semi-automatisée qui a pour but de détecter spécifiquement des métabolites réactifs dans des incubations *in vitro*. Elle nous a permis de détecter d'une manière très efficace, les métabolites réactifs formés par une série de médicaments connus.

Un troisième projet démontre une nouvelle méthodologie qui nous permet de mesurer la concentration absolue de l'adduit formé par l'acétaminophène et l'albumine, présent dans le sang. L'acétaminophène, pris en trop grandes doses, peut causer l'hépatotoxicité. En fait, l'acétaminophène est le premier responsable de l'insuffisance hépatique aigüe en Amérique du Nord et il n'existe aucun test capable de prédire la sévérité de l'hépatotoxicité du patient qui a subi une surdose. Puisque cette toxicité est causée par le métabolite réactif de l'acétaminophène qui se lie aux protéines pour induire la toxicité, cette méthode a un potentiel clinique très intéressant.

Un quatrième projet présente une nouvelle stratégie qui a pour but de permettre l'identification des protéines ciblées par les métabolites réactifs. Il y a beaucoup d'intérêt à identifier ces protéines car l'hypothèse courante veut que la différence

entre la toxicité démontrée par les composés qui peuvent former des métabolites soit dûe aux différences entre les protéines ciblées par ceux-ci. Cette nouvelle stratégie vise à purifier les adduits de métabolites réactifs de manière très spécifique grâce à la chimie click. Cette méthodologie est présentée et la faisabilité de cette approche analytique est démontrée.

Ces méthodologies permettent non seulement l'avancement des connaissances au sujet des métabolites réactifs, mais nos stratégies peuvent également s'appliquer au développement de techniques analytiques nécessaires à d'autres domaines de recherche. Un exemple de ceci, une nouvelle approche appliquée à la quantification du marquage isotopique de protéines est aussi présentée dans cette thèse.

Mots clés: Spectrométrie de masse, métabolites réactifs, développement de méthodes, toxicité de médicaments, bio-analyse.

CHAPITRE I

INTRODUCTION

1.1 MÉTABOLISME DE XÉNOBIOTIQUES ET MÉTABOLITES RÉACTIFS

Le métabolisme des xénobiotiques, molécules étrangères à un organisme, génère principalement des métabolites d'une polarité plus importante par rapport à la molécule de départ, dans le but de les rendre moins toxiques et d'ainsi favoriser l'élimination de ces molécules du corps humain.

Les transformations métaboliques sont souvent classées en deux catégories: celles de la phase I et celles de la phase II (Shewaita, 2000). D'abord, la phase I consiste à modifier des groupements fonctionnels, par oxydation, réduction ou hydrolyse. Typiquement, l'oxydation est la réaction enzymatique la plus courante lors du métabolisme de phase I. Ces réactions peuvent être catalysées par les enzymes de la famille des cytochromes P450 (CYP), famille enzymatique la plus importante parmi les enzymes du métabolisme de la phase I (Rendic, 2002). D'autres familles notables d'enzymes de phase I, parmi lesquelles sont comptées les monooxygénases contenant des flavines (FMO), des oxygénases de monoamines (MAO), les myéloperoxydases (MPO) et les cyclooxygénases (COX). Ces familles sont composées d'enzymes individuelles possédant des spécificités de substrat différentes, de sorte que les xénobiotiques, avec des structures chimiques différentes, seront métabolisés par une combinaison d'enzymes distinctes. Ces réactions ont pour double objectif, d'une part, de rendre le substrat plus soluble, facilitant ainsi son excrétion, ainsi qu'introduire de

nouveaux groupements fonctionnels qui seront ciblés par les enzymes métaboliques de phase II.

Subséquemment, le métabolisme de phase II comprend des réactions de conjugaison. En général, le métabolisme de phase II est plus efficace pour inactiver des composés biologiquement actifs et faciliter leur excrétion, étant donné qu'ils fixent à leurs substrats des molécules polaires. Quelques exemples de ces transformations sont l'ajout de l'acide glucuronique, d'un groupement sulfate, de groupements acétyles ou de glutathion. Le tableau 1.1 résume les réactions de biotransformation les plus rencontrées lors du métabolisme de xénobiotiques.

Tableau 1.1. Biotransformations courantes issues du métabolisme de phase I et phase II de xénobiotiques

Phase 1 Biotransformation	**Modification chimique**	**Phase 2 Conjugaison**	**Modification chimique**
Réduction	+2H	Glutathion	$+C_{10}H_{15}N_3O_6S$
Déhydrogénation	-2H	Glucuronide	$+C_6H_8O_6$
Hydroxylation	+O	Sulfate	$+SO_3$
Déméthylation	$-CH_2$	Acétyle	$+C_2H_2O$
Déméthylation	$-CH_2CH_2$	Glycine	$+C_2H_5NO_2$
Oxydative déamination	-NH-2H+O	Méthyl	$+CH_2$
Décarboxylation	$-CO_2$	Taurine	$+C_2H_5NO_2S$

Bien que le métabolisme des xénobiotiques ait lieu dans plusieurs tissus humains, le principal site de métabolisme est essentiellement le foie, en raison du rôle qu'il tient au sein du système digestif en plus de la proportion élevée d'enzymes métaboliques qui y sont présentes. Il est important de noter que la désignation numérique des phases I et II a pour but de classer les biotransformations en fonction du type de réaction et n'est nullement destiné à spécifier un ordre dans lequel ces réactions se produisent. Les molécules peuvent aussi subir des transformations exclusivement de phase I ou de phase II. Le métabolisme accélère non seulement l'excrétion des xénobiotiques à l'aide des transformations chimiques qu'il effectue, mais celles-ci aident normalement à inactiver les composés biologiquement actifs. Néanmoins, cette double action du métabolisme n'est pas toujours efficace, puisque certains xénobiotiques sont en fait des pro-médicaments et le métabolisme est donc nécessaire afin de libérer le composé actif. Les xénobiotiques peuvent également être bioactivés et transformés en espèces réactives, appelées métabolites réactifs, qui peuvent se lier à des macromolécules de leur environnement et causer des effets toxiques (Pirmohamed, 1996; Liebler, 2005; Guengerich 2011). La figure 1.1 montre un schéma général du métabolisme des xénobiotiques, illustrant la formation possible de métabolites réactifs.

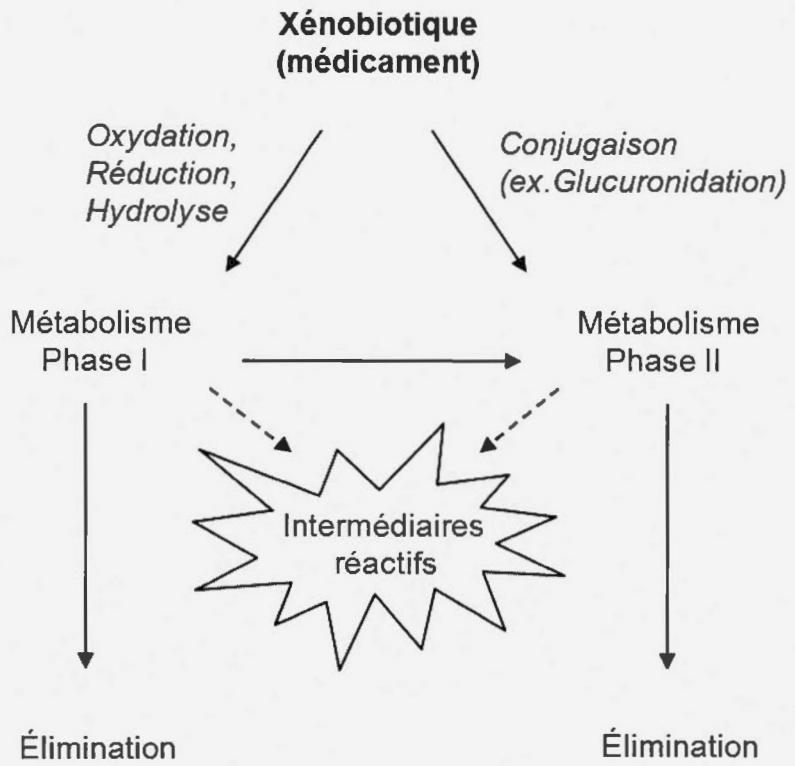

Figure 1.1. Métabolisme de xénobiotiques et formation de métabolites réactifs

Alors que les métabolites réactifs sont le plus souvent produits par les enzymes oxydatives de la phase I, les enzymes métaboliques de phase II peuvent également en générer (Zhou, 2005). Les précurseurs de métabolites réactifs possèdent des structures chimiques qui, une fois transformées par certaines enzymes métaboliques, donnent lieu à des molécules ayant une région de faible densité électronique. Ces métabolites réactifs sont donc considérés comme des électrophiles, capables de réagir avec des nucléophiles présents dans la cellule. Il existe de nombreuses structures chimiques précurseur à des espèces réactives (tableau 1.2).

Tableau 1.2. Exemples de groupements fonctionnels susceptibles de former des espèces réactives lors de transformations métaboliques (adapté de Kalgutkar, 2005)

Structures chimiques précurseurs	**Espèces réactives (via métabolisme)**
Amines aromatiques hydrazines, hydroquinones, phénols alkylés (*ortho* et *para*), méthylènedioxybenzènes	Quinones (incluant imidoquinones, et quinone-méthylène)
Amines aromatiques, arènes nitrosylés, amino-benzènes	Groupes nitroso
Formamides, sulfonylurées, thiourées, thiazolidinediones	Isocyanates
Furanes, thiophènes	Carbonyles insaturés en α et β
Thiourées, thiazolidinediones	Oxydes de souffre
Hydrazines, hydrazides	Diazènes

1.2 TOXICITÉ DES METABOLITES RÉACTIFS

Les protéines contiennent plusieurs sites nucléophiles qui peuvent se lier de manière covalente à des métabolites réactifs. Les groupements thiols libres, par exemple, présents sur les chaînes latérales de cystéines procurent un caractère fortement nucléophile et sont donc les cibles privilégiées des métabolites réactifs. La forte

corrélation reliant la quantité de protéines modifiées de manière covalente, et la toxicité d'un médicament est établie (Mitchell, 1973; Zhou, 2005). En fait, la modification covalente des protéines est une cause majeure de réactions indésirables des médicaments qui sont de nature idiosyncrasique, ou imprévisibles. Le tableau 1.3 démontre des exemples de médicaments présentant une toxicité due à la formation de métabolites réactifs.

Tableau 1.3. Exemples de médicaments dont la toxicité est causée par des métabolites réactifs

Médicament	Catégorie	Toxicité
acétaminophène	analgésique, antipyrétique	hépatotoxique
clozapine	antipsychotique	agranulocytose
carbamazépine	antiépileptique	hyper-sensibilité
phénytoïne	anti convulsant	hépatotoxique
ticlopidine	antiagrégant	agranulocytose
fipexide	nootrope	hépatotoxique, fièvre
felbamate	antiépileptique	anémie aplasique
diclophénac	anti inflammatoire	hépatotoxique
phénacétine	analgésique, antipyrétique	hépatotoxique

Le lien entre la toxicité des médicaments et la formation d'adduits de protéines avec des métabolites réactifs fut abordé au début des années 1970 lors d'une série de trois articles (Mitchell, 1973; Jollow, 1973; Potter, 1973). Dans ces études, il a été prouvé qu'il est nécessaire, pour que la liaison covalente entre la protéine et l'acétaminophène se fasse, que l'acétaminophène soit métabolisé. En outre, ils ont démontré la corrélation entre l'augmentation du métabolisme et l'augmentation des adduits de protéines *in vivo*. Il a été découvert, plus tard, que le métabolite réactif responsable de la toxicité de l'acétaminophène était le *N*-acétyle-imidoquinone (*N*-

acetyl-p-benzoquinone imine, NAPQI), une imidoquinone qui peut réagir avec les thiols libres des protéines.

Au cours des 40 dernières années, une multitude de réactions indésirables aux médicaments furent attribuées à la liaison irréversible de métabolites réactifs aux protéines (Zhou, 2005; Liebler, 2005; Guengerich, 2011). L'acétaminophène, dont l'hépatotoxicité accroit avec la dose, demeure toutefois sécuritaire lorsqu'il est utilisé selon la posologie suggérée. D'autres médicaments, tels que le fipexide et le troglitazone, furent retirés du marché pour cause de formation de métabolites réactifs toxiques. Compte tenu du coût très élevé de la mise en marché des médicaments, ainsi que du souci vis-à-vis de la santé des patients, l'industrie pharmaceutique teste systématiquement ses nouvelles entités chimiques pour évaluer leurs tendances à former des substances réactives. Lors du développement de médicaments, les nouveaux candidats subissent un test de dépistage afin de déterminer s'ils formeront d'éventuels métabolites réactifs et si tel est le cas, se lieront de façon covalente aux protéines. Par conséquent, les composés susceptibles de former ces espèces sont souvent retardés dans leur développement clinique. Les chimistes médicinaux prennent le plus grand soin, lors de la conception et la synthèse des composés, pour que les molécules candidates ne contiennent pas de groupement chimique pouvant former des métabolites réactifs. Au cours des deux dernières décennies, la quantité de médicaments développés a diminué de façon significative et l'avancement de la compréhension des problèmes causés par les métabolites réactifs peut être considéré comme l'un des facteurs contributifs.

La prudence affichée par l'industrie pharmaceutique à l'égard des métabolites réactifs semble être raisonnable en raison de la sévérité des effets secondaires indésirables. Bien qu'il existe une forte corrélation entre la formation de métabolites réactifs et la toxicité d'un médicament, cette relation demeure complexe et mal comprise. Comme

le présente le tableau 1.3, tous les médicaments donnant lieu à des métabolites réactifs n'engendrent pas la même toxicité et s'il y a une toxicité, cette dernière ne sera pas toujours d'une même sévérité. De plus, certains composés peuvent former des adduits protéiques sans causer d'effet toxique. Un exemple souvent cité est l'analogue de l'acétaminophène, le 3-acétamidophénol, qui se lie de manière covalente aux protéines sans toutefois conduire à une hépatoxicité (Rashed, 1990; Fountoulakis, 2000). L'acétaminophène, analgésique et antipyrétique largement utilisé, ne serait pas commercialisé considérant les normes qui existent aujourd'hui dans l'industrie pharmaceutique.

Il est clair que les processus biologiques impliqués dans la toxicité causée par la liaison des métabolites réactifs aux protéines sont complexes. La liaison irréversible des substances réactives aux protéines peut provoquer la toxicité via plusieurs mécanismes différents (Uetrecht, 2008). Cependant, la relation entre la structure chimique de métabolites réactifs et la toxicité résultante n'est encore pas totalement comprise. Il est nécessaire de mieux comprendre cette relation car en-outre, le rejet systématique de composés prometteurs, trop tôt dans le processus de développement de médicaments, pourrait ainsi être contourné. Il y a plusieurs groupes de recherche académique et industrielle, qui explorent cette relation entre la structure chimique des médicaments, celle de leurs intermédiaires réactifs et leurs liaisons covalentes aux protéines.

1.3 ANALYSE DU MÉTABOLISME *IN VITRO*

Une méthode couramment utilisée pour l'évaluation du métabolisme de composés médicamenteux emploie l'incubation *in vitro* du médicament avec des microsomes

hépatiques (*liver microsomes*, LM). Les microsomes sont des fractions cellulaires contenant principalement la membrane du réticulum endoplasmique. Il s'agit de la composante cellulaire comportant la plus forte concentration d'enzymes métaboliques. La plupart des enzymes de la phase I sont présentes dans la membrane du réticulum endoplasmique et par conséquent, les microsomes hépatiques sont bien adaptés pour réaliser des expériences de métabolisme *in vitro*. Un composé d'intérêt peut facilement être ajouté à des microsomes pour y être ensuite incubé à température et pH physiologique pour produire des métabolites. La nicotinamide adénine dinucléotide phosphate (NADPH) doit également être ajoutée au mélange tamponné car cette molécule demeure un cofacteur essentiel lors du métabolisme oxydatif (pour les enzymes contenant le cytochrome et la flavine). Ces tests *in vitro* sont souvent les premières expériences effectuées dans l'espoir de comprendre le métabolisme d'un composé et de déterminer les structures des métabolites de phase I. Les incubations microsomales sont également utiles lors du développement de médicaments afin d'obtenir une première impression de la biodisponibilité d'un médicament, puisque les composés qui se métabolisent trop rapidement ont aussi tendance à être éliminés rapidement *in vivo*. Les groupements chimiques susceptibles d'être transformés métaboliquement peuvent ainsi être caractérisés lors de l'analyse de ces incubations par spectrométrie de masse (Jia, 2007).

Les incubations microsomales *in vitro* sont aussi régulièrement utilisées pour évaluer la tendance des composés à former des métabolites réactifs et ensuite, pour caractériser leurs structures. Étant donné que ces métabolites réactifs sont des espèces instables qui se lient rapidement de manière covalente à des nucléophiles présents sur des protéines microsomales, un agent piégeant doit être ajouté à l'incubation. L'agent piégeant généralement employé pour ces expériences est le glutathion (GSH), un tripeptide contenant une cystéine avec un groupement thiol libre (figure 1.2). Le glutathion est une molécule endogène présente à des concentrations élevées dans des

cellules de mammifères. L'une de ses fonctions est d'agir comme antioxydant afin de se lier à des espèces électrophiles dans les cellules. Le glutathion a donc un rôle de protecteur contre le stress oxydatif et les métabolites réactifs. Dans les incubations microsomales, le glutathion est généralement ajouté en excès pour s'assurer que les espèces réactives se lieront de manière covalente, préférentiellement à son thiol libre, et non à des cystéines sur des protéines microsomale.

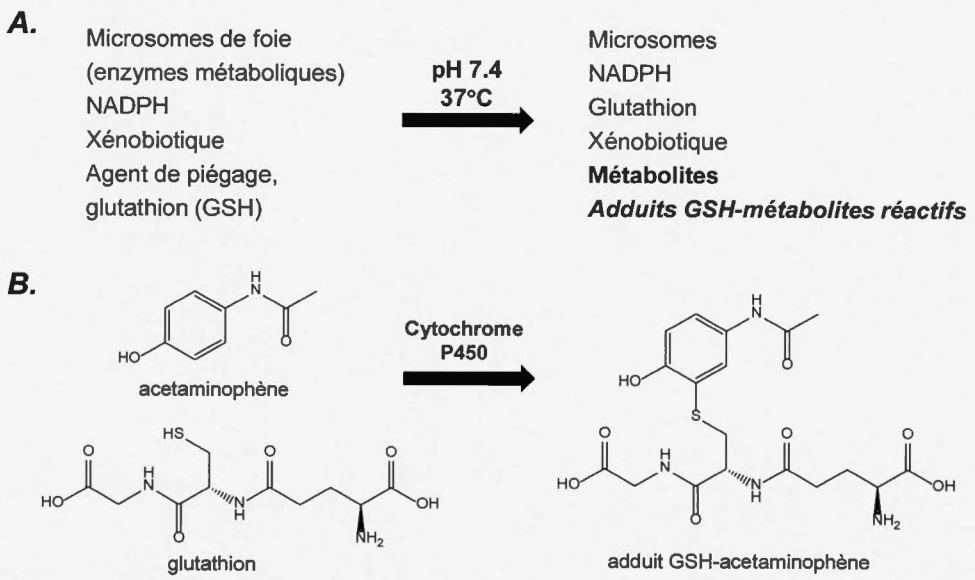

Figure 1.2. Incubation microsomale et piégeage de métabolites réactifs par le glutathion. A. Composition du milieu d'incubation. B. Exemple de la formation de l'adduit de l'acétaminophène.

L'analyse des incubations microsomales nécessite une technique sensible, sélective et capable d'élucider les structures des métabolites. En général, les médicaments sont incubés à une concentration comprise entre 10 et 50 µM, dans un volume total variant entre 200 et 500 µl (2 à 25 nmol). Une portion du médicament est ensuite transformée

en divers métabolites et, lorsqu'on piège ces métabolites réactifs avec le glutathion, des adduits glutathion-médicament sont obtenus. La concentration de métabolites et des adduits de glutathion peuvent avoir des ordres de grandeur inférieurs à celle du composé original, d'où l'importance que la technique utilisée puisse détecter et caractériser ces produits métaboliques avec une grande sensibilité. La sélectivité de la technique est également essentielle, car les incubations microsomales contiennent un mélange complexe de molécules biologiques. En outre, les structures des produits du métabolisme formés ne sont pas connues *a priori*, de sorte que l'analyse doit être en mesure à la fois de détecter les produits métaboliques présents, tout en ayant la capacité de déterminer leurs structures chimiques.

La chromatographie liquide couplée à la spectrométrie de masse (*liquid chromatography-mass spectrometry*, LC-MS) est la technique la plus utilisée pour analyser des incubations microsomales de médicaments. La séparation par chromatographie liquide à haute performance (*high performance liquid chromatography*, HPLC) permet d'isoler les produits du métabolisme et est essentielle afin de réduire la complexité de la matrice présente dans l'échantillon. La détection par spectrométrie de masse (*mass spectrometry*, MS) réunit sensibilité, sélectivité et capacité d'interprétation de structures chimiques. Cependant, la principale difficulté, lors de l'analyse d'incubations *in vitro*, provient du fait que les formules chimiques des analytes, à ce point, ne sont pas connues. La structure du médicament parent est bien caractérisée et sa fragmentation peut être étudiée par spectrométrie de masse en tandem (MS/MS). L'identification des produits métaboliques et la détermination de leurs structures ont donc été traditionnellement effectuées par des techniques de LC-MS/MS. Ces techniques peuvent confirmer la similitude entre la structure du médicament et ses produits métaboliques, puis identifier les sites de biotransformation. En utilisant la spectrométrie de masse à haute résolution, les mesures de masses précises peuvent en outre aider à déterminer la

formule chimique des analytes et de leurs fragments, et ainsi faciliter la détermination des structures chimiques. Avec la prévalence accrue des instruments MS à haute résolution au cours des dernières années, différentes stratégies permettant le dépistage des produits du métabolisme ont également vu le jour. Le chapitre 2 présentera une technique de criblage, basée sur la spectrométrie de masse à haute résolution, appliquée à la découverte des produits du métabolisme. L'atrazine et trois de ses analogues, des molécules qui ont déjà été étudiées dans le passé, ont été analysées en utilisant cette nouvelle méthode dans le but de trouver de nouveaux produits métaboliques.

Lorsque l'objectif est de détecter les métabolites réactifs présents dans des incubations microsomales, des méthodologies spécifiques sont largement utilisées pour le dépistage de la présence d'adduits de glutathion. Les deux approches les plus répandues sont basées sur la spectrométrie de masse en tandem en exploitant la fragmentation spécifique du glutathion. La première approche consiste à surveiller la perte de l'acide pyroglutamique tandis que la deuxième détecte la perte du glutathion-SH_2. Le principal problème relié à ces stratégies relève du fait que les adduits de glutathion ne se fragmentent pas tous de la même manière, étant donné que les structures des métabolites réactifs peuvent influencer leurs fragmentations. La différence entre les patrons de fragmentation des adduits GSH de différentes structures peut donc conduire à de faux négatifs. De plus, ces techniques se fient uniquement sur la fragmentation du glutathion, ce qui peut entrainer ainsi de faux positifs. Le mode d'analyse et la polarité de l'ionisation utilisés pour ces tests peuvent également engendrer un manque de sensibilité. Le chapitre 3 présentera une nouvelle méthodologie conçue pour surmonter les limitations des stratégies actuellement utilisées pour détecter la présence d'adduits GSH dans les incubations *in vitro*. Cette stratégie utilise un nouvel agent piégeant analogue au glutathion contenant un atome de brome, donc possédant un patron isotopique, un défaut de masse unique et exploite

ses propriétés chimiques uniques pour filtrer les données provenant de la spectrométrie de masse à haute résolution.

1.4 ANALYSE D'ADDUITS MÉDICAMENTS-PROTÉINES

Le piégeage des métabolites réactifs avec le glutathion dans des incubations de microsomes de foie et l'analyse subséquente par LC-MS est le moyen le plus utilisé pour détecter et déterminer la structure de ces espèces réactives autrement instables et indétectables. La présence d'adduits GSH est une indication de la capacité de ces espèces à se lier aux protéines, mais il est important de garder à l'esprit que la liaison protéique n'est pas directement détectée. L'expérience traditionnelle, encore utilisée de manière routinière, détermine si un composé peut se lier de manière irréversible aux protéines microsomales par l'incubation d'un analogue radioactif du médicament. La radioactivité mesurée provenant de la fraction de protéines microsomales (après la précipitation des protéines suivant l'incubation) est donc une indication de la quantité de médicament liée aux protéines. Cette méthode est intéressante car les composés qui ont tendance à former des adduits de protéine peuvent être identifiés tôt lors du développement de médicaments. Cette méthode ne permet pas, toutefois, de tirer de l'information quant à la structure chimique du métabolite réactif et la nature de la liaison covalente avec les protéines.

D'après des études antérieures (Cho, 1994; Evans, 2004), nous connaissons l'identité de certaines protéines qui ont tendance à être modifiées par différents métabolites réactifs. Selon une approche protéomique, une protéine ciblée peut être purifiée et digérée enzymatiquement en peptides pour ensuite être analysée par LC-MS/MS. Les différences de masse entre les principaux fragments ioniques d'un peptide représentent généralement la perte séquentielle d'acides aminés individuels et permettent le séquençage du peptide. Idéalement, lorsqu'un acide aminé est modifié,

la nouvelle masse du peptide est obtenue par la somme de sa masse, incluant la modification, en plus des masses provenant des ions fragments contenant le site de modification affectées similairement. La différence de masse entre les fragments correspondant à la perte de chacun des acides aminés individuels (à l'exception de l'acide aminé modifié) restent cependant les mêmes, ce qui permet le séquençage du peptide modifié. Le ou les site(s) de modification de la protéine cible peuvent donc être déterminés et la formule chimique de l'agent électrophile confirmée. Ces expériences peuvent fournir une preuve directe, quant à la structure de l'espèce électrophile responsable de la liaison covalente en plus de l'identité de ses cibles nucléophiles sur la protéine *in vivo*.

L'albumine et l'hémoglobine ont été découvertes comme étant ciblées par des intermédiaires électrophiles de produits chimiques cancérogènes depuis les années 1970, et l'idée de les exploiter en tant que biomarqueurs d'exposition aux cancérogènes fut introduite. Ces protéines sont très abondantes et contiennent des sites nucléophiles susceptibles de réagir avec les espèces électrophiles. En outre, elles sont présentes dans la circulation sanguine, ce qui rend l'échantillonnage *in vivo* relativement simple et non invasif. Depuis, l'évolution des techniques modernes d'analyse de protéines par spectrométrie de masse, qui ont vu le jour grâce au développement de techniques d'ionisation douces (Fenn, 1989; Tanaka, 1988; Karas 1988), suivi des progrès majeurs dans le domaine de la protéomique (Mann, 2001; Aebersold, 2003; Walther, 2010), l'étude des protéines modifiées a connu un intérêt grandissant en raison de leurs liens avec une multitude de processus biologiques. Plus précisément, en ce qui concerne les liaisons covalentes d'électrophiles, un intérêt particulier à l'albumine modifiée lui fut apporté en tant que biomarqueur. Plusieurs études ont été effectuées dans le but d'identifier et de caractériser les adduits d'albumine, sans toutefois proposer des méthodes quantitatives pour mesurer la concentration de ces adduits. Le chapitre 4 présentera une nouvelle approche qui

permettra la quantification d'adduits acétaminophène-albumine. Ceci représente la première méthode qui permet de déterminer de manière fiable la concentration absolue d'un adduit médicament-protéine *in vivo*.

1.5 IDENTIFICATION DES CIBLES PROTÉIQUES DE MÉTABOLITES RÉACTIFS

Quoique certaines protéines ciblées par des métabolites réactifs soient connues, le nombre de protéines visées demeure relativement peu nombreux. Il existe présentement un manque d'informations quant aux cibles protéiques des substances réactives. Nous avons vu que les médicaments qui peuvent former des métabolites réactifs et des adduits protéiques ne démontrent pas tous les mêmes effets secondaires, et n'expriment pas tous la même intensité. L'hypothèse veut que d'avantage d'information sur les variations entre les cibles protéiques de métabolites réactifs de structures différentes aiderait à expliquer les différences dans les effets secondaires (Ma, 2009; Evans, 2005; Zhou, 2005; Uetrecht, 2008). Il y a donc un grand intérêt pour identifier les cibles protéiques de ces espèces. Une identification exhaustive des cibles protéiques de chaque médicament serait indispensable pour établir et comprendre la relation entre la structure d'un composé et la toxicité induite par ses métabolites réactifs.

Il y a de nombreux défis analytiques associés à l'identification des protéines modifiées par des substances réactives. Même si les méthodologies protéomiques destinées à identifier les protéines dans des échantillons complexes sont devenues routinières, l'identification des protéines modifiées par des xénobiotiques peut s'avérer plus laborieuse. Les protéines sont généralement identifiées en utilisant un logiciel spécialisé capable de séquencer les peptides digérés, à l'aide de bases de données (contenant des séquences de protéines), en utilisant à la fois la masse

mesurée du peptide et son spectre de fragmentation obtenus par l'analyse MS/MS. Les modifications chimiques peuvent compliquer ces spectres MS/MS, rendant la tâche plus ardue d'identifier les peptides (et ainsi les protéines modifiées) avec un haut degré de certitude. De plus, un autre grand défi, associé cette fois à la faible concentration des protéines modifiées présentes dans les échantillons, est dû au fait que ces modifications soient assez rares. La faible concentration des modifications peptidiques, surtout à l'intérieur d'un mélange complexe contenant une quantité énorme de peptides non modifiés, peut gêner l'acquisition de spectres MS/MS de haute qualité, empêchant l'analyse des peptides d'intérêt.

Jusqu'à présent, la plupart des tentatives d'identification de protéines ciblées par les métabolites réactifs s'appuient sur l'immunochimie (Pohl, 1993; Griffin, 1998; Halmes, 1998; Cribb, 1996; Khojasteh, 2012) ou la radioactivité (Koen, 2007; Ikehata, 2008; Tzouros, 2009). En règle générale, des incubations microsomales sont réalisées avec des composés formant des adduits protéiniques dont la fraction protéique sera ensuite séparée sur des gels d'électrophorèse (1D ou 2D). Les bandes (1D), ou des taches (2D) qui produisent soit un signal d'anticorps ou de la radioactivité sont excisées, digérées et identifiées par MS/MS. Ces études illustrent la nécessité d'utiliser des méthodes plus sensibles et plus sélectives, car aucune d'entre elles n'a pu confirmer la présence ou même l'emplacement des modifications dans la séquence d'un peptide. Ces méthodes ont également le défaut de pouvoir produire de faux positifs, car les protéines identifiées ont possiblement été sélectionnées grâce à leur co-migration avec l'origine d'un signal provenant de l'anticorps ou de la radioactivité.

Une étude dont le travail est à souligner (Tzouros, 2009), utilise un mélange équimolaire d'un médicament et son analogue radioactif, et par la suite, sépare les peptides issus de la digestion de protéines (séparées ultérieurement sur un gel 2D) par

chromatographie d'échange d'ions couplée à un détecteur de radioactivité. Les pics générant un signal sont ensuite récupérés, digérés et analysés par LC-MS/MS. La signature isotopique des peptides, produite par le mélange d'isotopes, offre une confirmation supplémentaire de la présence d'une modification. Comme certaines des études mentionnées précédemment, celle-ci a le désavantage de se fier à la détection par radioactivité, garantissant une faible sensibilité. Cette étude a réussi le séquençage de quatre peptides, issus de trois protéines différentes, soulignant la nécessité d'employer des méthodes de détection plus sensibles et des méthodologies plus efficaces si l'on vise à obtenir une liste plus complète des adduits protéiques présents dans des microsomes.

La nécessité de développer des méthodes plus sensibles n'est pas surprenante, puisque les concentrations de métabolites réactifs générés dans des incubations *in vitro* sont typiquement de faible niveau, généralement de l'ordre de 0,01 à 1 µM. Ces espèces peuvent alors réagir avec plusieurs protéines parmi les centaines de milliers présentes dans les microsomes. Autrement dit, il y aura non seulement une petite quantité totale de protéines modifiées, mais aussi une très faible proportion d'une protéine ciblée qui sera modifiée. Le plus grand défi pour l'identification des protéines cibles est de s'assurer d'obtenir la sensibilité requise pour effectuer le séquençage de leurs peptides après digestion enzymatique. Pour ce faire, il serait idéal de développer une méthode pour extraire ou purifier les protéines cibles, car autrement, le mélange sera trop complexe pour les analyser d'une manière fiable.

À cet effet, le travail du groupe Liebler (Shin, 2007; Wong, 2008) représente une avancée significative dans le domaine, puisqu'ils ont conçu des sondes électrophiles contenant de la biotine, utilisée pour la purification par affinité des adduits de protéines. Bien qu'un des aspects important de leurs travaux repose sur la reproductibilité de la technique (les cibles ne sont pas aléatoires, suggérant une

certaine spécificité de l'électrophile), les sondes utilisées sont en fait des agents ciblant à alkyler les groupements thiols. Leurs structures ne représentent donc pas le type de réactivité qui existe chez les métabolites réactifs de médicaments. De plus, les groupements électrophiles ne sont pas générés par le biais d'enzymes métaboliques, mais sont plutôt ajoutés à des concentrations beaucoup plus élevées que lors d'incubations *in vitro*, dans le but de produire des échantillons plus concentrés de protéines modifiées. La structure encombrante de la biotine, ainsi que la taille et la nature chimique des sondes, peuvent aussi jouer un rôle quant à la spécificité de ces agents électrophiles, qui ne sont aucunement reliés d'une manière structurale à de vrais médicaments conduisant aux métabolites réactifs.

Afin d'améliorer les stratégies ci-dessus, notre groupe de recherche a concentré ses efforts sur l'élaboration d'une méthode incorporant la «chimie click» et des sondes analogues à des médicaments qui peuvent former des métabolites réactifs, dans le but d'identifier leurs cibles protéiques dans des incubations microsomales. Le chapitre 5 présentera le développement d'une nouvelle méthodologie qui permettra la purification sélective de peptides modifiés par des espèces électrophiles, produites par la transformation biologique, ayant des structures similaires aux métabolites réactifs de vrais médicaments. Nous envisageons que la sensibilité acquise via cette procédure (en développement) permettra d'identifier quelles sont les protéines modifiées par de vrais métabolites réactifs et de déterminer où les modifications ont lieu sur la protéine.

1.6 SPECTROMÉTRIE DE MASSE

Le thème central de cette thèse est l'utilisation de techniques à la fine pointe en spectrométrie de masse appliquée à la caractérisation de métabolites réactifs et de

leurs adduits. La spectrométrie de masse à haute résolution (HRMS), ainsi qu'en tandem (MS/MS) sont des outils cruciaux dans l'optique d'identifier et de quantifier des composés importants d'un point de vue biologique dans les matrices complexes. La puissance de détection par MS est sans paire, compte tenu de la sensibilité et la spécificité nécessaires pour bien caractériser les métabolites réactifs et leurs adduits dans les échantillons très complexes. Cette section énumèrera les principaux avantages à utiliser la HRMS et la spectrométrie de masse en tandem. Je vais aussi traiter des caractéristiques majeures des types d'instrumentation qui ont été utilisés par les méthodologies décrites dans cette thèse.

Les deux premières études présentées dans cette thèse utilisent la spectrométrie de masse à haute résolution pour le dépistage de composés dans des mélanges complexes. La haute résolution fournit un niveau de sélectivité accru puisque les ions de masses similaires sont bien séparés dans les spectres acquis. La figure 1.3 démontre comment un spectre complexe peut être efficacement simplifié par la simple extraction d'une gamme de masse très étroite. À l'aide de critères très précis, nous pouvons analyser des données à haute résolution pour déterminer la présence de composés d'intérêt dans des échantillons complexes. Les instruments à haute résolution peuvent également fournir des mesures de masses exactes qui aident à raffiner les formules chimiques possibles pour les pics non identifiés. De plus, les mesures de masses précises permettent également de confirmer l'identité de pics provenant d'analytes d'intérêt, si bien que la plupart des journaux scientifiques exigent maintenant que les nouvelles molécules soient analysées par HRMS pour leur caractérisation.

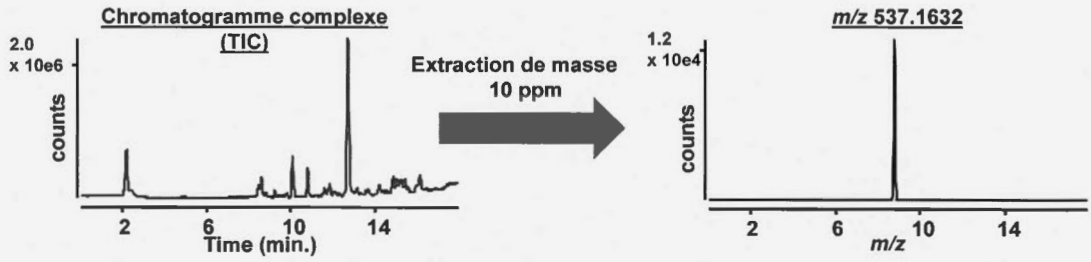

Figure 1.3. Exemple de la sélectivité que peut procurer la spectrométrie de masse à haute résolution lors de l'analyse d'un mélange complexe

Les instruments ayant la capacité de produire des spectres de masse à haute résolution avec des mesures de masses précises contiennent des analyseurs de masse de type résonance cyclotronique ionique (*Ion cyclotron resonance*, ICR) et « orbitrappe », tous deux basées sur la transformée de Fourier, ainsi que des analyseurs à temps-de-vol (*time-of-flight,* TOF). Les instruments à haute résolution qui sont relevés dans cette thèse sont basés sur des analyseurs TOF. La figure 1.4 montre un schéma illustrant les principes de l'analyseur TOF, où les ions sont accumulés puis pulsés à travers un tube de vol sans champ électrique ou magnétique. Chaque ion reçoit une quantité égale d'énergie cinétique, de sorte qu'ils vont atteindre le détecteur dans l'ordre inverse de leur taille. Le rapport *m/z* des ions peut donc être calculé à partir du temps nécessaire pour traverser le tube-de-vol. Les instruments TOF sont très sensibles lors de l'acquisition des données sur une large gamme de masse et ils ont un temps d'acquisition de spectre très rapide. Le temps qu'il faut pour que les ions se déplacent à travers le tube de vol et acquièrent un spectre de haute résolution est de l'ordre de quelques microsecondes, par rapport aux instruments basés sur la transformée de Fourier, qui prennent plus de temps pour acquérir des spectres de résolution comparable.

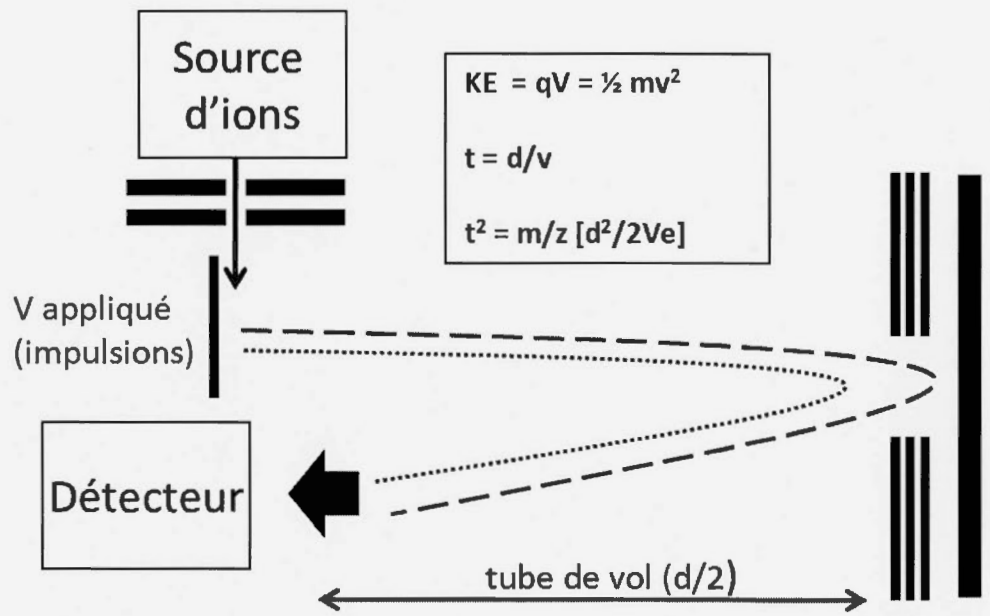

Figure 1.4. Principe d'un analyseur de masse à temps-de-vol (TOF MS)

Il existe plusieurs systèmes intégrant de multiples analyseurs de masse pour effectuer des analyses MS/MS. Le spectromètre de masse en tandem classique est le triple quadripôle, qui comprend deux quadripôles séparés par une cellule de collision, ayant la capacité d'effectuer une dissociation induite par collisions (*collision-induced dissociation*, CID) d'ions précurseurs filtrés par le premier quadripôle. Les utilisations les plus courantes de la spectrométrie de masse en tandem comprennent l'élucidation de structure et la quantification des espèces provenant de matrices complexes. La fragmentation sélective des ions précurseurs (molécules protonées ou déprotonées) de molécules biologiques peut fournir de l'information structurale lorsque le deuxième analyseur de type quadripôle est utilisé pour balayer les ions produits qui en résultent (figure 1.5). Quand un ion fragment est sélectionné (et filtré spécifiquement) par le troisième quadrupole (*selected reaction monitoring*, SRM ou MRM), la détection de la molécule ciblée est encore plus sélective, et est habituellement utilisée pour la

quantification d'analytes précis dans les matrices complexes. La figure 1.6 illustre le schéma général d'un instrument de type triple quadripôle et énumère ses différents modes de balayage. L'un des instruments décrit dans cette thèse est un instrument hybride quadripolaire-piège-à-ions linéaire (*quadrupole linear ion trap*, QqLIT). Ce type d'instrument peut être utilisé de la même manière qu'un instrument triple quadripôle, car le piège-à-ions linéaire peut fonctionner comme un simple quadripôle. Bien que cet instrument dispose des fonctionnalités supplémentaires par rapport à un triple quadripôle, les méthodes décrites dans cette thèse utilisant cet instrument hybride contiennent seulement des modes de balayage de type triple quadripôle.

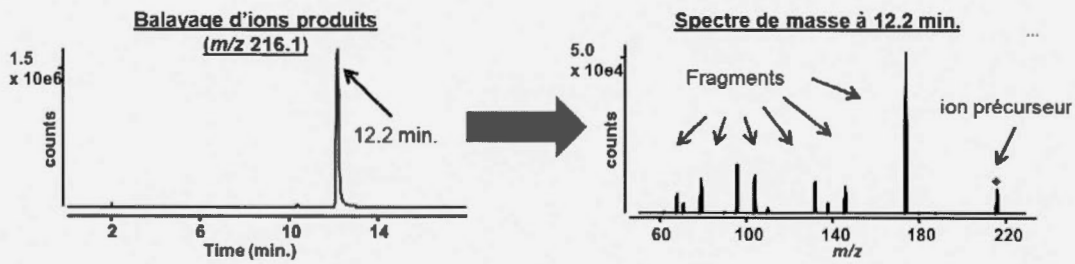

Figure 1.5. Exemple d'un spectre d'ions produits

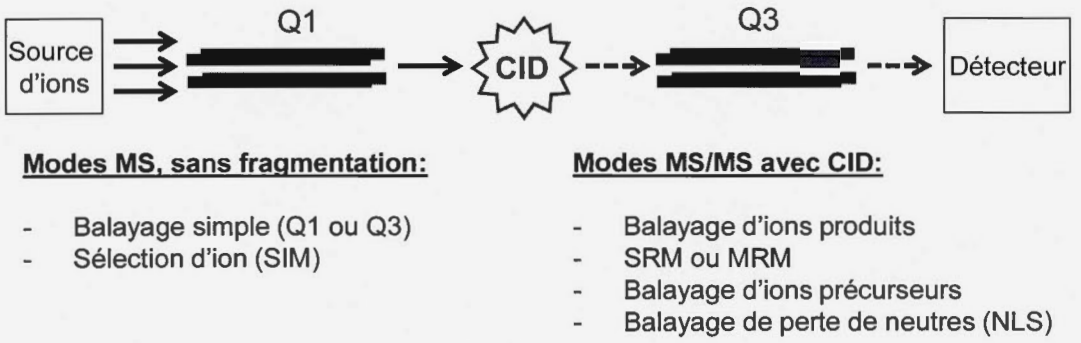

Figure 1.6. Différents modes d'analyse disponibles avec un instrument triple quadripôles

Bien sûr, les instruments les plus modernes combinent à la fois la haute résolution et la spectrométrie de masse en tandem. Ces instruments hybrides ont évolué rapidement au cours des vingt dernières années et sont devenus beaucoup plus populaires, principalement en raison de leur utilisation courante dans le domaine de la protéomique. Un tel instrument qui est décrit dans cette thèse est un instrument hybride quadripôle-temps-de-vol. Cet instrument dispose de la plupart des fonctionnalités d'un instrument triple quadripôle, mais à haute résolution et en ayant des capacités d'analyse très rapides. Des instruments tels que ceux-ci sont à la fine pointe de la spectrométrie de masse moderne en raison de leur polyvalence. La sensibilité et la résolution disponibles chez ces instruments ne cessent d'augmenter. Leur constante évolution permet le développement de nouvelles méthodologies pour répondre à une multitude de questions biologiques.

CHAPITRE II

ARTICLE SCIENTIFIQUE: "ATRAZINE METABOLITE SCREENING IN HUMAN MICROSOMES: DETECTION OF NOVEL REACTIVE METABOLITES AND GLUTATHIONE ADDUCTS BY LC-MS"

André LeBlanc and Lekha Sleno*

*Université du Québec à Montréal, Pharmaqam, Chemistry Department, P.O. Box 8888, Downtown Station, Montréal, Québec, Canada H3C 3P8

Article published in:

Chemical Research in Toxicology 2011, 24, 329-339.

Received: September 7, 2010

Published: March 02, 2011

Cet article présente les résultats d'une étude portant sur le métabolisme de l'atrazine et trois autres pesticides analogues. Il y a controverse entourant l'atrazine, un pesticide couramment utilisé en Amérique du Nord, dû au fait qu'il pourrait engendrer des effets toxiques chez les humains et les animaux. Nous avons utilisé la spectrométrie de masse à haute résolution pour le dépistage de ses métabolites formés dans des incubations microsomales. Nous avons découvert de nouveaux métabolites de l'atrazine, incluant des métabolites réactifs.

Sous la supervision du professeure Lekha Sleno, je fus responsable de la rédaction du manuscrit, ainsi que de toutes les manipulations, expérimentations et analyses de données.

2.1 ABSTRACT

Atrazine (ATZ), one of the most widely used herbicides worldwide, has been the subject of several scientific studies associated with its human and ecological risks. In order to study atrazine's toxicity, the formation of its metabolites and the result of their exposure must be assessed. This relies on our ability to detect and identify all of atrazine's metabolites, however, no previous untargeted screening method has reported the detection of all known metabolites and glutathione conjugates at once. In this study, a compound-specific, post-acquisition metabolic screening method was employed following a generic HPLC separation coupled with high resolution time-of-flight mass spectrometry (TOF-MS) to detect Phase I metabolites and glutathione conjugates generated by *in vitro* human liver microsomal incubations. Our method was designed to be unbiased and applicable to a wide variety of compounds since methods that can detect a broad range of metabolites with high sensitivity are of great importance for many types of experiments requiring thorough metabolite screening. Based on incubations with atrazine and three closely-related analogs (simazine, propazine and cyanazine), we have proposed a new Phase I metabolism scheme. All known Phase I transformations of atrazine were successfully detected, as well as a new *N*-oxidation product. Novel reactive metabolites were also detected as well as their glutathione conjugates. These newly detected species were produced via imine formation on the *N*-ethyl group, a biotransformation not previously observed for atrazine or its analogs.

2.2 INTRODUCTION

Atrazine (ATZ) is one of the most widely used agricultural herbicides worldwide, with approximately 80 million pounds applied yearly in the United States alone (Kiely *et al.*, 2004). It is employed in order to control broadleaf and grassy weeds and is mostly applied on corn, sorghum, and sugar cane crops, as well as, to a lesser extent, on residential lawns. Because of its widespread use, its ability to infiltrate water systems and its resistance to further degradation by hydrolysis and photolysis, atrazine and its byproducts are some of the most frequently detected in ground and surface waters (Nelson & Frankenberry, 2001; Gaynor *et al.,* 2000; Clay *et al.,* 2000). Atrazine is also routinely detected in drinking water, especially close to highly treated areas (Jiang *et al.,* 2006; Gojmerac *et al.*, 1996; Hua *et al.*, 2006). In October 2009, the U.S. Environmental Protection Agency (EPA) launched a comprehensive re-evaluation of atrazine due to the growing number of scientific studies associated with its human and ecological risks (EPA, 2009).

There has been much debate over the environmental and toxicological effects of atrazine (Solomon *et al.,* 2008; Gammon *et al.*, 2005) Animal toxicological studies have mainly focused on endocrine disruption end points such as mammary gland tumor production (*Wetzel et al., 1994*; Ueda *et al.*, 2005) or modulation of luteinizing hormone release (Cooper *et al.*, 1996; McMullin *et al.*, 2004). In addition, recent studies suggest that environmentally relevant levels of atrazine can reduce fathead minnow reproduction (Tillitt *et al.*,2010). and induce feminization in male African clawed frogs (Hayes *et al.*, 2010)). Several studies have also been conducted investigating the link between atrazine exposure and human health, but these have yielded mixed conclusions. There remains a need for more in-depth scientific studies in order to draw a more complete picture of the potential impact of atrazine on human health.

Exposure to atrazine not only implies exposure to its environmental degradates but also to its metabolism products. For the study of atrazine's toxicology, the formation of its metabolites and the result of their exposure need to be assessed. This obviously relies on our ability to detect and identify all of atrazine's metabolites. Atrazine metabolite screening studies have been conducted from *in vivo* bioanalysis experiments in rats (Bakke *et al.*, 1972) or from *in vitro* liver microsomal incubations in human or other vertebrate species such as rat, pig, mouse, and chicken (Adams *et al.*, 1990; Lang *et al.*, 1996) A more recent study, has investigated atrazine metabolism in human liver with both microsomal and S9 fractions (Joo, *et al.,* 2010). These studies and others show that atrazine typically undergoes *N*-dealkylation by the hepatic cytochrome P450 system (Lang *et al.*, 1997) Glutathione conjugation of atrazine or its *N*-dealkylated metabolites by chlorine substitution has been reported and detected (Joo, *et al.,* 2010). as well as the subsequent formation of mercapturic acid (Adams *et al.*, 1990) conjugates. Evidence of the formation of reactive metabolites also includes protein covalent binding of atrazine metabolites (Dooley *et al.*, 2006) and the depletion of glutathione stocks in rat erythrocytes (Singh *et al.*, 2010; McMullin *et al.,* 2003)

Screening methods used to identify novel atrazine metabolites and glutathione adducts from *in vivo* (Bakke *et al.*, 1972) and *in vitro* (Adams *et al.*, 1990) studies have used ^{14}C-labeled atrazine and relied on the detection of radioactive spots from thin layer chromatography (TLC) experiments. Liquid chromatographic separation of *in vitro* incubations coupled with UV detection (Lang *et al.*, 1996) has also been used and has led to the detection of the isopropyl-hydroxylated metabolite of atrazine. The ethyl-hydroxylated metabolite was first described using a combination of UV detection and full scan MS using a linear ion trap instrument (Joo, *et al.,* 2010). The more recent *in vivo* metabolism studies have analyzed atrazine and its previously identified metabolites in order to investigate disposition and pharmacokinetics in animal models (McMullin *et al.,* 2003; Ross *et al.*, 2009) or to detect human

metabolites in bioanalytical assays (Lucas *et al.*, 1993; Buchholz *et al.*, 1999; Barr *et al.*, 2007) The most recent analytical methods have predominantly been quantitative in nature and have been developed to improve biomonitoring techniques in urine.(Zhou *et al.*, 2007; Panuwet *et al.*, 2008; Ross & Filipov, 2006). Typically, these methods employ a targeted analysis of the parent compound and specific metabolites by liquid chromatography coupled with mass spectrometry (LC-MS) without searching for any new metabolite species.

None of the above-mentioned untargeted screening methods have reported the detection of all known atrazine metabolism products at once. The differences in the physical properties between atrazine and its metabolites have been a challenge for the efficient extraction and separation of the analytes of interest. More importantly, the sensitivity and specificity of these techniques have been a factor in limiting the number of metabolites detected. Methods that can detect a broad range of metabolites with high sensitivity and selectivity are of great importance for many types of experiments requiring thorough metabolite screening, as in biological or environmental monitoring studies. These screening techniques are also crucial in finding potential avenues of toxicity, for instance, via reactive metabolite formation.
The goal of this study is 3-fold. The first is to detect all known Phase I biotransformations and GSH conjugates of atrazine produced by human liver microsomes (HLM) with a single untargeted and generic screening method. The second is to find any new unreported atrazine metabolites and GSH conjugates formed in HLM, and last, to verify that all detected metabolites and conjugates were metabolism-dependent by comparison with a full set of controls. The result is a newly proposed Phase I metabolism scheme for herbicidal chloro-S-triazines based on the detection of *in vitro* generated metabolites from human liver microsomal incubations with atrazine, as well as three of its derivatives (simazine, propazine, and cyanazine). This new metabolism scheme includes novel reactive metabolites detected via glutathione trapping as well as a newly reported *N*-oxidation product. A thorough,

compound-specific, metabolic screening method following a generic separation by reverse phase liquid chromatography coupled with high resolution mass spectrometry on an electrospray-time-of-flight (ESI-TOF) instrument was used to reveal the oxidative metabolites and glutathione adducts formed by atrazine and its analogues, on the basis of accurate mass data. Molecular structures were subsequently confirmed by LC-MS/MS analysis on a triple quadrupole (QqQ) mass spectrometer.

2.3 EXPERIMENTAL

2.3.1 MATERIALS

Analytical grade atrazine (97.2%), propazine (99.3%), and cyanazine (99.7%), as well as reduced l-glutathione (GSH), β-nicotinamide adenine dinucleotide 2′-phosphate reduced tetrasodium salt (β-NADPH), formic acid (ultra pure), potassium phosphate (monobasic), and potassium hydroxide were obtained from Sigma-Aldrich (Oakville, ON, Canada). Analytical grade simazine (96%) was purchased from Alfa Aesar (Ward Hill, MA, USA). Human liver microsomes were purchased from BD Biosciences (Mississauga, ON, Canada). HPLC grade acetonitrile (ACN), methanol, and acetone were obtained from Fisher Scientific (Ottawa, ON, Canada), and ultrapure water was supplied by a Barnstead NANOpure Diamond UV ultrapure water system from Thermo Scientific (Mississauga, ON, Canada).

2.3.2 *IN VITRO* INCUBATIONS

Human liver microsomal incubations (1 mg/mL protein) were performed with 50 μM herbicide (atrazine, simazine, propazine, or cyanazine), 1 mM NADPH, and 1 mM

GSH for 2 h at 37 °C in a potassium phosphate buffered solution (50 mM, pH 7.4) in a total volume of 250 µL. Samples were then quenched with an equal volume of ice-cold ACN, vortexed, and centrifuged at 13000 rpm for 10 min. The supernatant was evaporated to dryness using a centrifuge concentrator (model RC10.10, Jouan, Winchester, VA, USA) and reconstituted in 250 µL of 10% ACN prior to injection onto the LC/MS system. Control incubations were quenched at time = 0 (t0) (prior to the addition of pesticide) and/or performed without the addition of GSH, NADPH, and/or microsomes.

2.3.3 LC/MS ANALYSIS

All samples were separated on an Thermo BetaBasic-C18 column (2.1 × 150 mm, 5 µm particles) using an Agilent 1200 HPLC system (including binary pump, in-line degasser, high performance autosampler, and thermostated column compartment) with the following gradient: initial conditions of 5% B with a 2 min hold, up to 95% B at 13 min, and held for 3 min before re-equilibration, where mobile phases A and B were water and acetonitrile (both containing 0.1% formic acid), respectively, at a flow rate of 0.3 mL/min, a column temperature of 35 °C, and 20 µL injection volume. Mass spectrometric analysis was performed on an Agilent 6210 ESI-TOF instrument (Agilent Technologies, Mississauga, ON, Canada) in positive ESI mode using MassHunter acquisition software (version B.02.00). The dual ESI source was operated with a capillary voltage of 4000 V and gas (ultrapure nitrogen) temperature of 350 °C with a flow of 12 L/min. The nebulizer pressure was maintained at 35 psi and the fragmentor and skimmer voltages were 100 and 60 V, respectively. Data were acquired from *m/z* 100-1000 with internal calibration using the reference masses *m/z* 121.050873 and 922.009798 in the Agilent reference mass solution (#G1969085001),

sprayed continuously through the reference electrospray needle. All raw TOF data were processed using MassHunter Qualitative Analysis software (version B.02.00).

The collision-induced dissociation (CID) fragmentation patterns of oxidative metabolites and glutathione adducts found during screening were analyzed by LC-MS/MS on an Agilent 6410 triple quadrupole instrument for structure confirmation using the above LC method. The multimode ionization source was operated in ESI positive mode with a capillary voltage of 2500 V and a gas temperature and flow of 300 °C and 5 L/min (ultrapure nitrogen), respectively. The vaporizer temperature was held at 150 °C, and the nebulizer pressure was maintained at 60 psi. The charging and fragmentor voltages were set at 2000 and 135 V, respectively. The product ion scans were acquired with unit resolution and an 800 ms total scan time at 0.1 amu step size. The scanned *m/z* range consisted of *m/z* 50 to parent+10, with a collision energy of 20 V. All raw MS/MS data were also processed using MassHunter Qualitative Analysis software.

2.3.4 POST-ACQUISITION METABOLITE SCREENING

Prior to filtering the data, Phase I metabolism products and glutathione conjugates were predicted on the basis of each compound's structure. An exhaustive list of potential metabolites and their masses was generated for each compound considering all common Phase I metabolic transformations. Only biotransformations that were not structurally feasible were disregarded. Glutathione adduct formation was added to the list of possible biotransformations in order to screen for potential electrophilic reactive metabolites and because previous microsomal studies had detected GSH conjugates. The list of screened biotransformations for the four tested herbicides was the following: dehydrogenation (-2H), hydroxylation (+O), dechlorination (-HCl),

hydration (+H2O), *N*-dealkylation (compound-dependent: -C2H4, -C3H6, or -C5H6N), and glutathione addition (+C10H17N3O6S (+GSH)). The exact masses of the resulting hypothetical metabolism products were calculated for all possible combinations including up to four separate biotransformations. Extracted ion chromatograms (EICs) of each of the resulting masses within a 10 ppm window were then extracted from the total ion chromatogram (TIC) of all samples and controls for a given compound. All EICs that had no detected chromatographic peaks were discarded. The remaining EICs were analyzed and directly compared to the EICs of the corresponding mass in the various control samples.

2.4 RESULTS

2.4.1 POST-ACQUISITION DATA MINING

Our approach for data acquisition was designed to be unbiased and applicable to a large variety of compounds. The screening employed for this study relies uniquely on post-acquisition data mining based on the chemical structures of atrazine, simazine, propazine, and cyanazine (figure 2.1). The TOF-MS enables us to detect all ions (*m/z* 100-1000) with high resolution and high sensitivity without omitting any potential metabolic species, in contrast to more targeted acquisition methods such as single ion monitoring (SIM) and multiple reaction monitoring (MRM) on a triple quadrupole instrument. Using a high resolution mass spectrometer not only allows us the use of narrow mass extraction (±10 ppm) for high specificity but also allows us the use of generic acquisition parameters applicable to a wide range of compounds. The HPLC run is also a generic gradient that can be used for a multitude of compounds and metabolites with broad range in polarities. The use of a thorough set of controls performed without the addition of GSH, NADPH, and/or microsomes, in combination

with incubations quenched at t_0 (prior to the addition of pesticide) are crucial in determining whether a species is dependent on the presence of microsomes, NADPH, and/or glutathione once the initial screening has been performed. This allows us to confirm whether the formation of a given metabolite is entirely reliant on metabolism (enzymatically formed). In addition, testing several S-chloro-triazine analogues in the same study is a useful strategy to help understand the effect that different functional groups have on the metabolism of compounds within the same family.

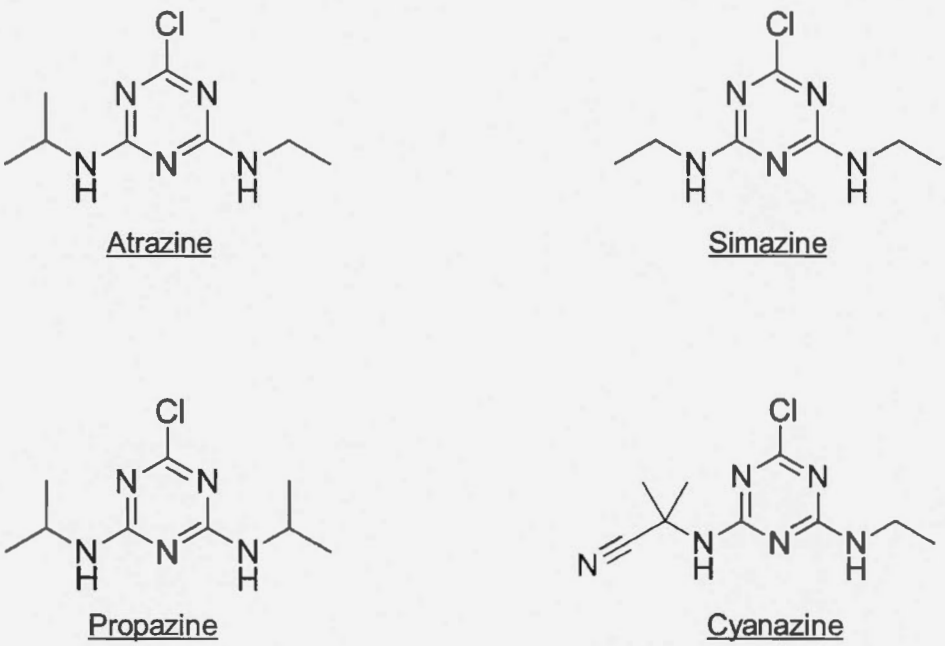

Figure 2.1. Chemical structures of atrazine and other S-chloro-triazine herbicide analogues used in this study.

2.4.2 MS/MS

The internally calibrated high resolution MS yields accurate mass data, which is crucial for elemental formula confirmation. However, since high resolution data is not sufficient for structural elucidation of metabolites, MS/MS data for each detected species is also necessary. The collision-induced dissociation (CID) fragmentation patterns of atrazine, simazine, propazine, and cyanazine were studied and used for comparative purposes to confirm the identity of all screened species. Figure 2.2 illustrates atrazine's MS/MS spectrum from which we have proposed a comprehensive fragmentation scheme (Scheme 2.1), complemented by the MS/MS data of atrazine's ^{37}Cl isotope (M+2) at *m/z* 218 to confirm the chlorine-containing fragments (data not shown). The fragmentation pattern of atrazine is mostly dominated by *N*-dealkylations ($-C_2H_4$ and $-C_3H_6$) and dechlorination (-HCl). These fragmentation mechanisms are very useful for identifying the location of the transformations sustained by atrazine and its analogues since they are the most likely targets of metabolism.

2.4.3 SCREENING RESULTS

Following raw data collection, we proceeded with compound-specific screening by extracting exact masses for each of the hypothetical metabolites of atrazine and its three analogues. Once a given elemental formula was confirmed as metabolism-dependent, we then elucidated the metabolite's structure by MS/MS on a triple quadrupole instrument. A summary of all MS/MS characterized peaks for each herbicide is given in Table 2.1 (with base peaks noted in bold).

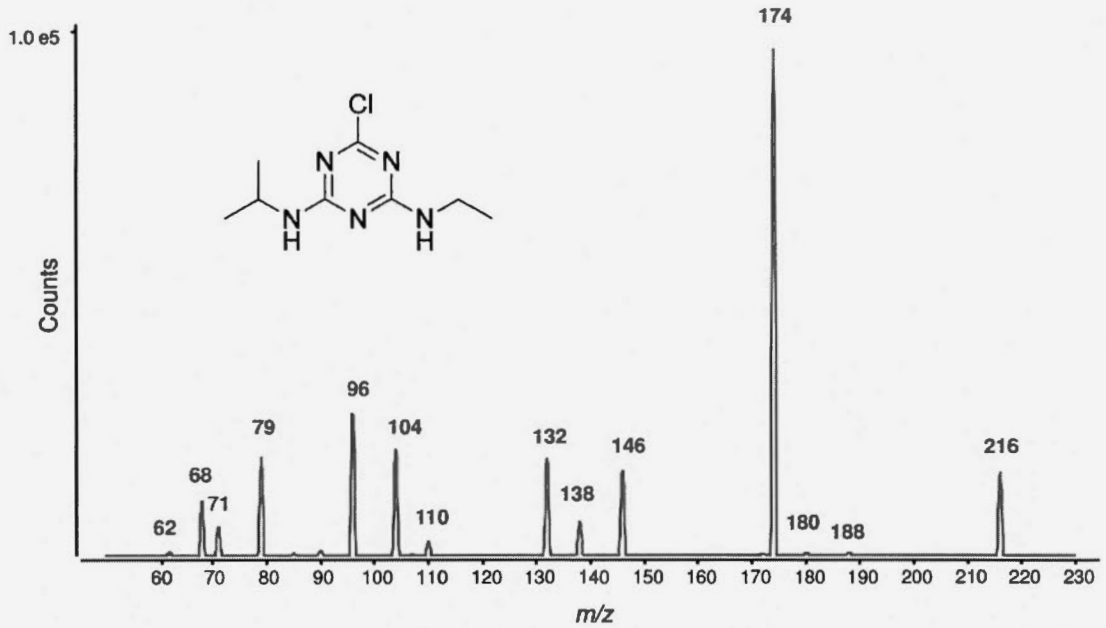

Figure 2.2. Collision-induced dissociation (MS/MS) spectrum of atrazine (*m/z* 216).

Atrazine:

First, we notice that all previously reported biotransformations of atrazine were successfully detected. These include *N*-dealkylations ($-C_2H_4$ and $-C_3H_6$), hydroxylation (+O), and chlorine substitution by glutathione conjugation (-HCl +GSH). Two of the major species detected (Figure 2.3) are the mono-*N*-dealkylation products: deisopropylated atrazine (DIA) and deethylated atrazine (DEA). The didealkylated metabolite of atrazine (diaminochlorotriazine or DACT) is considered a major metabolite *in vivo*. However, the non-quantitative nature of the LC-MS screening method coupled with DACT's early retention time, and therefore its susceptibility to matrix suppression and decreased organic content of the mobile phase during its elution, contribute to the relatively small signal obtained compared to the monodealkylated metabolites. This is in line with other *in vitro* studies that have not been able to detect DACT at all, presumably due to sample preparation and

chromatographic conditions. Also, three chromatographically distinct oxidation products were found and characterized by MS/MS (Figure 2.4). As reported by Joo *et al.*, (2010) two of these species correspond to adding an oxygen atom onto the ethyl side chain (hydroxy-ethyl atrazine, or HEA) and the isopropyl side chain (hydroxy-isopropyl atrazine, or HIA). The MS/MS data of the third oxidation product (see Discussion below) indicates that it is an *N*-oxidation of the *N*-ethyl group (*N*-hydroxy ATZ, or NHA). While hydroxylation of both aliphatic groups has been previously detected, this is the first report of atrazine *N*-hydroxylation.

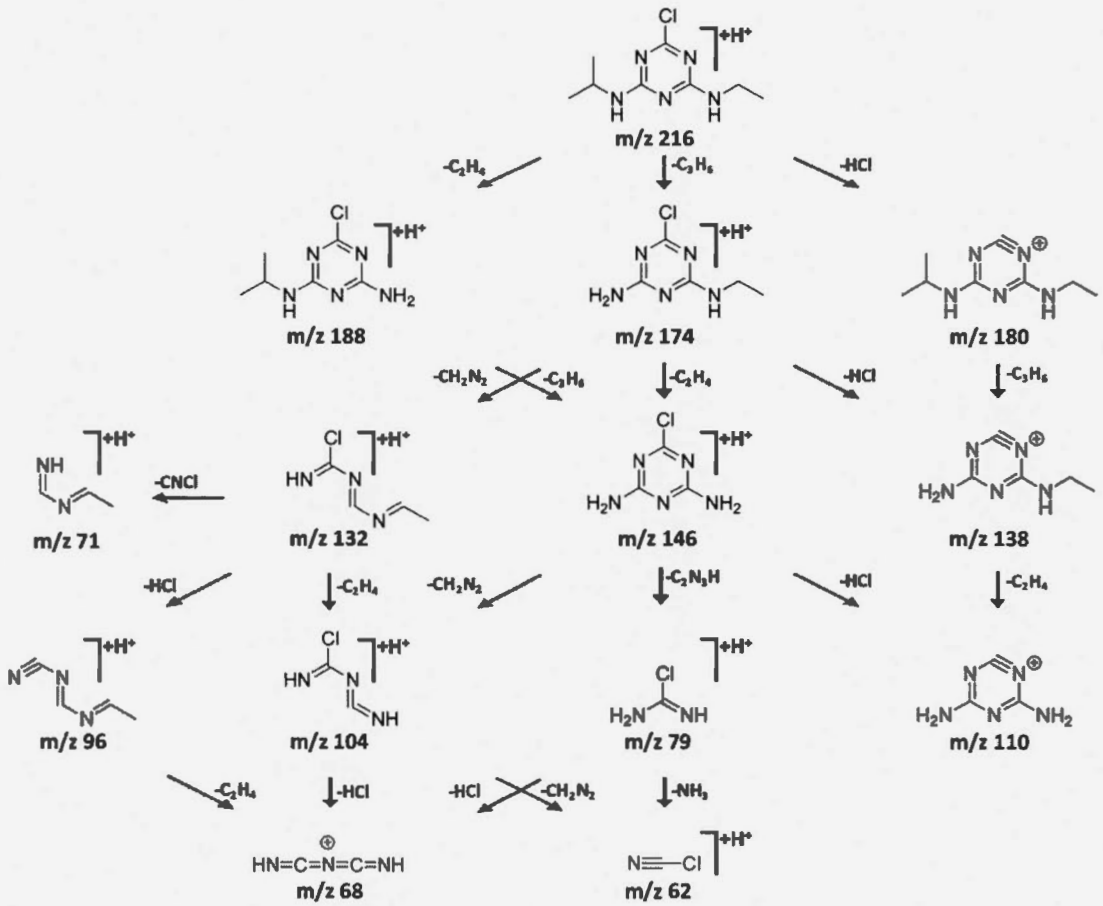

Figure 2.3. Proposed Fragmentation Scheme for Atrazine

Table 2.1. Summary of all MS/MS Data for Metabolites and GSH Conjugates of Atrazine and Analogues

	Metabolite // GSH Conjugate	Chemical Formula	Exact Mass (MH^+)	ppm	RT (min.)	MS/MS Fragments[b]	%[c]
Atrazine	DACT (-C_3H_6-C_2H_4)	$C_3H_4N_5Cl$	146.0228	5.5	2.2	110, 104, **79**, 68, 62,	< 0.1
	DIA (-C_3H_6)	$C_5H_8N_5Cl$	174.0541	2.3	8.5	146, 138, 132, 110, 104, 96, 79, 71, **68**	7.0
	DEA (-C_2H_4)	$C_6H_{10}N_5Cl$	188.0697	0.5	10.1	**146**, 110, 104, 79, 68, 62	17.7
	DHA (-2H)	$C_8H_{12}N_5Cl$	214.0854	-0.5	13.1	**172**, 136, 130, 105, 104, 94, 79, 69	2.7
	ATZ	$C_8H_{14}N_5Cl$	216.1010	1.4	12.7	**174**, 146, 138, 132, 104, 96, 79, 71, 68	87.7
	HDHA (-2H +O)	$C_8H_{12}N_5OCl$	230.0803	0.9	10.9	188, **146**, 110, 104, 79	0.1
	HIA (+O)	$C_8H_{14}N_5OCl$	232.0960	2.2	10.2	214, **174**, 146, 132, 104, 96, 79, 71, 68	1.9
	NHA (+O)	$C_8H_{14}N_5OCl$	232.0960	3.9	10.4	214, 190, 174, **172**, 136, 104, 94, 79	0.2
	HEA (+O)	$C_8H_{14}N_5OCl$	232.0960	1.3	10.8	214, 188, 172, **146**, 110, 104, 79, 68	7.1
	DEA +GSH -HCl	$C_{16}H_{26}N_8O_6S$	459.1769	1.5	5.3	313, 274, 256, 199, **186**, 153, 145, 130	0.1
	ATZ -HCl +GSH[a]	$C_{18}H_{30}N_8O_6S$	487.2082	3.1	9.2	358, 214, **199**, 145	0.5
	DHA +GSH	$C_{18}H_{29}N_8O_6SCl$	521.1692	2.3	9.7	**308**, 233, 214, 179, 162, 76	0.7
	HDHA +GSH	$C_{18}H_{29}N_8O_7SCl$	537.1641	0.7	8.8	**308**, 233, 230, 179, 162, 76	0.5
Simazine	DACT (-C_2H_4-C_2H_4)	$C_3H_4N_5Cl$	146.0228	4.8	2.1	110, 104, **79**, 68, 62	0.1
	DES (-C_2H_4)	$C_5H_8N_5Cl$	174.0541	1.7	8.5	146, 138, 132, 104, 96, 79, 71, **68**	21.2
	DHS (-2H)	$C_7H_{10}N_5Cl$	200.0697	0.5	12.3	172, 132, 130, 122, 104, **94**, 71, 69, 68	2.1
	SIM	$C_7H_{12}N_5Cl$	202.0854	0.5	11.7	174, 166, **132**, 124, 104, 96, 90, 71, 68	66.1
	NHS (+O)	$C_7H_{12}N_5OCl$	218.0803	-0.9	9.4	**200**, 172, 164, 140, 132, 122, 104, 96, 94	0.1
	HES (+O)	$C_7H_{12}N_5OCl$	218.0803	-0.9	9.8	200, **174**, 146, 138, 132, 104, 96, 79, 68	3.9
	DES -HCl +GSH	$C_{15}H_{24}N_8O_6S$	445.1612	1.1	2.2	316, 274, 199, **172**, 145	0.3
	SIM -HCl +GSH[a]	$C_{17}H_{28}N_8O_6S$	473.1925	2.3	8.6	344, **200**, 145	0.2
	DHS +GSH	$C_{17}H_{27}N_8O_6SCl$	507.1536	2.6	9.3	308, 291, 233, 200, **179**, 162, 76	0.5
	HDHS +GSH	$C_{17}H_{27}N_8O_7SCl$	523.1485	2.3	6.2	**308**, 291, 233, 216, 179, 162, 76	0.3
Propazine	DACT (-C_3H_6-C_3H_6)	$C_3H_4N_5Cl$	146.0228	10.3	2.2	110, 104, **79**, 68, 62	< 0.1
	DIP (-C_3H_6)	$C_6H_{10}N_5Cl$	188.0697	0.0	10.1	**146**, 110, 104, 79, 68	18.3
	Prop	$C_9H_{16}N_5Cl$	230.1167	1.7	13.6	188, **146**, 110, 104, 79, 68	83.4
	HIP (+O)	$C_9H_{16}N_5O$	246.1116	0.4	11.1	228, 204, 188, 186, **146**, 104, 79, 68	7.5
	DIP -HCl +GSH	$C_{16}H_{26}N_8O_6S$	459.1769	2.8	4.7	330, 199, **186**, 145	0.1
	Prop -HCl +GSH[a]	$C_{19}H_{32}N_8O_6S$	501.2238	1.2	9.8	372, **228**, 145	0.4
Cyanazine	DEC (-C_2H_4)	$C_7H_9N_6Cl$	213.0650	1.4	10.0	**186**, 177, 146, 145, 110, 104, 83, 79, 68	1.7
	DHC (-2H)	$C_9H_{11}N_6Cl$	239.0806	0.0	12.3	**212**, 176, 171, 134, 130, 119, 105, 94, 69	0.2
	Cya	$C_9H_{13}N_6Cl$	241.0963	1.7	11.9	**214**, 205, 174, 132, 104, 96, 71, 68	86.6
	DEC +O	$C_9H_{13}N_6OCl$	257.0912	3.5	10.3	230, 213, 212, **186**	0.1
	DEC -HCl +GSH	$C_{17}H_{25}N_9O_6S$	484.1721	1.4	8.0	355, 274, 256, 211, 204, **199**, 152, 145, 127	0.1
	Cya -HCl +GSH	$C_{19}H_{29}N_9O_6S$	512.2034	1.0	9.7	383, 274, 239, 212, 199, **180**, 145, 127	0.9
	DHC +GSH	$C_{19}H_{28}N_9O_6SCl$	546.1645	2.7	9.6	**308**, 239, 233, 179, 162, 76	0.1

[a] Represents compound with a peak area within 20% that of control incubation (no NADPH)

[b] Base peak fragment ions are shown in bold

[c] Percent peak area *vs.* parent in control incubation (relative quantitation using response factor of parent compound)

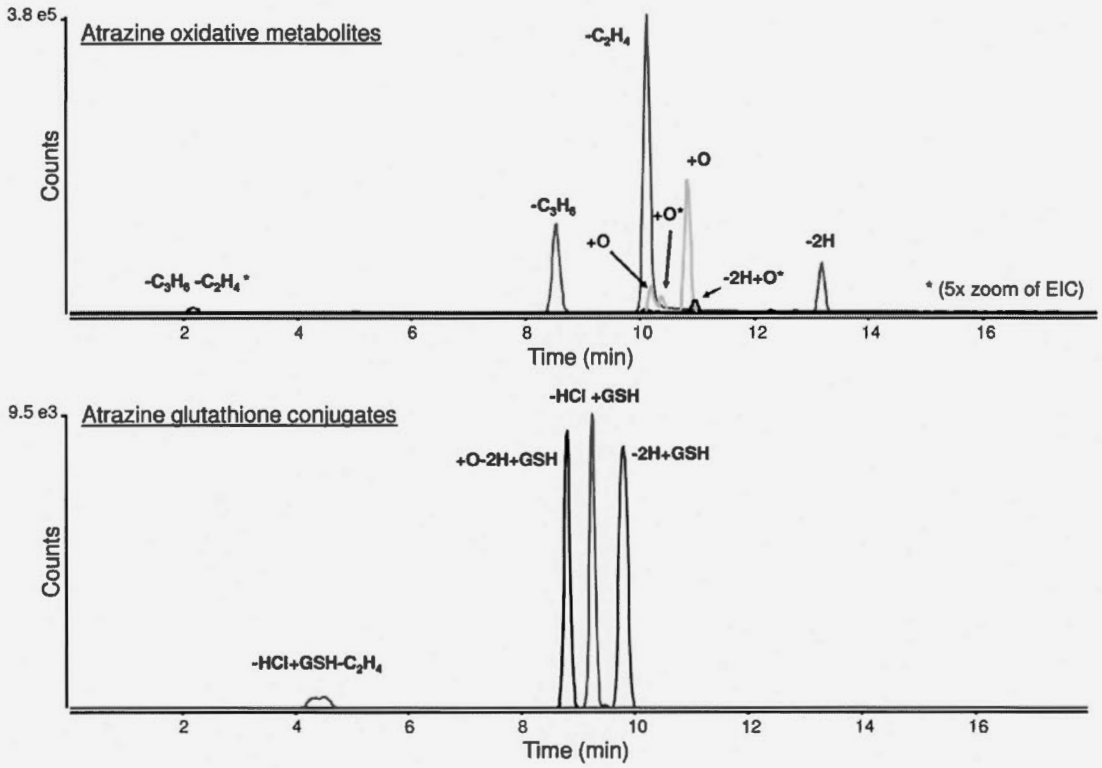

Figure 2.4. Overlaid extracted ion chromatograms (EICs) of oxidative metabolites (+NADPH) and GSH adducts (+NADPH+GSH) of atrazine from LC-TOF-MS analysis of atrazine (50 μM) incubated for 2 h with human liver microsomes. Peaks with * represent 5× zoom of EIC trace, in order to have all peaks detected on the same scale.

In addition to these previously known transformations, two novel metabolites involving a new transformation were also formed: ATZ-2H (dehydrogenated atrazine, DHA) and ATZ-2H+O (hydroxy-dehydrogenated atrazine, HDHA). This is the first report of an atrazine biotransformation of this type (-2H), and the MS/MS data (see Discussion below) supports our conclusion that the resulting double bond must occur on the *N*-ethyl group.

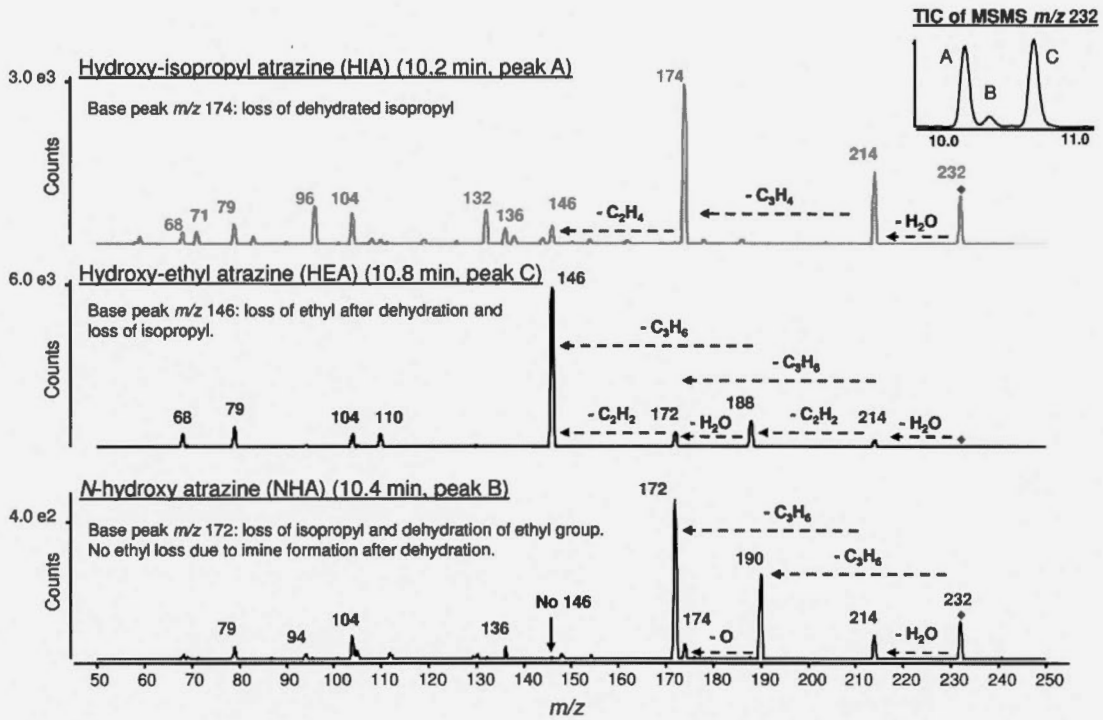

Figure 2.5. MS/MS spectra of the three hydroxylated atrazine (ATZ+O) metabolites from LC-QqQ analysis of atrazine HLM incubation. The TIC of the MS/MS for *m/z* 232 in the upper right corner shows three chromatographically distinct peaks (A, B, and C) each having different CID spectra.

Not only were these metabolites detected but also their corresponding glutathione conjugates (ATZ-2H+GSH and ATZ-2H+O+GSH) were found, not only confirming that these species are being formed but also implying their reactive nature. These GSH conjugates are the first reported for atrazine that are not the result of chlorine substitution by GSH.

Simazine:

The only structural difference between simazine and atrazine is the replacement of atrazine's isopropyl side chain by a second ethyl group. We should therefore see a very similar metabolism pattern for this compound, except for metabolites that are exclusively due to the presence of the isopropyl group. As expected, all the corresponding previously reported transformations for atrazine are also detected for simazine: *N*-dealkylation (-C2H4, forming DES), hydroxylation (+O), and glutathione adduction by chlorine substitution (-HCl+GSH). Additionally, dehydrogenated simazine (DHS or SIM-2H) with its corresponding glutathione conjugate (SIM-2H+GSH) confirms our initial observation from the atrazine screening that these newly detected species result from the biotransformation of the ethyl side chain. The detection and MS/MS data of the second, hydroxy-dehydrogenated glutathione conjugate (SIM+O-2H+GSH) confirms our observation for atrazine as well. There were also two distinct oxidation (SIM+O) metabolites detected. Since simazine contains two *N*-ethyl groups, they cannot be due to the oxygenation of two different alkyl groups. They are formed via the oxidation of the ethyl side chain and *N*-oxidation, as was also seen for atrazine. The proposed structures for the two +O metabolites of SIM are also supported by MS/MS data (Table 2.1). Both MS/MS spectra show characteristic peaks for simazine, with one corresponding to hydroxylation of the α-carbon while the other, less abundant species consistent with *N*-oxidation.

Propazine:

There is a noticeable reduction in the number of detected metabolites in the propazine incubations when compared to the atrazine and simazine incubations that is due to the absence of any dehydrogenated product. Since propazine contains two *N*-isopropyl groups and no ethyl side chain, this confirms the MS/MS data from the dehydrogenated (-2H) product of atrazine that the resulting double bond is formed on the *N*-ethyl group. The detected species in the propazine incubation mixture

correspond to the products of the other remaining transformations seen in the atrazine and simazine incubations: *N*-dealkylation (-C3H6), and hydroxylation (+O). The fact that we see a single +O metabolite (hydroxy-isopropyl propazine, HIP) for propazine helps confirm our proposed *N*-hydroxylation of the *N*-ethyl group of atrazine and simazine. In addition, the chlorine substituted GSH conjugate was also detected for propazine.

Cyanazine:

On the basis of the results from the other tested compounds, most of the predictable transformation products for cyanazine were detected. Since cyanazine contains an ethyl group, the dehydrogenated (-2H) metabolite with its corresponding glutathione adduct (-2H+GSH) is found, as well as the products of *N*-dealkylation (-C2H4), oxidation (+O), and chlorine-substituted glutathione adduction (-HCl+GSH).

2.5 DISCUSSION

2.5.1 *N*-OXIDATION PRODUCT

While hydroxylation of the ethyl and isopropyl groups has already been reported, a newly detected +O metabolite was found using our LC-TOF-MS screening method. The MS/MS data shown in Figure 2.4 compares the fragmentation patterns of the three +O metabolites of atrazine. The first thing we notice in the MS/MS data for NHA is the loss of the intact isopropyl group (-C3H6) from both the parent (*m/z* 232) and the dehydrated (-H2O) fragment (*m/z* 214), indicating that the isopropyl group has not been modified.

What is most interesting about the fragmentation pattern of NHA is the absence of a loss of the ethyl moiety. This can be explained by the effect that the loss of water has on subsequent fragmentation, as evidenced by the characteristic peak at *m/z* 214 seen in all three oxygenation products. The difference between dehydration of the hydroxy-alkyl metabolites (DEA and DIA) and the *N*-hydroxy product (NHA) is the location of the resulting double bond. The dehydration of hydroxy-alkyls results in terminal alkenes that facilitate subsequent *N*-dealkylation fragmentation. This is especially apparent in the fragmentation pattern of DEA where we see a facile loss of ethylene (-C2H2), in contrast to atrazine, which does not lose its ethyl group as favorably. However, dehydration of the *N*-oxidation product yields an imine that prevents fragmentation of the ethyl group altogether, explaining the lack of any de-ethylation or loss of ethylene. In addition, we see a minor loss of *m/z* 16 (-O) in the NHA MS/MS spectrum (from *m/z* 190 to *m/z* 174), a characteristic loss common to *N*-hydroxy species, which was not seen in any other atrazine related spectra.

As reported by Joo *et al.*, (2010) it is unlikely that the oxygen is added to the β-carbon of the ethyl group, since the *N*-ethyl α-carbon is the only known target of oxidative attack (Lang *et al.*, 1997). In any case, oxidation of the β-carbon could only yield a dehydration product containing a terminal ethene and would therefore yield MS/MS data similar to DEA.

This proposed structure for the *N*-oxidation product is further strengthened by the simazine data, where we see the formation of a similar *N*-hydroxy metabolite, also supported by analogous MS/MS data (Table 2.1).

Novel Reactive Metabolites and GSH Adducts

While the chlorine-substituted glutathione conjugates were previously reported, we thoroughly screened our data with the explicit intent to search for any novel reactive metabolites through GSH trapping *in vitro*. GSH trapping in microsomal incubations

is a commonly used assay to help identify potential reactive metabolites formed via Phase I oxidative metabolism (Ma & Subramanian, 2006). Electrophilic reactive metabolites have often been linked to toxicity via their ability to covalently bind to proteins (Uetrecht, 2007). Since differences in their chemical structures can cause varying toxicological effects, it is important to identify every possible reactive metabolite originating from a particular compound.

The novel dehydrogenated (-2H) metabolites found in our incubations were formed via the dehydrogenation of the *N*-ethyl groups. The MS/MS spectrum of DHA (Figure 2.5, top) shows the presence of a large fragment of *m/z* 172, corresponding to the loss of the intact isopropyl group. In addition, there is a systematic -2 *m/z* shift for all fragments retaining the ethyl group (see Scheme 2.1), indicating that the double bond must be on the ethyl group. The spectrum of DHA also reveals evidence as to the location of the added double bond. As with the *N*-oxidation product discussed above, the fragmentation of DHA does not yield any loss of the ethyl moiety. This indicates that the imine is being formed, as opposed to the ethene, since we know from the MS/MS data of the oxygenation products that the formation of the terminal alkene favors the loss of the ethene moiety.

The loss of two hydrogen atoms (-2H) is a common Phase I oxidative metabolism transformation for many xenobiotics, but was not previously observed for atrazine. In fact, there are no reports of a microsomal dehydrogenase acting on an analogous aliphatic group, suggesting that this transformation is not the result of direct enzymatic dehydrogenation. It is possible, however, that the dehydrogenation product is the result of the spontaneous dehydration of the newly reported *N*-hydroxy metabolite. This hypothesis combined with the MS/MS data and the fact that the dehydrogenated metabolite was only observed on the *N*-ethyl group leads us to conclude the formation of an imine reactive metabolite.

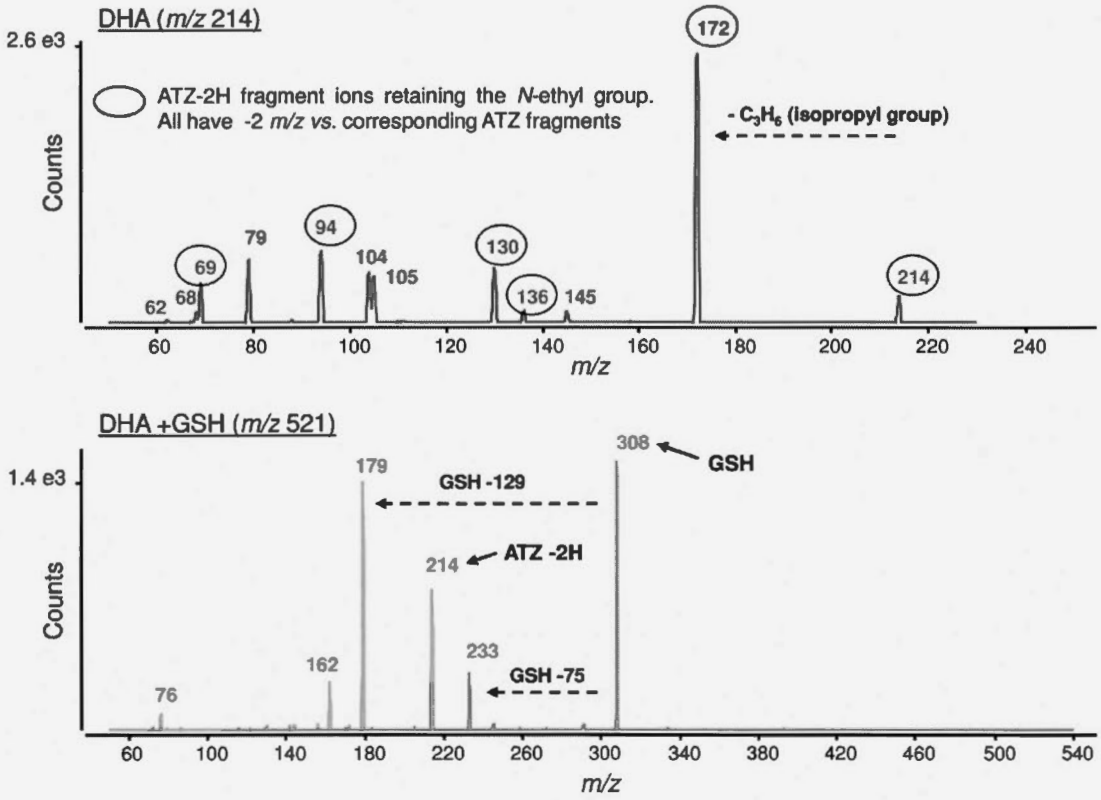

Figure 2.6. MS/MS spectra of dehydrogenated atrazine (DHA) reactive metabolite (above) and corresponding GSH conjugate (below).

The MS/MS spectrum of the corresponding glutathione conjugate, however, does not reveal the exact location of GSH addition due to its facile cleavage during CID, as evidenced by the base peak of *m/z* 308 corresponding to the mass of protonated glutathione. The remaining peaks are predominantly typical glutathione fragments (*m/z* 76, 162, 179, and 233), resulting from the losses of the glycine (-75) or γ-glutamic acid (-129 and -146), except for the large *m/z* 214 peak from dehydrogenated atrazine (Figure 2.5, bottom). Neutral loss scanning of 129 Da is often used to screen for GSH conjugates by tandem mass spectrometry (Ma & Subramanian, 2006; Baillie & Davis, 1993). However, in this case, no peak would have been seen using a neutral loss scan (NLS) of 129 Da from the intact ATZ-

2H+GSH conjugate due to the facile cleavage of the bond between ATZ-2H and GSH. The MS/MS data for all dehydrogenated glutathione adducts from atrazine, simazine, and cyanazine yield similar spectra dominated by GSH peaks. All these spectra include a large peak with a mass corresponding to the protonated intact dehydrogenated metabolite. While the MS/MS data for the GSH conjugates may not reveal the exact structures of these newly detected species, it does confirm their identity especially when combined with the high resolution data obtained from the initial screening. We consider dehydrogenated atrazine (DHA) along with the analogous simazine and cyanazine metabolites to be newly reported reactive metabolites. The imine double bond formed on the ethyl group can act as an electrophilic Michael acceptor capable of covalently binding to glutathione. In addition, these dehydrogenated reactive metabolites may be formed by the spontaneous dehydration of the newly reported *N*-oxidation products of triazines containing an *N*-ethyl group.

The MS/MS data from the hydroxylated dehydrogenated metabolite of atrazine (HDHA, or ATZ-2H+O) is consistent with the data obtained for DHA. The CID spectrum for HDHA is dominated by two peaks at *m/z* 188 and 146. These major fragments correspond to consecutive losses of *m/z* 42, the first being the loss of the intact isopropyl, indicating that dehydration as well as hydroxylation is occurring on the ethyl side chain. Unlike DHA, the imine formed in HDHA does not prevent the loss of the ethyl group for the fragment ion of *m/z* 146. This is due to the presence of the hydroxyl group. Hydroxylation of the imine carbon allows keto-enol type resonance and subsequently results in the facile loss of $COCH_2$ (*m/z* 42). The MS/MS data for the GSH conjugate of HDHA, similarly to the GSH conjugate of DHA, is dominated by glutathione fragments, with the exception of the peak at *m/z* 230, corresponding to intact HDHA.

2.5.2 GSH-ATZ AND OTHER CHLORINE SUBSTITUTIONS

Atrazine mercapturates, derived from the substitution of chlorine by glutathione, are commonly considered products of atrazine metabolism and have frequently been detected *in vivo* (Lucas *et al.,* 1993; Buchholz *et al.*, 1999; Ross & Filipov, 2006). In our set of incubations and controls, the substitution of chlorine by glutathione displays an interesting detection pattern. For all four compounds tested, the substitution product (-HCl+GSH) is observed in all samples that included glutathione, independent from metabolism. Figure 2.6 (top) shows that even without the presence of microsomes, GSH-ATZ is formed with a comparable intensity to the 2 h incubation sample as well as the control without the addition of NADPH. This is strong evidence that the chlorine substitution with glutathione is formed nonenzymatically under these incubation conditions. The nonenzymatic formation of this GSH conjugate has previously been discussed (Ross *et al.,* 2009; Abel *et al.,* 2004). Current techniques used for metabolite identification typically rely on a direct comparison with a control sample, and therefore this species would not be identified as a metabolite using our untargeted screening method, in contrast to the newly reported GSH conjugates, which are entirely reliant on metabolism for their formation (Figure 2.6, bottom). This data shows that in our incubation system, there is no significant enzymatic contribution to the formation of GSH-ATZ. This observation is consistent with the study conducted by Abel *et al.*, (2004) where it was concluded that the only GST isozyme (pi class GST) found to have any significant activity toward atrazine is not normally present in human liver. The authors pertinently mention, however, that this GST isozyme is very present in skin and lung tissues and may play an important part in the metabolism of atrazine, especially among agricultural workers, the population most exposed to atrazine.

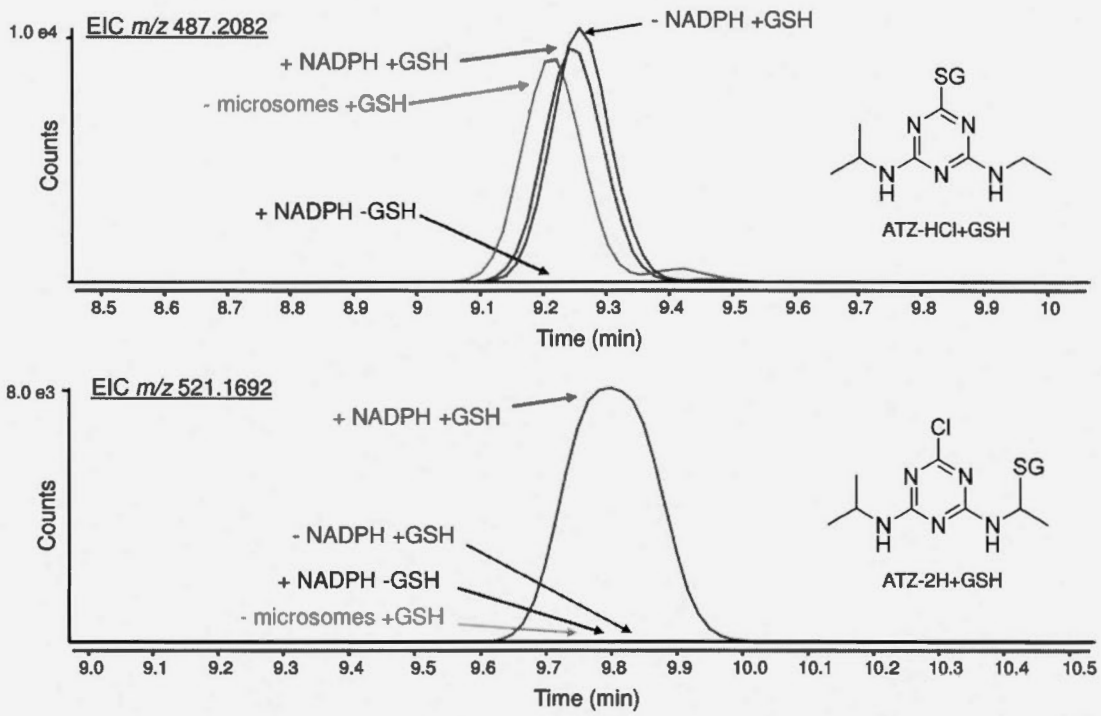

Figure 2.7. Overlaid EICs for atrazine glutathione-chlorine substitution product (ATZ-HCl+GSH) and the GSH conjugate from dehydrogenated atrazine (ATZ-2H+GSH) in control and metabolism samples incubated for 2 h.

Another Cl substitution product of atrazine, hydroxy-atrazine (OH-ATZ), was first identified as an important atrazine metabolite by Bakke (1972) and has since often been considered as a metabolite; however, subsequent metabolism studies have frequently been unable to detect it.(Adams *et al.,* 1990; Lang *et al.,* 1990; Lucas *et al.,* 1993) The study conducted by Joo *et al.*(20) was the first to note that OH-ATZ was not produced enzymatically, concluding that it was formed through a sample enrichment step. Our screening method, which does not include any sample enrichment, has identified OH-ATZ in the incubation mixture and with similar intensities in all samples and controls.

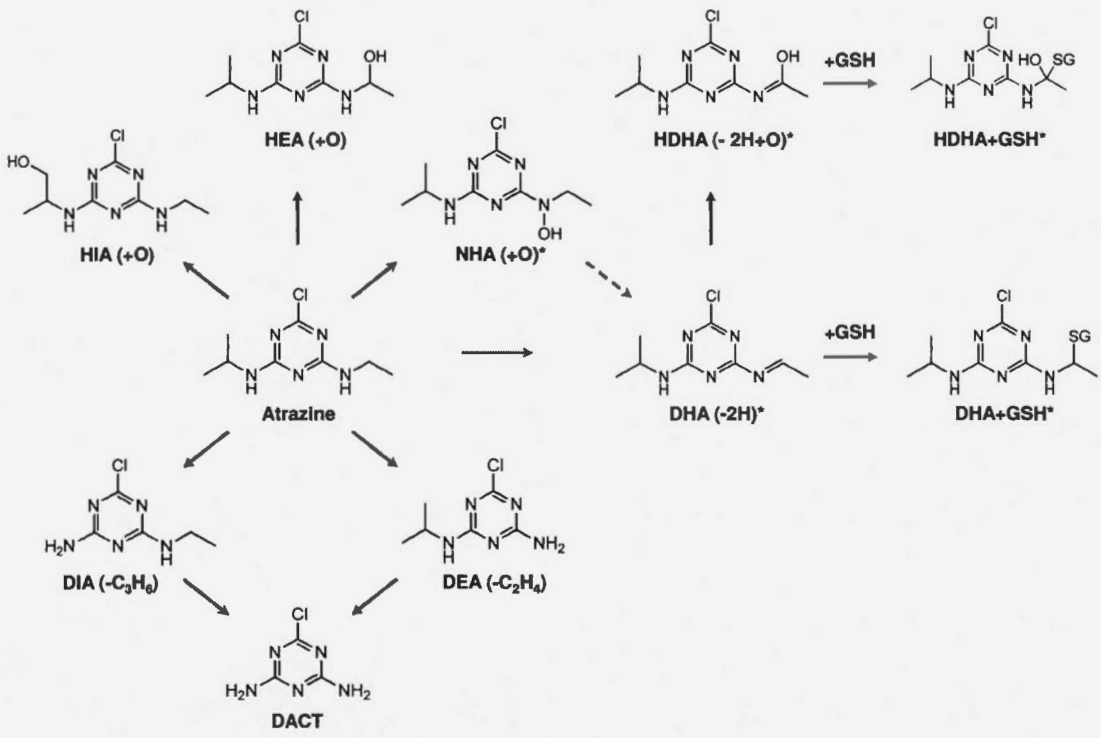

Figure 2.8. Classification of atrazine transformations detected in this study (novel oxidative metabolites and glutathione conjugates are noted by * and dotted line indicates the proposed pathway for the formation of the imine-containing reactive metabolites (DHA and HDHA) via the *N*-hydroxy atrazine).

The presence of OH-ATZ in all controls clearly shows that it does not depend on metabolism for its formation, especially considering it is also detected when analyzing the stock solution used for incubation (Table 2.2). Similarly, hydroxy-simazine (OH-SIM) and hydroxy-propazine (OH-PROP) are also detected in all samples and controls, as well as in the simazine and propazine stocks, respectively. Hydroxy-cyanazine (OH-CYA), however, is not detected in any of the samples or controls and is absent in the cyanazine stock. This data strongly suggest that the hydroxy substitution of chlorine in the S-chloro-triazine ring is not a product of

metabolism. Since a previous study described "OMe-ATZ" (Atraton) as a novel atrazine metabolite (Li *et al.,* 2006), this species was also screened for and was, similarly to OH-ATZ, detected in all samples, controls, and stocks (data not shown). We therefore do not consider this species to be metabolism-dependent, but to originate from atrazine stock impurities as well.

Table 2.2. Chlorine Substitution Product (-HCl + H2O) in Analytical Stocks

Compound	% peak area relative to parent
ATZ	3.5
SIM	0.9
PROP	< 0.1
CYA	Not detected

2.5.3 GENERAL CONSIDERATIONS FOR UNTARGETED METABOLIC SCREENING METHODS

Using a generic HPLC separation in combination with untargeted high resolution mass spectrometric detection allows for a broadly applicable method relevant for metabolite screening of a wide range of xenobiotics. This approach is adaptable to many different experiments, such as other types of incubations (cytosolic or S9) *or in vivo* samples from biological matrices. As well, it can be used in combination with various purification or sample enrichment methods such as solid phase extractions. The HPLC method can equally be altered in terms of gradient elution or column type to obtain complementary data if required based on the chemical properties of the compound of interest.

It is important to stress that the TOF-MS enables us to collect data with high sensitivity and without leaving out any potential metabolic species. Other notable advantages of using this approach include the accessibility and ease of use of the TOF instrument, minimal time spent on method development, and straightforward data mining. Of course, the weakness of this type of post-acquisition screening is its reliance on the prediction of all species present in the sample. There are MS software packages available that can help predict metabolism products based on all known biotransformations which can speed up listing potential metabolic species and reduce the chance of omitting a particular biotransformation. Newer mass spectrometers may also feature data-dependent acquisition and automatic background subtraction that can be very helpful in identifying metabolism products. Some of these newer instruments, based on quadrupole-time-of-flight and LTQ-orbitrap hybrid platforms, have the capability to collect high resolution full scan data and perform MS/MS experiments of all potential metabolism products in the same chromatographic run. These instruments, however, are not always accessible and require much more expertise than a simple ESI-TOF-MS.

With any mass spectrometric method, quantitation is only possible by comparison with a standard for each individual species. This is usually not feasible for the majority of metabolism studies. Semi-quantitative data can be extracted, for example, by comparing the integration of the peaks from each metabolite species to the area of the parent compound (as in Table 2.1). The accuracy of this data, however, relies on the assumption that the response factor for each metabolism product is comparable to the response factor of the parent compound. Because of ion suppression caused by matrix effects or coelution, mobile phase composition, detector dynamic range, and changes in the structure during metabolism, response factors will inevitably vary between each species; thus, all semiquantitative data of this type must only be viewed as a general indication of relative abundance.

The full set of controls used in this study was very useful in determining whether a species was dependent on the presence of microsomes, NADPH, and/or glutathione, however this type of data is rarely shown in metabolism studies. Depending on the type of experiment or incubation performed, there is biologically relevant information potentially available when performing a full set of controls, as demonstrated in this study. At the very least, detected species cannot be considered metabolites if they are not detected with a significantly larger response than in controls without enzymes or appropriate cofactors for the metabolic pathway of interest.

2.6 CONCLUSIONS

By thoroughly mining data produced by *in vitro* microsomal incubations while including appropriate control samples, we have been able to detect novel reactive metabolites along with their corresponding glutathione adducts and redefine the metabolism of atrazine (Figure 2.7) and other S-chloro-triazine pesticides containing an *N*-ethyl group. It therefore remains important that all of the novel metabolites and conjugates described here be further studied to understand their potential relevance to toxicity.

All known transformations of atrazine were detected with a single untargeted experiment using an LC-TOF-MS method that is applicable to a broad range of compounds. There are many other compounds with previously characterized metabolic pathways that have been studied using older methods that could benefit from this kind of unbiased screening approach. The use of generic acquisition and separation methods relying only on post-acquisition processing for compound-specific screening is an accessible way to verify the presence of all potential

transformations relevant to metabolism studies or even biological and environmental monitoring studies.

CHAPITRE III

ARTICLE SCIENTIFIQUE: "IMPROVED DETECTION OF REACTIVE METABOLITES WITH A BROMINE-CONTAINING GLUTATHIONE ANALOG USING MASS DEFECT AND ISOTOPE PATTERN MATCHING"

André LeBlanc, Tze Chieh Shiao, René Roy and Lekha Sleno*

*Université du Québec à Montréal, Pharmaqam, Chemistry Department, P.O. Box 8888, Downtown Station, Montréal, Québec, Canada H3C 3P8

Article published in:

Rapid Communications in Mass Spectrometry 2010, 24, 1241-1250.

Received: January 7, 2010

Accepted: February 16, 2010

Cet article présente une nouvelle stratégie conçue pour effectuer le dépistage des adduits formés par les métabolites réactifs lors d'incubations microsomales *in vitro*. Cette stratégie utilise un nouvel agent de piégeage, analogue au glutathion, et la spectrométrie de masse à haute résolution. Le patron isotopique et le défaut de masse uniques de notre nouvel agent de piégeage, surnommé « GSHBr », sont exploités lors du traitement de données. En utilisant notre méthodologie, nous démontrons que notre agent de piégeage augmente l'efficacité du dépistage versus le glutathion.

Sous la supervision de la professeure Lekha Sleno, je fus responsable de toutes les manipulations, expérimentations et analyses de données. Tze Chieh Shiao, grâce à la collaboration avec le laboratoire du professeur René Roy, a effectué la synthèse de la molécule « GSHBr ».

3.1 ABSTRACT

Drug bioactivation leading to the formation of reactive species capable of covalent binding to proteins represents an important cause of drug-induced toxicity. Reactive metabolite detection using *in vitro* microsomal incubations is a crucial step in assessing potential toxicity of pharmaceutical compounds. The most common method for screening the formation of these unstable, electrophilic species is by trapping them with glutathione (GSH) followed by liquid chromatography/mass spectrometry (LC/MS) analysis. The present work describes the use of a brominated analog of glutathione, *N*-(2-bromocarbobenzyloxy)-GSH (GSH-Br), for the *in vitro* screening of reactive metabolites by LC/MS. This novel trapping agent was tested with four drug compounds known to form reactive metabolites, acetaminophen, fipexide, trimethoprim and clozapine. *In vitro* rat microsomal incubations were performed with GSH and GSH-Br for each drug with subsequent analysis by liquid chromatography/high-resolution mass spectrometry on an electrospray time-of-flight (ESI-TOF) instrument. A generic LC/MS method was used for data acquisition, followed by drug-specific processing of accurate mass data based on mass defect filtering and isotope pattern matching. GSH and GSH-Br incubations were compared to control samples using differential analysis (Mass Profiler) software to identify adducts formed via the formation of reactive metabolites. In all four cases, GSH-Br yielded improved results, with a decreased false positive rate, increased sensitivity and new adducts being identified in contrast to GSH alone. The combination of using this novel trapping agent with powerful processing routines for filtering accurate mass data and differential analysis represents a very reliable method for the identification of reactive metabolites formed in microsomal incubations.

3.2 INTRODUCTION

The metabolism of xenobiotics most often catalyzes the formation of polar and, thus, readily excretable metabolites for the rapid elimination of drugs or other environmentally derived compounds. Certain molecules, however, can be bioactivated into reactive electrophilic metabolites, causing the formation of potentially toxic species capable of binding covalently to glutathione (GSH), proteins and DNA in the body (Zhang *et al.,* 2005). GSH acts as a natural scavenger to these electrophilic species due to its antioxidant activity and its ability to react with them quickly before more permanent damage can be done to cellular proteins or DNA. These GSH conjugates are then transported for direct biliary excretion (Zamek-Gliszczynski *et al.,* 2006) or further biotransformed to more polar mercapturic acid adducts for urinary excretion (Hinchman & Ballatori, 1994). Since reactive drug metabolites have often been linked to drug toxicity, (Zhang *et al.,* 2005; Uetrecht, 2007), it remains of utmost importance to screen for the formation of these species early on in drug discovery, in order to limit the potential for metabolism-induced side effects of new chemical entities (Evans *et al.,* 2004). The most common procedure for the rapid screening of reactive metabolite formation is to perform *in vitro* microsomal incubations in the presence of GSH, followed by liquid chromatography/mass spectrometry (LC/MS) analysis (Ma & Subramanian, 2006; Ma & Zhu, 2009). Several strategies have been reported for the detection of GSH conjugates using mass spectrometric detection and specialized data processing procedures. In comparing control (-GSH) incubations with those in the presence of the trapping agent, we can selectively screen for GSH adducts. A common method employs neutral loss scanning (NLS) of 129 Da, corresponding to the loss of the pyroglutamic acid moiety of GSH, in positive ion mode on a triple quadrupole instrument (Baillie & Davis, 1993). A precursor ion scan of *m/z* 272, resulting from the loss of H2S from the deprotonated GSH ion, in negative ion mode is often used in conjunction with the

NLS method on the same instrument (Dieckhaus *et al.,* 2005; Wen *et al.,* 2008). However, scanning techniques relying on specific fragmentation patterns of molecules in a triple quadrupole instrument are inherently less sensitive than acquisition of time-of-flight spectra, which has the added feature of accurate mass measurement capabilities for elemental formula confirmation. Furthermore, the neutral loss technique does not yield corresponding signals for all GSH adducts. For instance, benzylic thio-ether adducts are not detected by the NLS procedure (Dieckhaus *et al.,* 2005). False positives or limited sensitivity can be an issue with these screening strategies, since only the fragmentation of the GSH portion is used without consideration of the drug's fragmentation pathways. Alternatively, by using high-resolution mass spectrometers capable of providing accurate mass data for compounds present in the *in vitro* incubations, we can more easily screen for GSH adducts of specific drugs. With accurate mass data, mass defect filtering (MDF) can be performed, which takes into account the specific mass defect of the drug being tested. This filtering technique has been applied to the specific detection of drug metabolites (Zhang *et al.,* 2009) and glutathione adducts (Zhu *et al.,* 2007). MDF processing methods are usually performed on data obtained by high-resolution time-of-flight (TOF) and orbitrap mass spectrometers. Both these types of instruments are readily applicable to routine LC/MS acquisition of high-resolution data for small molecules. A generic MS method can be used for all drugs to be screened, followed by drug-specific post-acquisition processing techniques for identifying GSH adducts of interest. Yet another filtering technique which can be applied to the detection of reactive drug metabolites is based on specific isotope patterns. If, for instance, the drug molecule being screened contains a chlorine atom, with its unique M/M+2 isotope ratio of 1:0.35, it then has a different isotope pattern than most other molecules present in the incubation mixture. Most commercially available MS-based processing software should have the ability to easily filter out any ions not having a specific isotope pattern, and thus subtracting most of the background ions out of the total ion chromatogram (TIC). Some methods have been described for increasing the

selectivity of isotope pattern filtering by using a specific ratio of GSH with an isotopically labeled version of the trapping agent (Lim *et al.,* 2008; Rousu *et al.,* 2009; Yan *et al.,* 2005). All reactive metabolites will then form adducts with a unique isotope label for filtering purposes, no matter if the drug has a unique pattern or not. This technique works quite well; however, isotopically labeled GSH is very expensive, raising the cost of these screening assays considerably. Other research groups have reported the use of GSH analogs for screening reactive metabolites. Examples include a dansylated derivative (Gan *et al.,* 2005), yielding semi-quantifiable results if fluorescence is employed online with MS detection, as well as GSH containing a quaternary ammonium (Soglia *et al.,* 2006) or an ethyl ester moiety (Soglia *et al.,* 2004). Here, we have designed a novel bromine-containing GSH derivative (GSH-Br) specifically for the purpose of screening reactive drug metabolites by high-resolution TOF-MS. The choice of modification of GSH in the design of the new trapping agent was made with several features in mind: (1) the addition of a bromine for unique isotope pattern filtering and mass defect modification; (2) the introduction of an aromatic ring for bromine stability and increased hydrophobicity of adducts, hence improved chromatography; and (3) reaction on the free amine group via amide coupling for ease of synthesis without steric hindrance with the free thiol group. This new strategy has combined the advantages of several of the above-mentioned techniques, including specific isotope pattern and mass defect filtering as well as increased sensitivity and improved chromatographic behavior compared to regular glutathione. To present the usefulness of our novel screening method, we have compared the ability of detecting GSH adducts vs. GSH-Br adducts in *in vitro* microsomal incubations with four drugs known to form reactive metabolites, namely, acetaminophen, fipexide, trimethoprim and clozapine. The analytical approach presented here employs a generic LC/MS acquisition method, using electrospray ionization time-of-flight (ESI-TOF) instrumentation, followed by drug-specific processing routines for detecting GSH (and GSH-Br) adducts in a routine manner.

3.3 EXPERIMENTAL

3.3.1 MATERIALS

Fipexide hydrochloride, acetaminophen, trimethoprim, clozapine, β-nicotinamide adenine dinucleotide 2′-phosphate reduced tetrasodium salt (β-NADPH), reduced L-glutathione (GSH), oxidized glutathione (GSSG), sodium carbonate, formic acid (ultra-pure) and dithiothreitol (DTT) were obtained from Sigma-Aldrich (Oakville, ON, Canada). Potassium phosphate (monobasic) and potassium hydroxide were supplied by Riedel-de Haën (Seelze, Germany). *N*-(2-Bromobenzyloxycarbonyloxy)succinimide was purchased from Alfa Aesar (Ward Hill, MA, USA). Rat liver microsomes were purchased from BD Biosciences (Mississauga, ON, Canada). Acetone, ethyl acetate (EtOAc), HPLC grade acetonitrile (ACN) and methanol were obtained from Fisher Scientific (Ottawa, ON, Canada) and ultrapure water was supplied by a Barnstead NANOpure Diamond UV ultrapure water system from Thermo Scientific (Mississauga, ON, Canada).

3.3.2 SYNTHESIS OF GSH-BR

A solution of *N*-(2-bromobenzyloxycarbonyloxy)succinimide (*N*-(2-bromo-CBZ)-succinimide) (62 mg; 0.185 mmol, 2.50 equiv) in acetone (750 µL) was added dropwise to a solution of oxidized glutathione (GSSG) (45.5 mg; 0.074 mmol, 1.00 equiv) in a saturated solution of NaHCO3 (500 µL). The reaction mixture was stirred at room temperature for 40 min. A solution of DTT (47 mg, 0.37 mmol, 5.0 equiv) in 1 M Na2CO3 (500 µL) was then added. After 1 h, a solution of 2 M NaOH (100 µL) was added into the mixture to keep the pH at 10 and stirred for a further 15 min. The reaction was quenched by adding EtOAc and the aqueous layer was washed again

with EtOAc. The aqueous layer was acidified with a solution of 5 M HCl to pH 2–3 and extracted twice with EtOAc. The organic layer were dried over anhydrous Na2SO4, filtered and concentrated under vacuum to afford GSH-Br as a white solid (70 mg, 0.135 mmol, 91%).

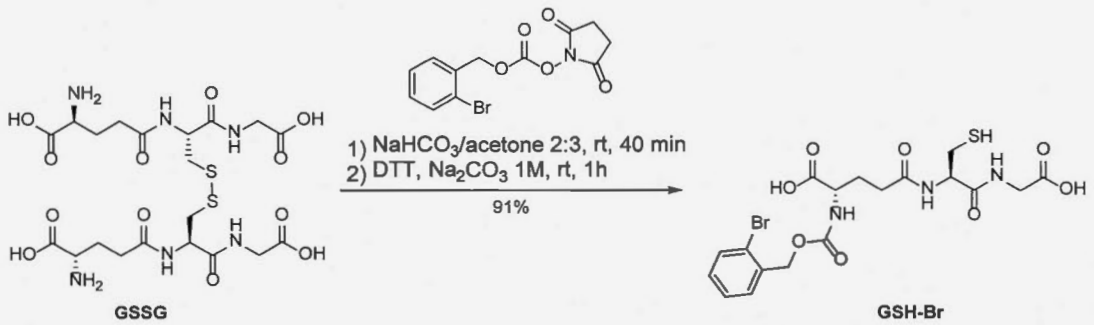

Figure 3.1. Synthesis of GSH-Br.

For characterization of the synthesized compound, NMR spectra were recorded for solutions in DMSO-d6 with a Varian Innova AS600 600 MHz spectrometer. Proton and carbon chemical shifts (δ) are reported in ppm downfield with internal reference of residual solvents (Gottlieb *et al.,* 1997). Coupling constants (J) are reported in Hertz (Hz), and the following abbreviations are used for signal multiplicities: singlet (s), doublet (d), triplet (t), multiplet (m). Analysis and assignments were made using COSY, DEPT, and HETCOR experiments. 1H NMR (600 MHz, DMSO-d6, 20°C): δ = 8.06–7.69 (m, 7H, H-ar and NH), 5.60 (s, 2H, PhCH2O), 5.08 (t, 1H, 3JH,H = 5.8Hz, CHCH2SH), 4.77–4.73 (m, 1H, HO2CCHNH), 4.40 (d, 2H, 3JH,NH = 4.4Hz, NHCH2CO2H), 3.34 (t, 1H, 3JSH,CH2 = 7.8 Hz, SH), 2.99–2.67 (m, 2H, CH2SH), 2.50–2.48 ppm (m, 4H 2 × CH2); 13C NMR (150 MHz, DMSO-d6): δ = 173.4, 172.6, 171.0, 170.8 (CO), 156.6 (NHCOO), 137.0 (Cq-arom), 133.2, 130.2, 130.0, 128.4 (Carom), 122.9 (Carom-Br), 66.0 (PhCH2O), 55.5 (CHCH2SH),

54.0 (CHNHCO2CH2Ph), 41.1 (CH2CO2H), 32.3 (NHCHCH2CH2), 27.9 (CH2SH), 26.7 (NHCHCH2CH2) ppm. High-resolution mass spectrometry (HRMS) data was acquired on an Agilent 6210 ESI-TOF instrument (see below for source conditions). In positive ESI mode, the protonated molecule [M+H]+ was measured as *m/z* 520.0390 (1.2 ppm, C18H22N3O8SBr).

3.3.3 *IN VITRO* INCUBATIONS

Rat liver microsomal incubations (1 mg/mL protein) were performed with 50 µM drug (acetaminophen, fipexide, trimethoprim or clozapine), 1 mM NADPH (absent in controls) and 1 mM GSH (or GSH-Br) for 2 h at 37°C in a phosphate-buffered solution (50 mM, pH 7.4) and a total volume of 250 µL. Samples were then quenched with an equal volume of ice-cold ACN and centrifuged at 13000 rpm for 10 min. Supernatant was evaporated to dryness using a model RC10.10 centrifuge concentrator (Jouan, Winchester, VA, USA) and reconstituted in 250 µL of 20% ACN prior to injection onto the LC/MS system

3.3.4 LC/MS ANALYSIS

All samples (10 µL injections) were separated on an Thermo BetaBasic-C18 column (2.1 × 150 mm, 5 um particles) on an Agilent 1200 HPLC system (including binary pump, in-line degasser, high performance autosampler, and thermostated column compartment) using the following gradient: initial conditions of 10% B with a 1 min hold, up to 100% B at 9 min and held for 5 min before re-equilibration, where mobile phases A and B were water and methanol (both containing 0.1% formic acid), respectively, at a flow rate of 0.25 mL/min and a column temperature of 35°C.

Mass spectrometric analysis was performed on an Agilent 6210 ESI-TOF instrument (Agilent Technologies, Mississauga, ON, Canada) in positive ESI mode using MassHunter acquisition software (version B.02.00). The dual ESI source was operated with a capillary voltage of 4000 V and gas temperature and flow of 350°C and 11.5 L/min (ultra-pure nitrogen), respectively. The nebulizer pressure was maintained at 35 psi and the fragmentor and skimmer voltages were 100 and 60 V, respectively. Data were acquired from *m/z* 100–1300 with internal calibration using the reference masses *m/z* 121.050873 and 922.009798 in the Agilent reference mass solution (reference #G1969-85001), sprayed continuously through the reference electrospray needle.

All raw TOF data was processed by molecular feature extraction (MFE) in MassHunter Qualitative Analysis software for compounds eluting in the retention time range of 2.5–17 min, using ions from *m/z* 200–1000, with a signal threshold of 100 counts (height). This processing step created MHD files, containing compound IDs (based on neutral mass and retention times) which were then amenable to further filtering and comparison of metabolism samples. Mass Profiler software (version B.02.00, Agilent Technologies) was then employed to compare incubations and filter the TOF data based on isotope patterns and mass defects of the formed GSH adducts. The Mass Profiler method was customized for each drug, based on the simple combination of each drug with GSH (or GSH-Br). The following filtering criteria were used:

- Neutral mass range: +50 and −150 Da from mass of (drug+GSH-2H) or (drug+(GSH-Br)-2H)
- Isotope filtering was based on the calculated theoretical isotope pattern of the (drug+GSH-2H) or (drug+(GSH-Br)-2H) adduct. We filtered based on all isotope peaks having a threshold of at least 25% intensity of the monoisotopic

peak, with an allowed error of ±15%. Therefore, any isotope peak (M+1, M+2, etc.) would be included in the filter if it was calculated as at least 25% of the height of the monoisotopic (M) peak.

- Mass defect filtering was performed based on the theoretical mass defect for drug+GSH-2H (or drug+(GSH-Br)-2H) ±40 mDa, allowing for all common phase I metabolic reactions (see Table 3.1).

3.4 RESULTS AND DISCUSSION

Each of the test compounds presented below was incubated separately with both trapping agents (GSH and GSH-Br) and compared to a control sample without glutathione. Each raw data file was processed with identical MFE parameters; however, Mass Profiler filtering methods were customized for each drug/trapping agent combination. The structures of GSH and GSH-Br are presented in Fig. 1, along with their theoretical isotopic patterns. A characteristic doublet is present for the M/M+2 peaks (where M is the monoisotopic peak) in GSH-Br due to the unique natural isotopic abundances of ^{79}Br and ^{81}Br. The four different drugs chosen for this study were acetaminophen, fipexide, trimethoprim and clozapine, all of which are known to form reactive metabolites with previously characterized GSH adducts. Figure 3.2 shows the structures of each of the test compounds. In our comparison between the two trapping agents, we chose to use a generic LC/MS method which could be used for all drugs. Screening of adducts was then based on accurate mass data, with stringent mass defect filtering, and isotope pattern matching. Table 3.2 presents a comprehensive summary of the unique molecular features found by the Mass Profiler software in both GSH and GSH-Br incubations for all four drugs, along with references for previous reports of each of the detected adducts.

Table 3.1. List of changes in mass defects caused by common phase I biotransformations

Phase 1 Biotransformation	Modification	Change in mass (Da)	Change in mass defect (mDa)	Change from -2H (mDa)
Reduction	+2H	+2,01565	+15.6	+31.3
De-hydrogenation	-2H	-2,01565	-15.6	0.0
Hydroxylation	+O	+15,99491	-5.1	+10.6
Di-oxidation	+2O	+31,98983	-10.2	+5.5
Quinone formation *or* CH_3 to COOH	+2O-2H	+29,97418	-25.8	-10.2
De-methylation	-CH2	-14,01565	-15.6	0.0
De-ethylation	-CH2CH2	-28,03130	-31.3	-15.6
Oxidative deamination	-NH-2H+O	-1,03163	-31.6	-16
Decarboxylation	-CO2	-43,98983	+10.2	+25.8

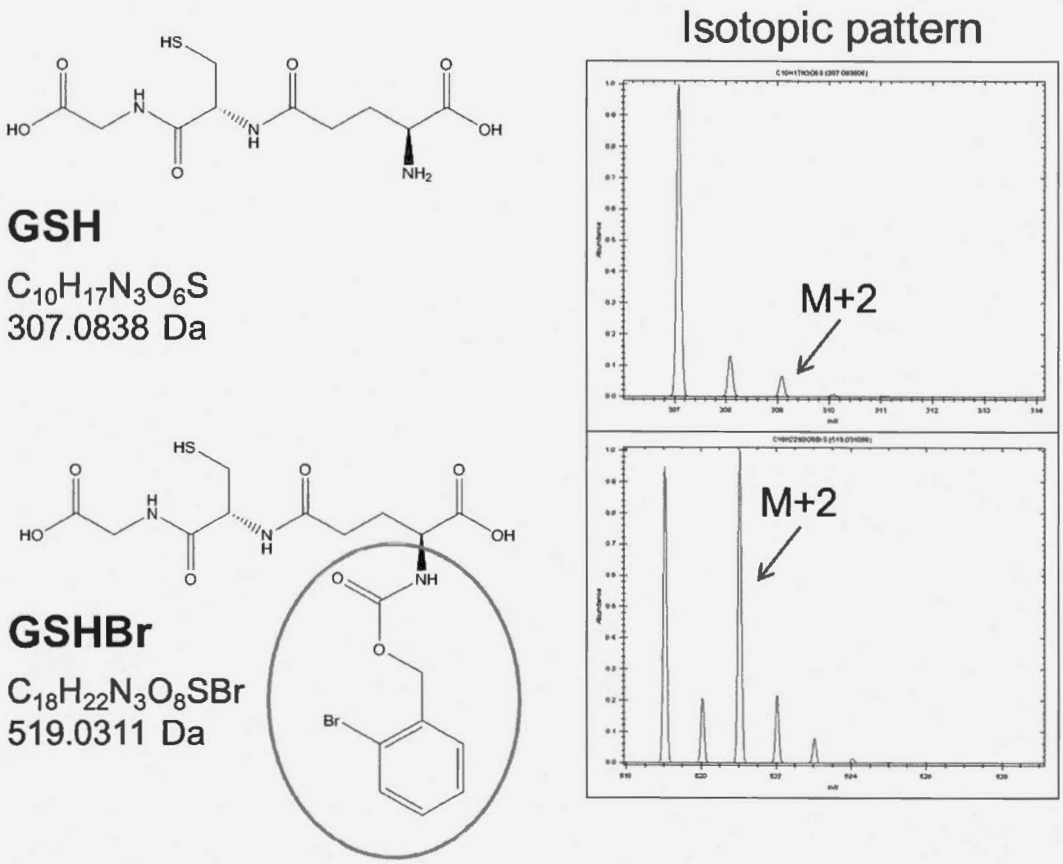

Figure 3.2. Structures of glutathione (GSH) and the brominated analog of glutathione (GSH-Br) used in this study, along with their isotopic patterns.

3.4.1 ACETAMINOPHEN

Acetaminophen (APAP) was the first drug used to test our newly developed GSH-Br analog for screening reactive drug metabolites by LC/MS. This model hepatotoxin is known as such since, at very high doses, the detoxifying phase II metabolic pathways of sulfation and glucuronidation become saturated, resulting in an increased amount of acetaminophen being oxidized to form the reactive *N*-acetyl-p-benzoquinoneimine

(NAPQI) (Bessems *et al.,* 2001; Prescott, 2000). The toxic NAPQI is often conjugated with glutathione, however, when cellular GSH pools are depleted, the remaining reactive NAPQI is free to covalently bind to liver proteins (Bartolone *et al.,* 1987; Potter *et al.,* 1974). Many cellular proteins have been reported to react with NAPQI, resulting in altered protein structure and function (Bessems *et al.,* 2001; Bartolone *et al.,* 1987; Cohen & Khairallah, 1997; Pumford *et al.,* 1990).

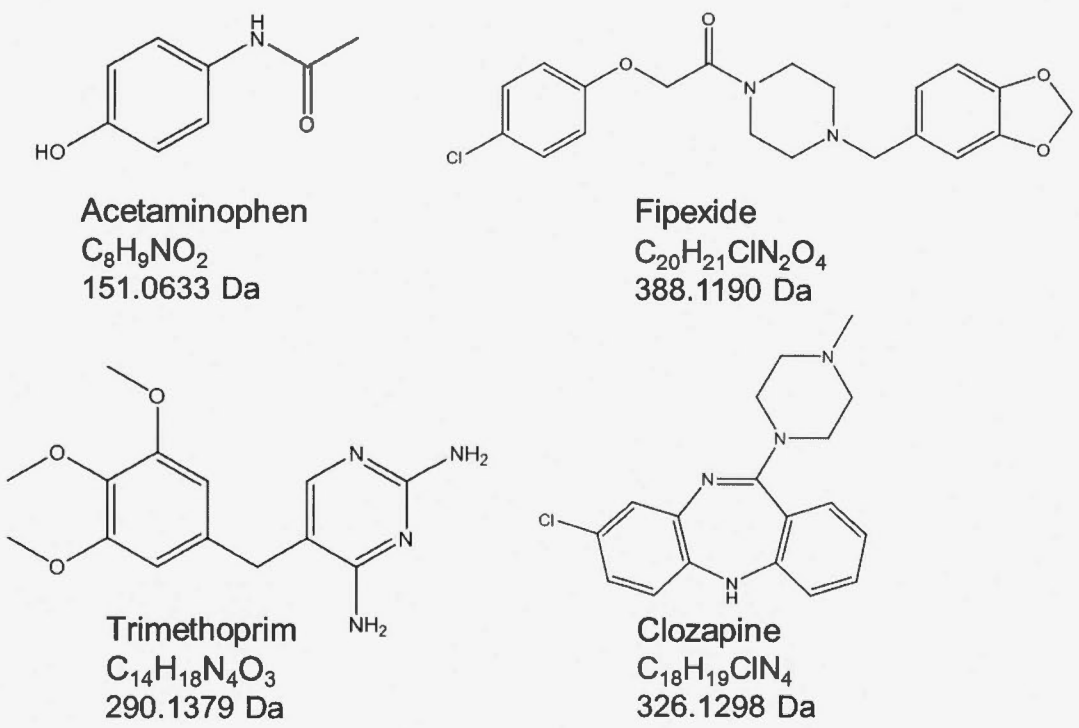

Figure 3.3. Structures of drugs tested for reactive metabolite formation in this study.

Table 3.2. Summary of unique molecular features found in GSH and GSH-Br incubations vs. control incubations (no GSH) by Mass Profiler software (RT: retention time in min)

Drug	GSH	GSH-Br	Structure	References
Fipexide	681.1887 Da 2.4 ppm (RT 10.1)	893.1325 Da -2.1 ppm (RT 12.2)	Fip + GSH(Br) - CH_2	(26)
	734.1903 Da - (RT 7.9)		False Positive!	
Acetaminophen		668.0783 Da -0.8 ppm (RT 12.0)	APAP + GSH(Br) - 2H	(10, 14)
Trimethoprim		807.1521 Da -1.5 ppm (RT 11.5)	TMP + GSH(Br) - 2H	(35, 36)
		793.1349 Da -3.5 ppm (RT 11.2)	TMP + GSH(Br) - 2H - CH_2	
Clozapine		861.1541 Da -2.0 ppm (RT 12.0)	Cloz + GSH(Br) + O	(44)
	649.2109 Da 3.7 ppm (RT 10.4)	861.1537 Da -2.4 ppm (RT 12.4)		
	647,1958 4.5 ppm (RT 11.1)	859,1396 -0.7 ppm (RT 12.7)	Cloz + GSH(Br) - 2H + O	(10, 12, 14, 15, 44)
		843.1452 Da -0.1 ppm (RT 12.3)	Cloz + GSH(Br) - 2H	(10, 12, 14, 15, 44)
	631.2002 Da 3.5 ppm (RT 10.3)	843.1448 Da* -0.6 ppm (RT 12.5)		
		843.1447 Da -0.7 ppm (RT 13.0)		
		843.1448 Da -0.6 ppm (RT 13.1)		
	617.1849 Da 4.2 ppm (RT 10.3)	829.1292 Da -0.5 ppm (RT 12.5)	Cloz + GSH(Br) - 2H - CH_2	(10, 12, 14, 15, 44)
	617.1846 Da 3.7 ppm (RT 10.9)	829.1276 Da -2.4 ppm (RT 13.1)		

* The Mass Profiler software identified an in-source fragment (-CO2) of this ion. The molecular feature has mass of 799.1568 Da (1.8 ppm from the decarboxylated species) with identical retention time (12.5 min).

The anticipated result, when acetaminophen was investigated with both GSH and GSH-Br, was an obvious adduct corresponding to the addition of each trapping agent to NAPQI. Surprisingly, when the control (-GSH) sample was compared to the incubation with added GSH, no unique features were identified in the GSH incubation using the Mass Profiler software (Fig. 3.3). When the GSH-Br analog was tested, however, a unique compound was detected with a neutral mass of 668.0783, corresponding to the NAPQI+(GSH-Br) adduct (APAP+(GSH-Br)-2H) with a mass accuracy of −0.8 ppm. In Fig. 3.3, the Mass Profiler results identifying this adduct are presented showing very consistent results between the three injections (denoted as individual dots in the graph of neutral mass vs. retention time). The question remained as to why the Mass Profiler software did not automatically recognize the GSH adduct with a neutral mass of 456.1315 (APAP+GSH-2H). When the raw data was verified manually, we noticed that, due to the polarity of this GSH conjugate, its retention time was less reproducible, and, therefore, the software did not identify the compound as being in all three injections of the GSH incubation. Figure 3.4 shows the comparison of the triplicate injections for both GSH and GSH-Br adducts of NAPQI. The overlaid extracted compound chromatograms (ECC) for both adducts are presented (neutral mass 456.1315 and 668.0788 Da for GSH and GSH-Br, respectively). The ECC corresponds to the sum of all extracted ion chromatograms of all ions attributed to the same compound (i.e., protonated ions, sodiated ions, isotopic peaks, multiply charged species, etc.), which is designated following molecular feature extraction. The GSH-Br adduct demonstrates extremely consistent chromatography between the three injections. On the other hand, the three ECC traces for the corresponding GSH adduct illustrates earlier retention time and wider peak shapes for this compound. The three injections were more variable in terms of chromatography, resulting in the software not being able to identify the three peaks as being the same compound with matching accurate masses and retention times. This is an important problem to address since we are increasingly relying on automatic

detection and identification by software due to the high-throughput nature of these types of screens. It therefore remains important to fully understand the limitations of such unsupervised processing routines and therefore design our studies with these limitations in mind. In the case of acetaminophen, if we had relied fully on the automated procedure using regular GSH as the trapping agent, we would not have identified any GSH adducts formed via APAP metabolism.

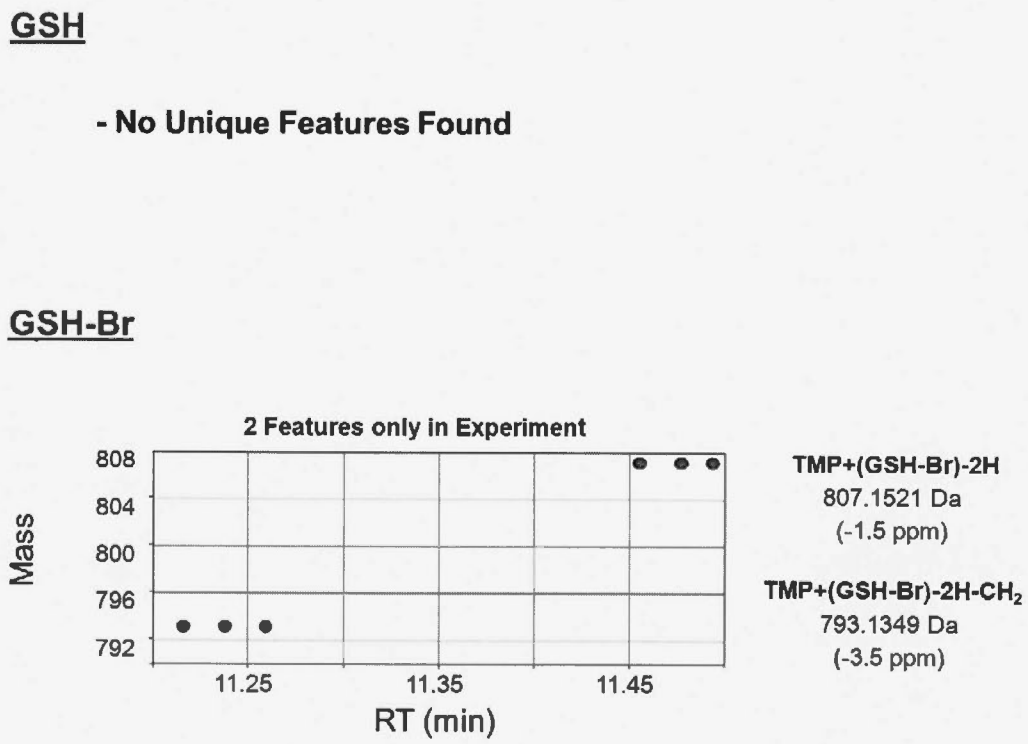

Figure 3.4. Mass Profiler results showing neutral mass and retention times for unique peaks in acetaminophen incubations compared to control (no NADPH) for GSH vs. brominated analog GSH-Br.

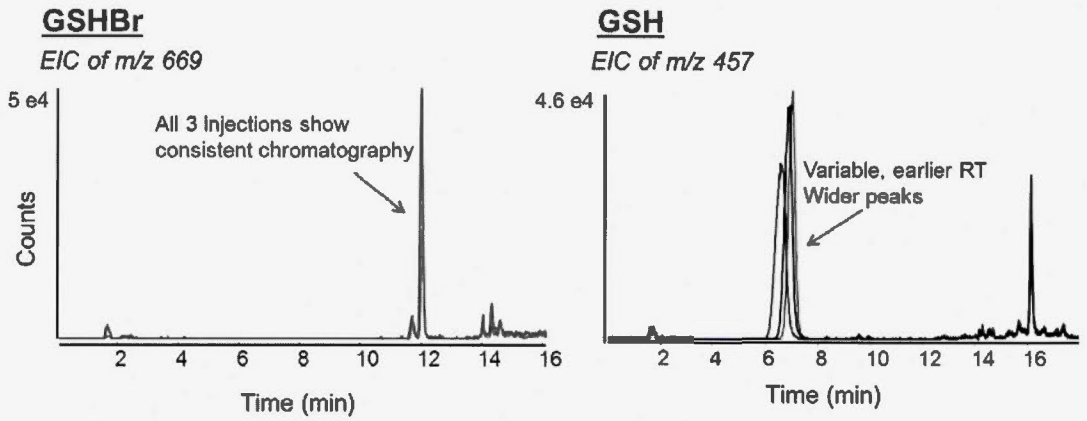

Figure 3.5. Extracted compound chromatograms (ECC) of triplicate injections (overlaid) for acetaminophen adduct peaks for GSH and GSHBr incubations.

3.4.2 FIPEXIDE

The next test compound was one that has recently been reported to form GSH adducts in microsomal and hepatocyte incubations (Sleno *et al.,* 2007; Sleno *et al.,* 2007).26, 27 This nootropic drug was designed and used as a treatment for cognitive disorders, (Bompani & Scali, 1986; Rolandi *et al.,* 1984) but was quickly withdrawn from the market due to severe and unexplained toxicity (Guy *et al.,* 1989; Das *et al.,* 1988). Since then, *in vitro* studies have shown the possibility of linking this toxicity to the formation of reactive metabolites (Sleno *et al.,* 2007) and covalent binding to proteins (Sleno *et al.,* 2007).The reactive metabolite identified in microsomal incubations is the catechol derivative of fipexide, which can easily be further oxidized to a quinone intermediate and subsequently attacked by GSH. This reactive metabolite is formed in relatively large proportion in *in vitro* microsomal incubations, and, therefore,

fipexide was thought to be an easy test compound for our GSH vs. GSH-Br comparison.

The Mass Profiler software clearly recognized the previously reported GSH adduct with a neutral mass of 681.1887 Da, as well as the corresponding GSH-Br species at 893.1325 Da (Fig. 5). However, an unforeseen second compound was identified in the GSH incubation at 734.1903 Da. Upon further examination of the molecular feature, it was concluded to be a false positive since the accurate mass did not coincide with any possible routes of metabolism of fipexide. This highlights an important advantage of using GSH-Br as a trapping agent, since it allows the filtering method to be extremely unique to both the drug of interest and GSH-Br. Both the isotopic pattern and the mass defect filtering parameters are more stringent due to the presence of bromine in the GSH-Br analog, thus alleviating the possibility of false positives being detected. In Fig. 6, the isotopic pattern for both GSH and GSH-Br adducts of the reactive metabolite of fipexide are shown. The presence of a chlorine atom in the structure of the drug already confers some specificity based on isotopic pattern which can be used to remove 'non-chlorinated' species from the list of proposed adducts. However, this isotopic pattern was not enough to weed out the related false positive compound in the GSH incubation. On the other hand, the isotopic pattern of the Fip+(GSH-Br)-CH_2 adduct is a result of the combination of chlorine and bromine, making the ratio of M/M+2/M+4 (M, being the monoisotopic mass) truly unique to a compound having both these elements.

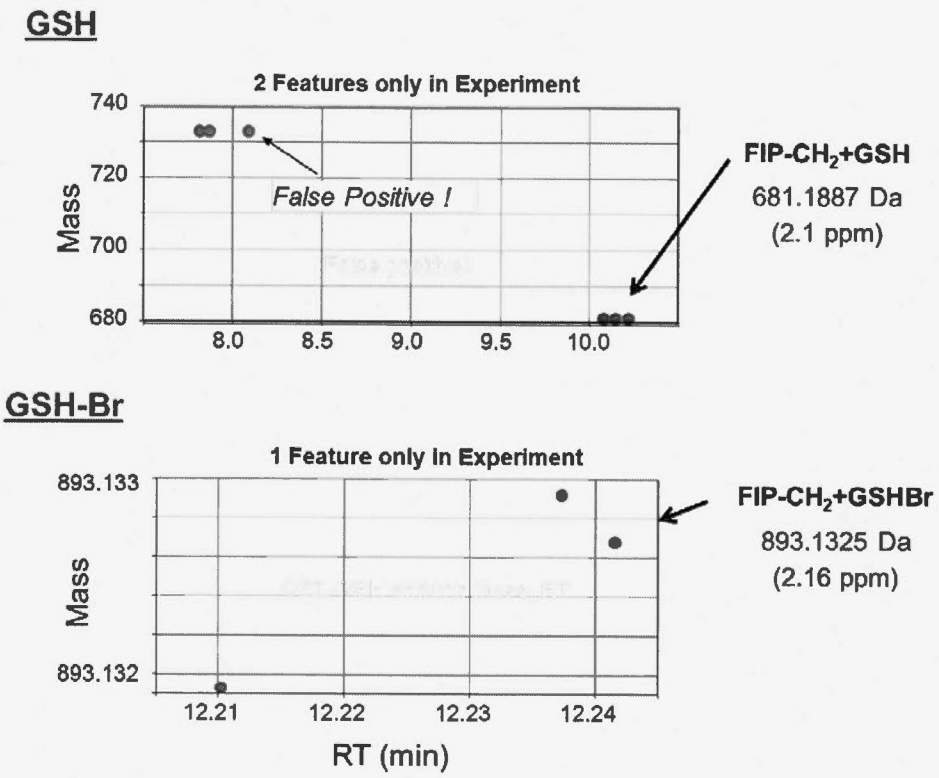

Figure 3.6. Mass Profiler results showing neutral mass and retention times for unique peaks in fipexide incubations compared to control (no NADPH) for GSH vs. GSH-Br.

It is also important to note that a second Mass Profiler filtering method was created in the case of the loss of the chlorine atom during metabolism, with the corresponding altered isotopic pattern for both GSH and GSH-Br samples. No unique features were identified in either case. It remains crucial to perform this secondary screening for all drug compounds containing chlorine (or other elements with unique isotopic abundances, and which can be lost through metabolism) since the loss of this atom changes the isotopic pattern drastically.

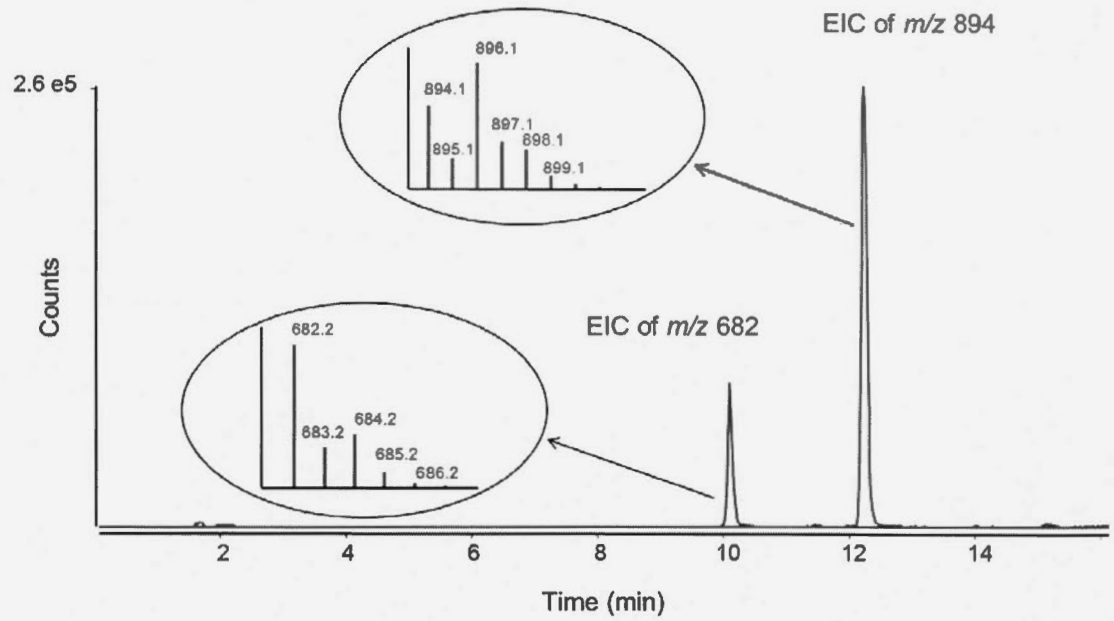

Figure 3.7. Extracted ion chromatograms (overlaid) for the $[M+H]^+$ ions of FIP+GSH-CH_2 (*m/z* 682) and FIP+(GSH-Br)-CH_2 (*m/z* 894) and the isotope patterns showing the increased sensitivity and retention for the brominated adduct as well as its specific isotope pattern.

Furthermore, when the EIC traces of only the protonated monoisotopic peaks, at *m/z* 682 and 894 for GSH and GSH-Br, respectively, were overlaid, another advantage of the latter trapping agent was exemplified (Fig. 3.6). Even though the isotopic pattern of the GSH-Br adduct causes the monoisotopic peak to decrease, the signal of this ion species in the mass spectrometer is still more than two-fold higher than the corresponding monoisotopic ion for the GSH adduct. This can be explained in part by the increased sensitivity of electrospray with a higher proportion of organic solvent in the mobile phase. Since the GSH-Br adduct is more hydrophobic, it elutes later from the column, and thus at higher organic content. Another reason is that, in modifying GSH at the free amine portion, we have lessened the propensity for a doubly

protonated ion to be formed (seen at *m/z* (M+2H+)/2), thus more of the ion's signal is concentrated in the singly protonated ion, making the GSH-Br adduct also easier to detect.

3.4.3 TRIMETHOPRIM

Trimethoprim (TMP) is a widely used antibacterial agent which has been shown to cause rare idiosyncratic reactions in humans, including skin rash, liver toxicity and neutropenia (Das *et al.,* 1988; Hawkins *et al.,* 1993; Wokolo *et al.,* 1988). The mechanism of trimethoprim-induced toxicities appears to be associated with its bioactivation and formation of reactive metabolites. A previous *in vitro* study detected a reactive pyrimidine iminoquinone methide metabolite as trapped *N*-acetyl-*L*-cysteine (NAC) adducts in human and rat liver microsomes (Lai *et al.,* 1999). Several GSH adducts were detected in a subsequent study with human and rat liver microsomes, as well as individual CYP enzymes (Damsten *et al.,* 2008).

When we compared the results from the Mass Profiler software for both GSH and GSH-Br incubations (shown in Fig. 3.7), two unique features were identified as GSH-Br adducts of TMP, yet no unique features were seen for GSH. The two adducts were detected at 807.1521 and 793.1349 Da, corresponding to TMP+(GSH-Br)-2H (−1.5 ppm) and TMP+(GSH-Br)-2H-CH_2 (−3.5 ppm), respectively. The first represents the adduct of the previously reported reactive iminoquinone methide intermediate, while the latter has lost one of its O-methyl groups. O-Demethylation of TMP has been reported as a major metabolic pathway in microsomal incubations (van't Klooster *et al.,* 1992), yet no mono-demethylated GSH adducts have been detected previously. Some of the GSH adducts which have been detected previously in rat liver microsomes (Damsten *et al.,* 2008) were not found in our study; however,

this could be due to different incubation conditions, specifically the concentration of TMP which was ten times the concentration we used here (500 μM). It is also noteworthy to mention that since TMP has a unique structure allowing multiple demethylation reactions (up to three) to occur (Damsten *et al.,* 2008), the MDF window of 40 mDa may not be enough to include tri-demethylated adducts. In order to assure that no demethylated metabolites were missed in our screening assay, we performed a secondary screen with the MDF widened to ±80 mDa. Even with the wider filter, no additional adducts were identified in the Profiler software in either GSH or GSH-Br incubations.

GSH

- No Unique Features Found

GSH-Br

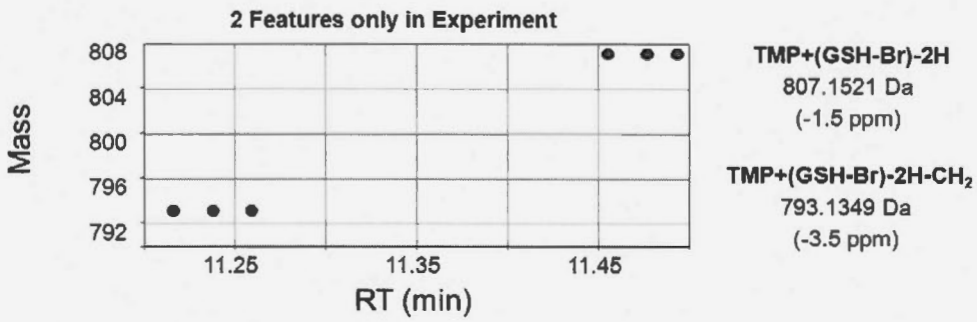

Figure 3.8. Mass Profiler results showing neutral mass and retention times for unique peaks in trimethoprim incubations compared to control (no NADPH) for GSH vs. GSH-Br.

Figure 3.8 presents the spectral transformation following molecular feature extraction (MFE) of raw TOF data. As described in the Experimental section, MFE was performed as a first step to identify all compounds within the specified filtering parameters, which consist mainly of signal thresholds, mass and retention time ranges. Individual MFE spectra, denoting all MS peaks related to a given compound, can be visualized in the MassHunter Qualitative Analysis software. This figure is included to convey the power of this processing routine in pulling out important adducts from the high background of electrospray ions seen in these types of incubations. The spectra on the right show that only the ions belonging to the neutral compounds at 793.1349 and 807.1521 Da are individually extracted out of the background for the two corresponding MFE spectra of the GSH-Br adducts.

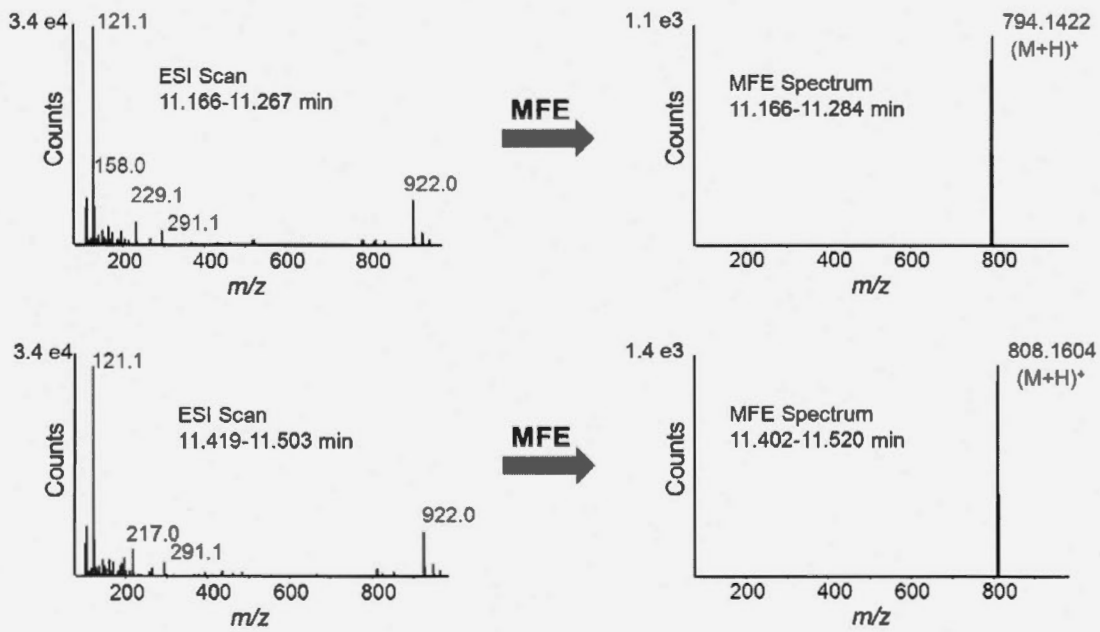

Figure 3.9. Molecular feature extraction (MFE) spectra for two GSH-Br adducts identified in trimethoprim incubations.

3.4.4 CLOZAPINE

Clozapine is an atypical antipsychotic used for the treatment of schizophrenia. It causes neutropenia and agranulocytosis in approximately 3% and 1% of patients, respectively (Alvir *et al.,* 1993; Atkin *et al.,* 1996; Krupp & Barnes, 1992), which may be due to the formation of toxic metabolites. Clozapine undergoes bioactivation to a toxic, chemically reactive nitrenium ion which can bind covalently to cellular proteins (Liu & Uetrecht, 1995; Maggs *et al.,* 1995) and deplete GSH levels in the cell (Williams *et al.,* 1997).

There have been several GSH adducts reported previously for clozapine, including the nitrenium GSH adduct combined with secondary metabolic pathways, such as mono-oxidation and *N*-demethylation (Zhu *et al.,*2007; Rousu *et al.,* 2009; Yan *et al.,* 2005). In our GSH incubations, five unique features were identified within the Profiler filtering parameters set within our method. As seen in Fig. 9, one adduct was detected for the nitrenium GSH adduct (Cloz+GSH-2H, 631.2002 Da) as well as two demethylated nitrenium adducts (Cloz+GSH-2H-CH2, 617.1849 and 617.1846 Da) and one mono-hydroxylated nitrenium adduct (Cloz+GSH-2H+O, 647.1958 Da). Additionally, an adduct was identified at 649.2109 Da, corresponding to a simple mono-oxidation reaction followed by GSH conjugation (Cloz+GSH+O) with a mass error of 3.7 ppm. This species has been described in a recent report, where negative ion precursor scanning of *m/z* 272 was employed (Jian *et al.,* 2009). The analogous NAC adduct was also detected in the same study. The Cloz+GSH+O adduct was also identified when a novel background subtraction algorithm was applied on high-resolution Orbitrap data of human liver microsomal incubations of clozapine (Zhang & Yang, 2008). Surprisingly, the Mass Profiler results for the GSH-Br incubation identified ten unique features with the new trapping agent. In addition to the same five adducts as seen in the GSH incubation, three more nitrenium ion adducts were

detected at 843.1452, 843.1447 and 843.1448 Da with retention times of 12.3, 13.0 and 13.1 min, respectively. In the past, as many as three such adducts had been detected at one time (Zhang & Yang, 2008); however, we detected four in our assay with the brominated analog of GSH. An additional Cloz+GSH+O species at 12.0 min was detected at 861.1541 Da (−2.0 ppm). The last feature, with a neutral mass of 799.1568 Da and retention time of 12.5 min, was recognized as an in-source fragment, formed by decarboxylation of one of the nitrenium ion adducts. This conclusion was made based on mass accuracy (measured mass error of 1.8 ppm) and co-elution with the largest nitrenium ion peak.

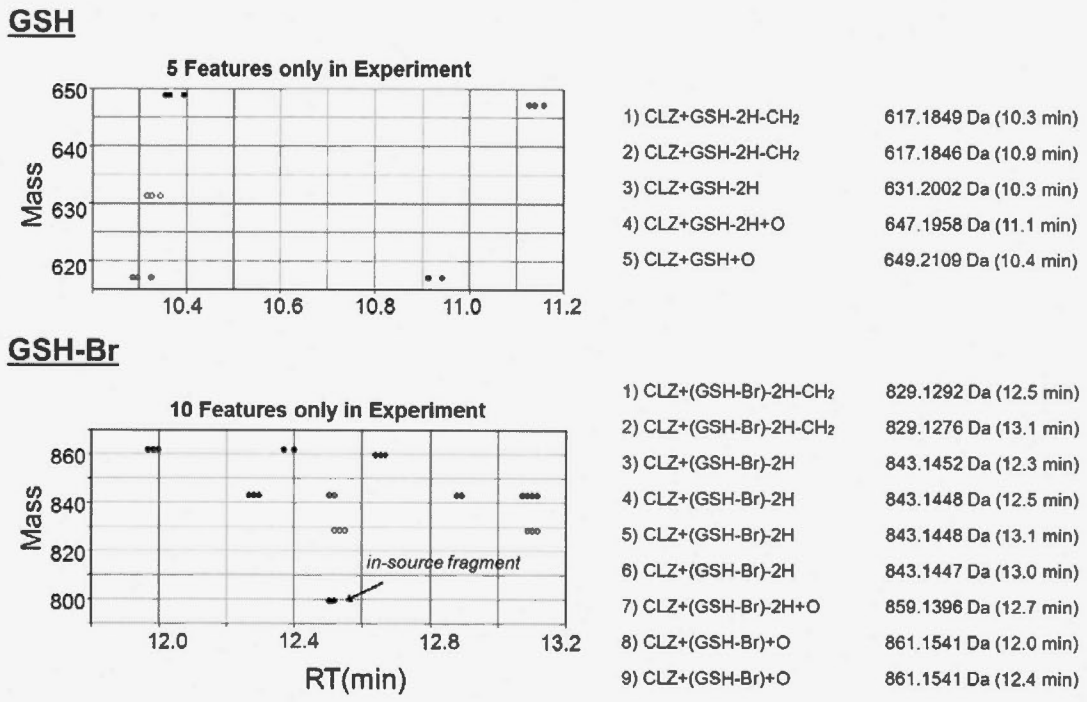

Figure 3.10. Mass Profiler results for unique peaks in clozapine incubations compared to control (no NADPH) for GSH vs. GSH-Br. Adducts identified in each case are listed on the right.

Since clozapine has a chlorine atom in its structure, we also need to consider a dechlorination reaction as part of the metabolism of this drug. As was done for fipexide, a second Mass Profiler filtering method was created with the isotopic pattern altered for the loss of the chlorine atom, for both GSH and GSH-Br, with no additional adducts being identified in either case.

3.5 CONCLUSIONS

We have combined mass defect and isotope filtering for screening reactive metabolites by accurate mass LC-MS with a novel bromine-containing GSH analog. Due to its increased hydrophobicity, this new analog increased the chromatographic retention of GSH adducts resulting in higher sensitivity, since they elute at higher organic content. The preparation of this compound was also very simple and inexpensive; in comparison to previously reported analogs (or stable-isotope-labeled compounds) used for this type of work. This new bromine-containing analog of GSH has several advantages for the detection of reactive metabolites. First of all, we can employ the specific isotope pattern of bromine for improved filtering of the data. Also, the unique mass defect of bromine minimizes spectral background compared to common organic compounds of similar mass (Shi *et al.,* 2009), thus having less potential for false positives using the mass defect filtering processing capabilities of many currently available types of software. The more hydrophobic adducts, in most cases, yield better peak shapes for the GSH-Br adducts vs. GSH adducts. These advantages have been exemplified using four drug compounds known to form reactive metabolites. The enhanced characteristics of the GSH-Br compound for reactive metabolite screening produces less false positives and more sensitive detection, thus more true adducts being identified in many cases.

CHAPITRE IV

ARTICLE SCIENTIFIQUE: "ABSOLUTE QUANTITATION OF NAPQI-MODIFIED RAT SERUM ALBUMIN BY LC-MS/MS: MONITORING ACETAMINOPHEN COVALENT BINDING *IN VIVO*"

André LeBlanc, Tze Chieh Shiao, René Roy, Lekha Sleno*

*Université du Québec à Montréal, Pharmaqam, Chemistry Department, P.O. Box 8888, Downtown Station, Montréal, Québec, Canada H3C 3P8

Article published in:

Chemical Research in Toxicology 2014, 27, 1632-1639.

Submitted: July 11, 2014

Accepted: August 28, 2014

Cet article présente une méthode pour déterminer la concentration absolue de l'adduit formé entre l'albumine et le métabolite réactif de l'acétaminophène *in vivo*. C'est la première fois qu'un tel adduit peut être mesuré d'une manière quantitative et ceci grâce à la conception d'une molécule qui a permis de construire une courbe d'étalonnage et d'utiliser un standard interne deutéré. Cette méthodologie engendre un intérêt clinique, car l'hépatoxicité causée par l'acétaminophène est la cause la plus fréquente de l'insuffisance hépatique aigüe en Amérique du Nord.

Sous la supervision de la professeure Lekha Sleno, je fus responsable de la conception de la méthode analytique et la rédaction du manuscrit, ainsi que de toutes les manipulations, expérimentations et analyses de données. Tze Chieh Shiao, grâce à la collaboration avec le laboratoire du professeur René Roy, a effectué la synthèse de la molécule «iodo-IPAP» et de son isotope deutéré.

4.1 ABSTRACT

Acetaminophen is known to cause hepatoxicity via the formation of a reactive metabolite, *N*-acetyl p-benzoquinone imine (NAPQI), as a result of covalent binding to liver proteins. Serum albumin (SA) is known to be covalently-modified by NAPQI and is present at high concentrations in the bloodstream and is therefore a potential biomarker to assess the levels of protein modification by NAPQI. A newly developed method for the absolute quantitation of serum albumin containing NAPQI covalently bound to its active site cysteine (Cys34) is described. This optimized assay represents the first absolute quantitation of a modified protein, with very low stoichiometric abundance, using a protein-level standard combined with isotope dilution. The LC-MS/MS assay is based on a protein standard modified with a custom-designed reagent, yielding a surrogate peptide (following digestion) that is a positional isomer to the target peptide modified by NAPQI. To illustrate the potential of this approach, the method was applied to quantify NAPQI-modified SA in plasma from rats dosed with acetaminophen. The resulting method is highly sensitive (capable of quantifying down to 0.0006 % of total RSA in its NAPQI-modified form), and yields excellent precision and accuracy statistics. A time-course pharmacokinetic study was performed to test the usefulness of this method for following acetaminophen-induced covalent binding at four dosing levels (75-600 mg/kg IP), showing the viability of this approach to directly monitor *in vivo* samples. This approach can reliably quantify NAPQI-modified albumin, allowing direct monitoring of acetaminophen-related covalent binding.

4.2 INTRODUCTION

Acetaminophen (or paracetamol) related toxicity is the most common cause of acute liver failure in North America (Lee, 2004; Sivilotti *et al.,* 2005). This hepatotoxicity is caused by an electrophilic reactive metabolite, *N*-acetyl p-benzoquinone imine (NAPQI), which forms covalent adducts with nucleophilic thiol groups in liver protein causing hepatic necrosis, tissue failure and death (Jollow *et al.,* 1973; Dahlin, *et al.,* 1984; Pumford *et al.,* 1989; Jaeschke & Bajt, 2010). Clinically, patients exhibiting acetaminophen-related toxicity must wait for the manifestation of generic signs of hepatic failure before deciding if a transplant is required (Larson *et al.*, 2005). The ability to measure the extent of protein covalent modification by NAPQI *in vivo* would therefore be extremely useful for monitoring acetaminophen toxicity. Previous reports have assessed the total amount of protein modification in plasma samples using radiolabeled drug or by measuring the total amount of modified cysteine following complete proteolysis (Devi *et al.,* 2007; McGill *et al.,* 2013). Immunochemical detection of acetaminophen protein adducts has also been reported (Hinson *et al.,* 1995).

Serum albumin (SA), present at high concentrations in blood, is covalently modified by NAPQI in several species, including humans (Damsten *et al.,* 2007). Importantly, Cys34 of SA is the only free cysteine (in rat and human) and has been previously reported as modified by NAPQI. For these reasons, and because blood sampling is much less invasive than tissue sampling, modified SA is therefore an ideal potential biomarker to assess acetaminophen-linked covalent binding, and could be used as a direct measure of this type of toxicity.

LC-MS-based methods have been used to characterize NAPQI-modified albumin and modifications by other reactive drug metabolites, heterocyclic amines, reactive

carbonyl species, and mustard gas (Meng *et al.,* 2013; Peng & Turesky, 2011; Dingley *et al.,* 1999; Aldini *et al.,* 2008; Aldini *et al.,* 2008; Noort *et al.,* 2008). Despite the obvious interest, there are no assays that accurately measure the concentration of SA containing a specific modification, due to the extensive challenges involved in developing such an assay. Generally, whether it is a shotgun approach or a targeted quantitative assay, proteins are enzymatically digested and peptides analyzed by LC-MS/MS (Domon, & Aebersold, 2006). Targeted multiple-reaction monitoring (MRM) assays, on triple quadrupole platforms, are regarded as the gold standard for quantitation due to the high sensitivity and selectivity they provide (Liebler & Zimmerman, 2013; Boja & Rodriguez, 2012). For MS-based quantitation, it has long been established that combining an appropriate standard using isotope dilution is the ideal strategy and this approach has been increasing in quantitative proteomics in recent years (Brun *et al.,* 2009). To be as accurate as possible for quantifying a specific protein, a protein-level standard together with an isotopically labeled internal standard (IS) would be used in conjunction with LC-MRM analysis, for producing an external calibration.

The major challenge in achieving robust assays for absolute quantitation of proteins has traditionally involved the implementation of appropriate standards. Since protein standards can be difficult to produce, the use of peptide standards has gained popularity (Gerber *et al.,* 2003). This approach can yield good results, but cannot compensate for differences during protein digestion. To correct for all variations possible in a proteomics workflow, the ideal standard remains the intact protein of interest. Nonetheless, the current benchmark for quantitation of post-translational modifications (PTMs) on a specific target protein is by synthesizing peptide standards containing the modification (Kirkpatrick *et al.,* 2005). While protein standards are evidently the best option, the synthesis of full-length proteins aren't very practical, especially when it comes to a modified protein, and therefore it remains unrealistic to produce a PTM-containing protein standard in precisely known quantities. In the case

of a NAPQI-modified protein, it would be exceptionally challenging to synthesize even a pure modified peptide standard in known quantities, since NAPQI itself is such an unstable species.

A recent article describing an assay for monitoring NAPQI covalent binding to mouse serum albumin acknowledged the difficulty in obtaining a standard for quantitation purposes and relied instead on measuring the relative abundance between modified and unmodified albumin after trypsin digestion by LC-MS (Switzar *et al.*, 2013). The relative quantitation was based on comparing peak areas between modified and unmodified peptides, from extracted ion chromatograms. This approach assumes that the LC-MS response factors of both species are equivalent despite having different structures, elution times and matrix effects, and without considering the assay's large dynamic range. Another study used a synthesized NAPQI-CPF tripeptide as a standard solution for quantifying modified human albumin (Damsten *et al.*, 2007). The assay employed a non-specific digestion (pronase) and albumin alkylated with mustard gas as an internal standard for normalization. The amount of NAPQI-modified albumin was estimated by comparing NAPQI-CPF from serum with and without spiking a constant amount of standard NAPQI-CPF prior to digestion. This procedure was used for comparing covalent binding between patient samples, but was not described as an accurate measurement for absolute quantitation of NAPQI-albumin. No previous method has been reported for the absolute quantitation of acetaminophen covalent binding to albumin.

Using a novel approach for producing a modified-protein standard, the absolute quantitation of NAPQI-modified rat serum albumin (NAPQI-RSA) has been achieved by LC-MRM with an external calibration curve and isotope-labeled internal standard. The applicability of the method was established by measuring NAPQI-RSA in rat plasma following acetaminophen dosing.

4.3 EXPERIMENTAL

4.3.1 MATERIALS

Peptide, LQKCPYEE (96.34% purity) was ordered from Biomatik (Cambridge, ON). Rat serum albumin (RSA, 99%), acetaminophen, ammonium bicarbonate, *n*-Dodecyl β-D-maltoside (DDM), dithiothreitol (DTT), iodoacetamide (IAM), methanol, pepsin, nicotinamide adenine dinucleotide phosphate, formic acid, ammonium hydroxide and phosphoric acid were obtained from Sigma-Aldrich (Oakville, ON). Acetonitrile (ACN) and potassium chloride were purchased from Caledon (Georgetown, ON). Potassium phosphate (dibasic) was from Anachemia (Montreal, QC). Human liver microsomes were purchased from BD Biosciences (Mississauga, ON). Blank male Sprague-Dawley rat plasma (Li Heparin) was purchased from Bioreclamation LLC (Baltimore, MD). Nanopure water was prepared from a Millipore Synergy® UV system (Billerica, MA). Iodo-APAP and D_4-iodo-APAP were synthesized in-house (described in supplemental material) for the chemical labeling of RSA and standard peptide to produce surrogate standard and internal standard for quantitation assay.

4.3.2 PREPARATION OF IODO-APAP-MODIFIED AND NAPQI-MODIFIED LKQCPYEE

Lyophilized LQKCPYEE (100 µg) was solubilized in 950 µl of 100 mM ammonium bicarbonate buffer pH 8.5 (ABC), treated with 25 µl 100 mM DTT and placed in a thermomixer (Eppendorf, Mississauga, ON) for 15 min at 37°C. Then, 25 µl of either iodo-APAP or D_4-iodo-APAP (300 mM in ACN) was added and incubated at 37°C

for 45 minutes in the dark. Modified LKQCPYEE solutions (0.1 mM) were diluted (10x) for MS/MS characterization.

To prepare NAPQI-modified LQKCPYEE, rat liver microsomes (1 mg/ml protein) were incubated with 50 µM acetaminophen, 1 mM NADPH, and 1 mM LQKCPYEE (2 h, 37°C) in potassium phosphate buffer (50 mM, pH 7.4), quenched with equal volume (250 µl) of cold ACN, vortexed, and centrifuged (16873 rcf, 10 min). The supernatant was evaporated to dryness and reconstituted in 250 µl of 10% ACN for LC-MS/MS analysis.

4.3.3 RAT DOSING

Dosing and blood collection were performed at INRS Centre de Biologie Experimentale (Laval, QC). Sprague-Dawley rats (450-550 g) were given acetaminophen (IP, solubilized in 60% PEG 200) at four dosing levels (75 (n=3), 150 (n=3), 300 (n=3) and 600 (n=4) mg/kg). Lithium heparin plasma was prepared from blood collected at: pre-dose, 1, 2, 4, 6 and 24 h post-dose, and kept at -80°C.
Iodo-APAP modified RSA standard solutions

RSA solution (250 µl, 4 mg/ml) was combined with DTT (25 µl, 100 mM) and DDM (25 µl, 2% in water) and incubated at 37°C (20 min). ABC (700 µl) and either iodo-APAP or D_4-iodo-APAP (25 µl, 300 mM in ACN) were then added and incubated (37°C, 45 min) in the dark. The resulting solutions consisted of 1 mg/ml RSA modified with either iodo-APAP (stock for standard solutions) or D_4-iodo-APAP (stock for IS solution). Standard spiking solutions were prepared in 0.1% DDM and diluted to appropriate concentrations for each standard, from 1000 µg/ml (no dilution) to 1.78 µg/ml. The IS working solution (ISWS) was prepared at 100 µg/ml.

4.3.4 RAT PLASMA EXTRACTION

Rat plasma (100 µl) was thawed followed by the addition of 25 µl of DDM (2%), 100 µl ABC and 100 µl DTT (100 mM) and samples were placed at 37°C. After 20 minutes, 40 µl of IAM (750 mM) was added for further incubation (37°C, 45 min) in the dark. After cysteine alkylation, 20 µl of ISWS was added. For calibration standards, 20 µl spiking solution was added to IAM-alkylated blank plasma. To adjust solvent composition and pH, 100 µl of 5% formic acid in 50% methanol was added prior to pepsin digestion (40 µl, 3 mg/ml pepsin) at 37°C for 18 h.
Digestion was quenched with 50 µl of 5% NH_4OH (final pH ~7.5) and diluted with 400 µl of water. Mixed mode reverse-phase/weak anion exchange solid phase extraction (SPE) was performed on 1cc (30 mg) Oasis MAX cartridges (Waters, Mississauga, ON). Samples were eluted with 1 ml methanol containing 2% formic acid and evaporated to dryness under vacuum.

Samples were reconstituted with 110 µl of 10% acetonitrile and 100 µl was injected onto a Zorbax™300-SCX column (2.1×150 mm) with 5 µm particles (Agilent Technologies, Palo Alto, CA). Separation by strong cation exchange (SCX) chromatography was performed on an Agilent 1200 series HPLC with UV detector (220 and 280 nm) and fraction collector. Mobile phase A was 10 mM KH_2PO_4 in 25% acetonitrile (pH 2.75), while mobile phase B had an additional 1 M KCl. The gradient was held for 2 min at 100%A, then increased linearly to 25%B at 9 min, to 55%B at 13 min with 100%B at 13.5 min (and held for 6 min), at a flow rate of 0.25 ml/min. The fraction between 10 and 12 minutes was collected and placed under vacuum to evaporate residual acetonitrile. SPE was then performed on Oasis HLB cartridges (1cc, 30 mg) with methanol elution (1 ml). Extracts were dried and reconstituted with 100 µl 5% ACN prior to LC-MS/MS analysis.

4.4 LC-MS/MS ANALYSIS

Samples (30 µl) were injected onto a Kinetex® XB-C_{18} 2.1×100 mm column, with solid core 1.7 µm particles (100Å) fitted with a SecurityGuard®-Ultra C_{18}-peptide guard column (Phenomenex, Torrance, CA) using a Nexera® UHPLC (Shimadzu, Columbia, MD). Mobile phases were water (A) and ACN (B), both containing 0.1% formic acid. The gradient included a 3 min hold at 5%B with a linear increase to 12%B until 17 min, then to 95%B at 23.5 min, at 300 µl/min flow rate and column temperature of 40°C. Multiple reaction monitoring (MRM) detection in positive mode was performed using a hybrid quadrupole linear ion trap (QqLIT) 5500 QTRAP® mass spectrometer (AB Sciex, Concord, ON) with a TurboIonSpray™ ion source, using the following source conditions: ion spray voltage (IS V) 5000 V, temperature 550°C, nebulizer and drying gases (GS1 and GS2) at 50 psi, and curtain gas at 35 psi. Declustering (DP), entrance (EP) and collision cell exit (CXP) potentials were maintained at 60, 10 and 13 V, respectively. The MRM transitions used for quantitation were *m/z* 579.8→917.4 and 581.8→921.4 for the analyte and deuterated internal standard, respectively, at a collision offset voltage of 25 V and CAD gas pressure of 5 (arbitrary units). Two transitions (*m/z* 579.8→1045.4 and 581.8→1049.4) were monitored for qualitative purposes with collision offset voltage of 26 V. The dwell time for each transition was 250 ms for a total cycle time of 1.02 s. To reduce source contamination from the sample matrix, an integrated switch valve was used to send the eluent to waste for the first 10 min of each LC run. The remaining acquisition window from 10-16.5 min ensured monitoring of analyte and internal standard peptides eluting from the column. Data Analyst® software version 1.5.2 was used for data acquisition and raw data were processed using MultiQuant® version 2.1.1 (AB Sciex, Concord, ON).

Product ion spectra of modified LQKCPYEE were collected on a quadrupole time-of-flight (QqTOF) TripleTOF® 5600 mass spectrometer (AB Sciex, Concord, ON) equipped with a DuoSpray™ source in positive mode with similar source conditions as above. MS/MS data (collision offset voltage 30 V) were collected on the ten most intense ions from a survey TOF-MS experiment (*m/z* 140-1250). Accumulation times were 250 and 100 ms for TOF-MS and MS/MS, respectively (1.3 s cycle time).

4.5 RESULTS AND DISCUSSION

The main hurdle in developing a quantitative assay for NAPQI-modified albumin has been the lack of a standard for an external calibration curve and a suitable internal standard to properly correct for digestion efficiency and matrix effects. While albumin is commercially available, the challenge is having a known quantity of NAPQI-modified albumin. It is extremely difficult to produce a protein standard in precise quantities containing a specific modification. While obtaining a suitable labeled IS for unmodified proteins can be quite difficult, requiring isotopic labeling of whole proteins, the advantage of a modified protein lies in the possibility of labeling the modification. Therefore, an ideal way to produce both a modified protein standard and an isotopically-labeled modified internal standard relies on quantitatively modifying the site of interest. The particular challenge in the case of reactive metabolites is their inherent instability and that they are formed enzymatically. Though they can sometimes be formed by chemical or electrochemical oxidation, there has yet to be an efficient enough method to produce a quantitatively-modified protein standard (Madsen *et al.*, 2007; Bessems *et al.*, 1996).

Iodo-APAP modified albumin as a surrogate protein standard

NAPQI is formed through the oxidative metabolism of acetaminophen, catalyzed by the cytochrome P450 system (Figure 4.1A). NAPQI is a quinone imine that covalently binds to protein via a Michael addition reaction with nucleophilic cysteine thiol groups (Mitchell *et al.*, 1973; Potter *et al.*, 1973). The resulting product is the addition of *N*-(4-hydroxyphenyl) acetamide with the cysteine sulfur atom directly bonded to an aromatic carbon, preferentially ortho to the hydroxyl group (Figure 4.1B).

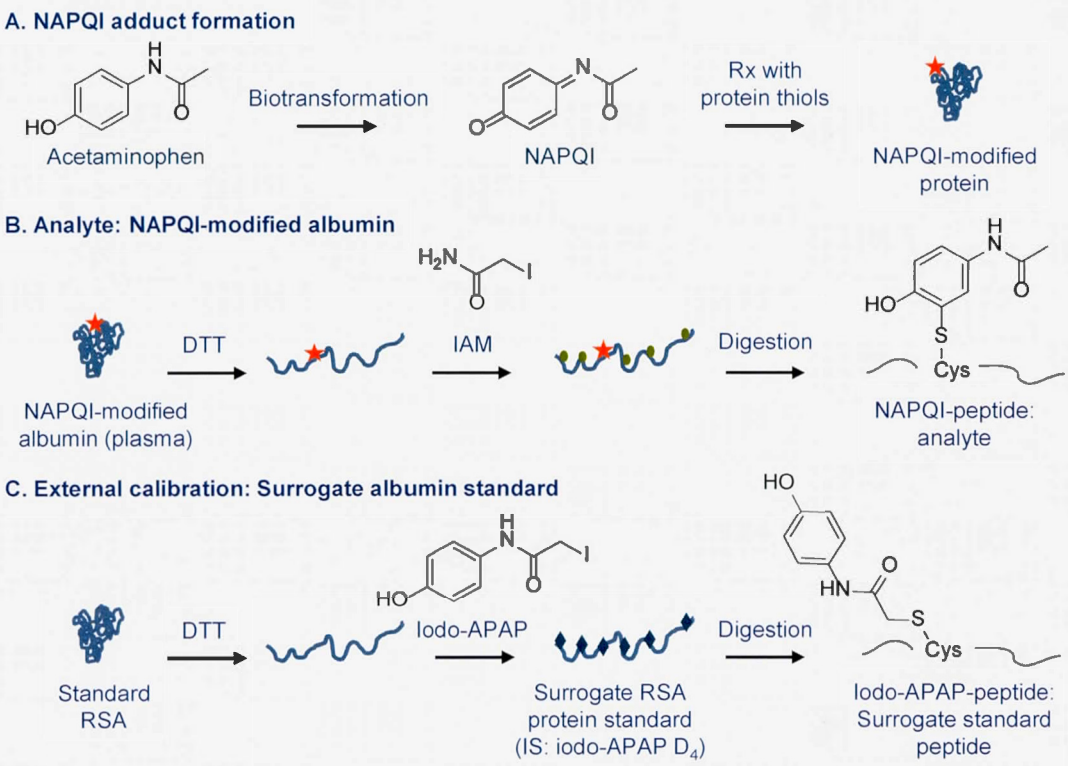

Figure 4.1. Formation of analyte (NAPQI-modified) and standard (iodo-APAP-modified) albumin and peptides.

To produce a suitable surrogate protein standard, iodo-APAP, an acetaminophen analog that can efficiently and quantitatively modify free cysteine residues (Figure 4.1C), has been synthesized. Iodo-APAP is also an analog of IAM, routinely used to alkylate and protect cysteine thiol groups, and reacts with free thiols resulting in the addition of *N*-(4-hydroxyphenyl) acetamide, through a thio-ether bond. The iodo-APAP product is therefore a positional isomer of the NAPQI product ensuring that the behavior of our standard will be as close as possible to the analyte during both sample preparation and LC-MRM analysis.

Iodo-APAP can quantitatively modify all cysteine residues in a known quantity of RSA, following treatment with DTT. Even though the modification site of interest is known to be the only free thiol group in RSA, the reduction of all disulfide bonds prior to alkylation ensures the protein is denatured prior to digestion, and that a fully alkylated RSA reflects the same treatment as the analyte NAPQI-RSA which is treated with DTT and IAM (along with other plasma proteins) prior to digestion. Iodo-APAP also allows an isotopically-labeled protein internal standard to be produced, simply by using D_4 ring-labeled iodo-APAP. A protein surrogate standard is produced to quantify NAPQI-modified albumin using an external calibration curve with a isotopically-labeled modified protein IS that can be spiked into all samples prior to digestion, resulting in a highly accurate method for measuring albumin adducts formed via APAP's reactive metabolite.

4.5.1 ALBUMIN DIGESTION

When a specific modification site is probed, there is an obvious lack of flexibility in choosing the analyte peptide for quantitation, since it must contain the modified residue in question. There is a great advantage in choosing between all possible

peptides for protein quantification, due to the very large sensitivity differences between peptides produced via enzymatic digestion. It was therefore important to optimize the digestion protocol to produce a specific active site peptide with high sensitivity by LC-MRM.

The most commonly used proteolytic enzyme in proteomic applications is trypsin. The efficiency and reproducibility of this enzyme is very important for protein quantitation workflows that use peptide standards for quantitation since these standards do not correct for variations in digestion efficiencies between samples. The disadvantage of trypsin for the quantitation of a modified protein is that there is normally only one fully tryptic peptide formed containing each modification site. Preliminary tests showed that the tryptic peptide of RSA was not very sensitive (unpublished data), and the fact that a lysine (trypsin cleavage site) lay next to the modified residue in question also complicated matters. Therefore, a digestion protocol was optimized to produce a sensitive Cys34-containing peptide. Since the surrogate standard is an intact protein; several strategies were assessed to produce a sensitive peptide for quantitation, without needing to be overly concerned with specificity of the protease. Following preliminary tests with trypsin, chymotrypsin, Glu-C and pepsin, an overnight pepsin digestion was chosen since it yielded the most sensitive Cys34 containing peptide (LQKCPYEE) amongst all the digestion protocols.

4.5.2 MRM METHOD

Once the analyte peptide was chosen, the MS/MS behavior of the surrogate peptide and analyte peptide were compared. Since the iodo-APAP modification is a positional isomer of the NAPQI-modification, it was necessary to confirm that the

fragmentation pattern would not vary between the two species. While producing the iodo-APAP LQKCPYEE is straightforward, the NAPQI-modified LQKCPYEE was produced via *in vitro* incubation of APAP with rat liver microsomes. Briefly, we added excess LQKCPYEE peptide in the acetaminophen incubation to trap the NAPQI formed through oxidative metabolism, similar to the procedure used to trap reactive metabolites using glutathione (Baillie & Davis, 1993). Figure 4.2 compares the high resolution MS/MS spectra obtained for the LQKCPYEE peptide containing NAPQI, iodo-APAP and D_4-iodo-APAP modifications. The product ion spectrum for the iodo-APAP peptide is virtually identical to that of the NAPQI peptide, therefore the same MRM transition can be used to quantify surrogate and analyte peptides. Differences in matrix effects are also minimized by their similar chromatographic profile. As highlighted in Figure 4.2, the precursor ion is detected at *m/z* 579.8 and the major fragment (y6) ion is found at *m/z* 917.4. The resulting transition (*m/z* 579.8→917.4) was thus the most sensitive, as well as being highly selective and was therefore chosen for quantitation, while the transition (*m/z* 579.8→1045.4) was used for a secondary qualitative confirmation.

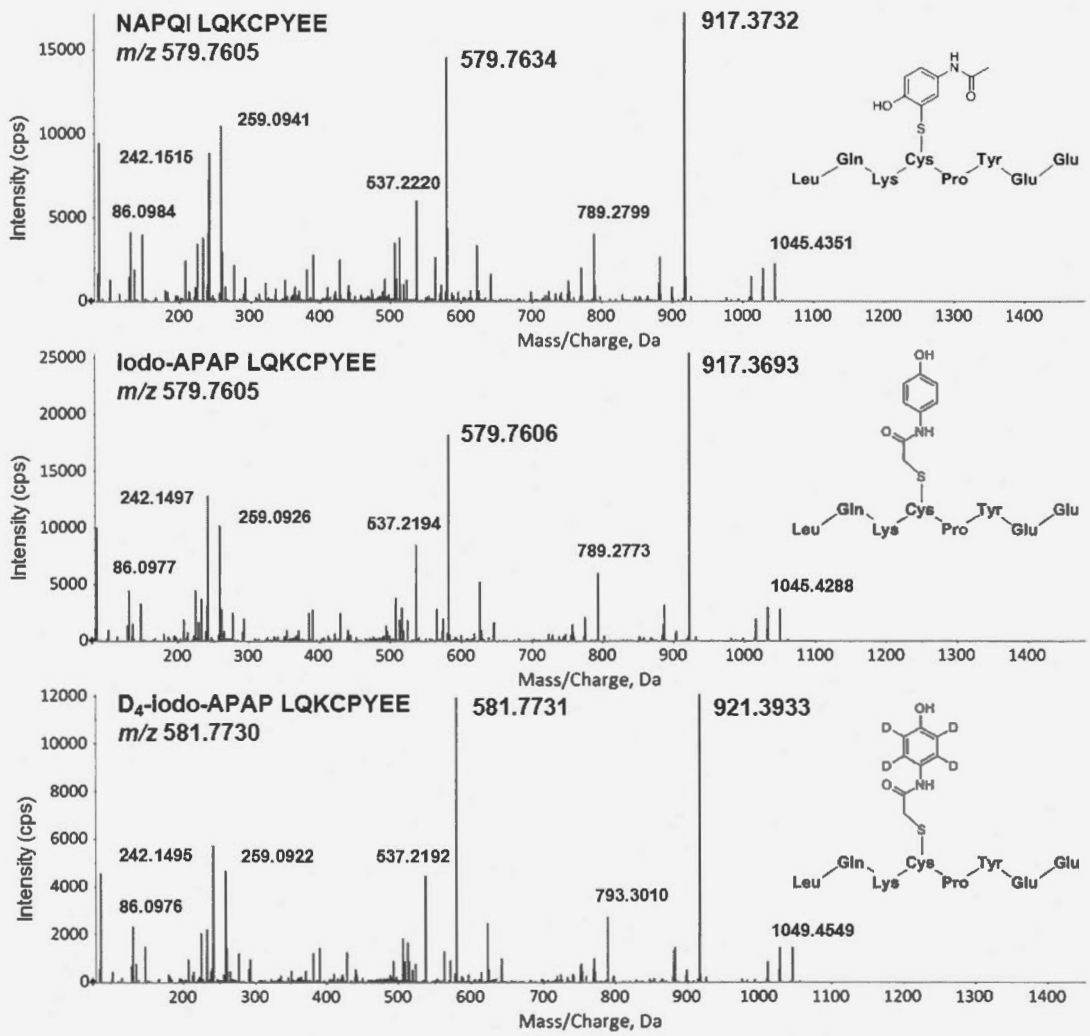

Figure 4.2. MS/MS spectra of NAPQI-modified LQKCPYEE (analyte peptide) and iodo-APAP modified LQKCPYEE (surrogate peptide) (theoretical precursor *m/z* 579.7605) along with that of the isotopically-labeled internal standard (theoretical precursor *m/z* 581.7730).

4.5.3 RAT PLASMA EXTRACTION

Since albumin accounts for about half the protein mass in plasma and the concentration of unmodified albumin is expected to be several orders of magnitude larger than that of NAPQI-modified albumin, sample clean-up was focused on the peptide level. LQKCPYEE contains a high proportion of acidic residues allowing for a good recovery by SPE using a weak anion exchange stationary phase. Even if mixed-mode weak anion exchange (MAX) proved to remove a large portion of the background present in the digested plasma samples compared to other tested SPE phases, including HLB and MCX, additional clean-up was needed to obtain the sensitivity required for the quantitation of relevant concentrations of NAPQI-adducted albumin. Fractionation by strong cation exchange (SCX) chromatography is routinely used in proteomics to reduce sample complexity and gain sensitivity to detect a greater number of peptides and thus expand proteomic coverage (Lau *et al.*, 2011). Combined with MAX-SPE, SCX fractionation further reduced the complexity of the peptide extract, followed by a final HLB SPE step to remove salts and concentrate the sample for LC-MRM analysis. Figure 4.3 illustrates the complete workflow for sample preparation and analysis of NAPQI-modified serum albumin from rat plasma.

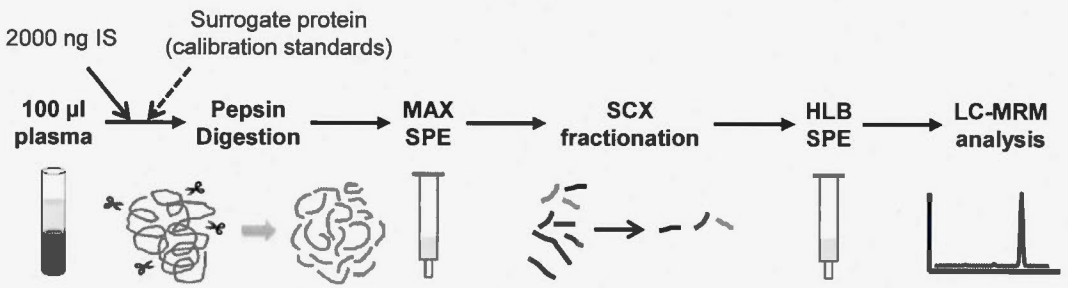

Figure 4.3. Scheme depicting sample preparation procedure for standard and rat plasma samples.

4.5.4 PRECISION AND ACCURACY

The performance of the method was evaluated in two separate runs using freshly prepared calibration curves and quality control samples (Table 4.1). The standard curve spans two and a half orders of magnitude with a lower limit of quantitation down to 0.296 µg/ml or approximately 0.0006% total (unmodified) albumin (calibration curves available in Supplemental Material). The calibration standards from 0.296-189 µg/ml of NAPQI-modified albumin consistently yielded excellent accuracies, ranging from 86-110 %. The QC samples were produced using separate batches of spiking stock solutions and very good results were seen in both evaluation runs; well within acceptable criteria. Linear regression (1/x2 weighting) for these calibration curves were reproducible and showed excellent linearity with R2 values of 0.99166 and 0.99459 (data included in supplemental material). These results confirm this approach can be used to produce a robust assay to determine absolute concentrations of NAPQI-modified albumin from plasma samples.

Table 4.1. Statistics for two separate (inter-day) assay performance evaluation runs

	Day 1		Day 2	
Standard conc. (µg/ml)	**% Accuracy**		**% Accuracy**	
	Curve A	Curve B	Curve A	Curve B
0.296	99.7	100.8	107.2	91.4
0.592	86.1	103.3	106.0	92.8
1.18	102.8	107.0	108.4	98.8
2.37	109.9	104.7	104.5	96.8
4.74	92.1	108.9	106.8	99.5
9.47	100.9	116.8	100.7	96.9
23.7	97.1	105.1	104.8	98.9
47.4	101.9	91.2	106.9	100.9
94.7	98.8	87.8	101.6	97.5
189	92.6	92.6	91.0	88.7
QC samples (µg/ml)	**% RSD (n=3)**	**% Accuracy (n=3)**	**% RSD (n=4)**	**% Accuracy (n=4)**
1.14	6.0	114.7	1.6	96.5
11.4	1.0	112.2	1.3	104.9
114	6.2	94.8	1.3	93.0

4.5.5 RAT STUDY SAMPLES

The assay's potential to monitor relevant *in vivo* levels of NAPQI-albumin was tested using plasma samples from rats dosed at four different acetaminophen concentrations. It is noteworthy to mention that the acetaminophen doses (75, 150, 300 and 600 mg/kg) were specifically chosen at non-toxic levels 31, 32 in order to demonstrate the capacity of the assay to quantify NAPQI-adducted albumin over an acceptable range in physiological concentrations and with the required sensitivity to differentiate between toxic and subtoxic doses. Figure 4.4 illustrates the LC-MRM traces used for

quantitation of NAPQI-LQKCPYEE from a blank plasma sample, the lowest calibration standard and a representative rat sample. While no peaks of interest were detected in blank plasma samples, all four dosing levels resulted in quantifiable concentrations of adducts for post-dose samples, even after 24h and in animals given the lowest dose. At 75 mg/kg, NAPQI-LQKCPYEE exhibited levels far above the quantitation limit of the assay, as can be seen from the representative LC-MRM trace from a sample after 2h following IP injection. Note that the slight retention time shift between the NAPQI-LQKCPYEE and the iodo-APAP-LQKCPYEE is due to the structure differences between these isomers.

Pharmacokinetic concentration curves with 6 time-points were produced for all rats (Figure 4.5), showing that NAPQI-RSA concentrations correlate well with dosage. In all dosing groups, there is an initial increase in adduct formation, however these levels increase less dramatically for the lower dose groups (75 and 150 mg/kg), since less reactive metabolite is formed in these animals than for the higher doses. At the highest dose, the levels of albumin adduct continue increasing even at 24 h, giving an indication of a decreased capacity for eliminating the reactive metabolite in these animals. This experiment clearly shows the viability of this approach to directly monitor acetaminophen covalent binding from *in vivo* samples.

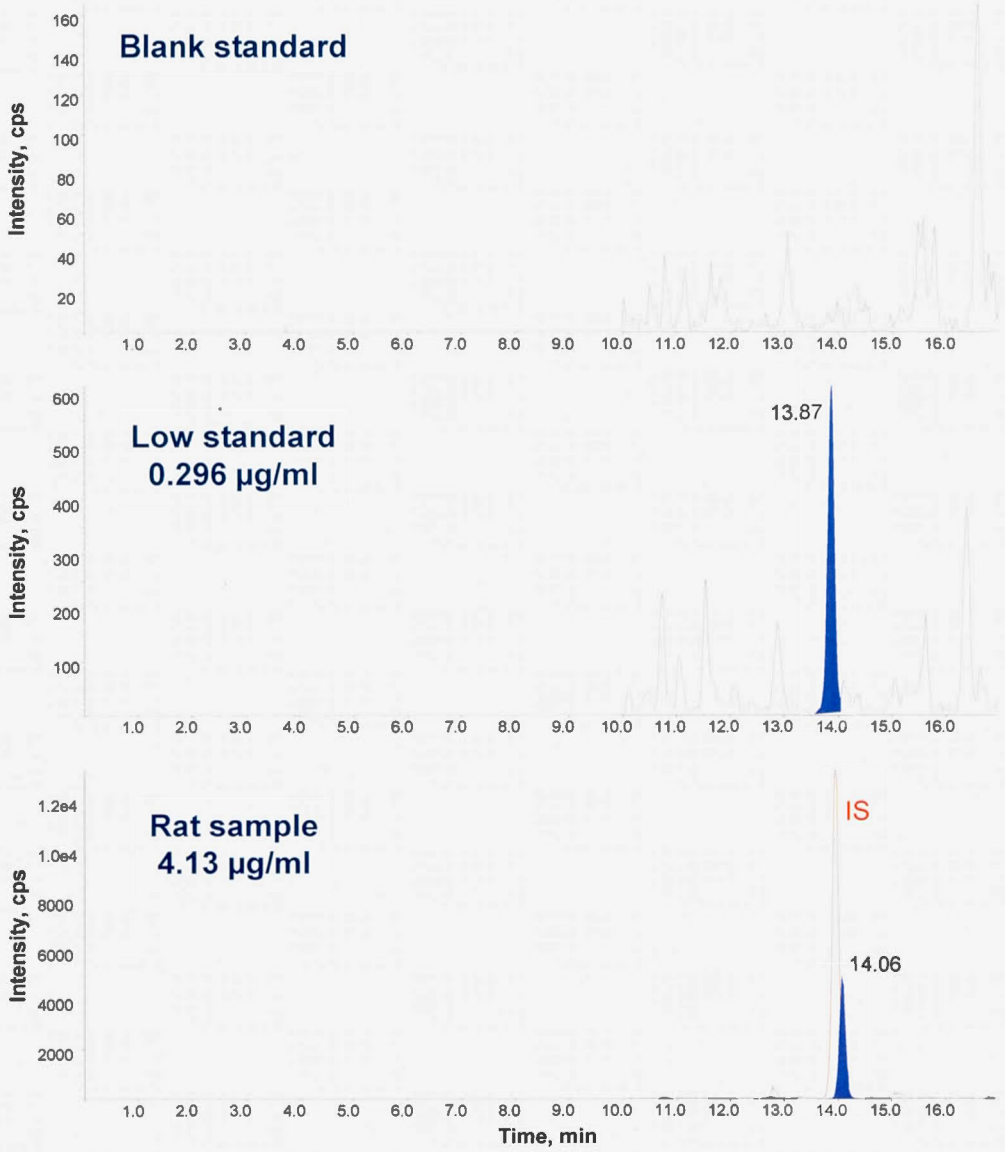

Figure 4.4. Representative chromatograms in a sample analysis run showing the MRM transition (*m/z* 579.8→917.4) used for quantitation of both NAPQI-LQKCPYEE (sample) and iodo-APAP-LQKCPYEE (standard). Rat sample chromatogram also shows the MRM transition (*m/z* 581.8→921.4) for the internal standard (IS, $_{D4}$-iodo-APAP-LQKCPYEE).

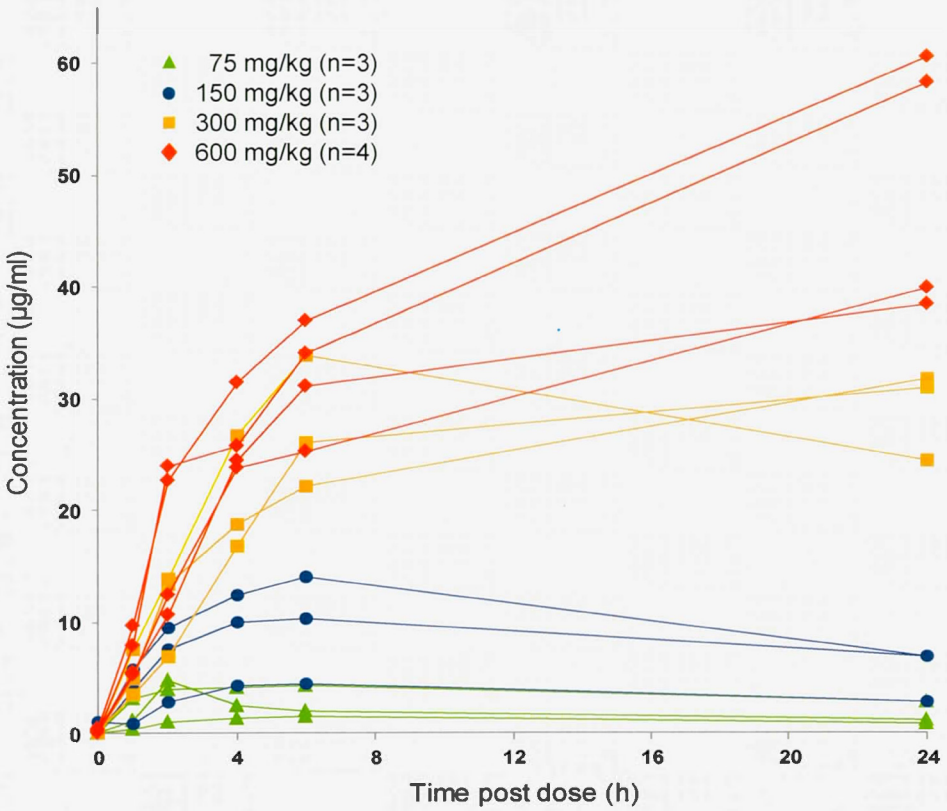

Figure 4.5. Measured concentrations for NAPQI-adducted albumin in rat plasma for 4 different acetaminophen (IP) dosing groups sampled over a 24 h time period (color legend in title).

4.6 CONCLUSIONS

A method has been described for the absolute quantitation of NAPQI-modified serum albumin. This work represents the first absolute quantitation of a modified protein (with very low modification stoichiometry) using a targeted isotope dilution LC-MS/MS assay. A customized alkylation reagent was used to create a surrogate

standard, enabling absolute quantitation of the extent of acetaminophen-induced covalent binding to albumin *in vivo*. The applicability of the method was verified by measuring plasma levels of NAPQI-RSA in rats dosed with acetaminophen. Following this proof of concept study in rat, an analogous assay is being developed and further validated for the quantification of NAPQI-modified human serum albumin for use in clinical studies.

CHAPITRE V

PURIFICATION OF PEPTIDES VIA CLICK CHEMISTRY FOR THE IDENTIFICATION OF PROTEINS COVALENTLY MODIFIED BY REACTIVE METABOLITES IN HUMAN LIVER MICROSOMES

Ce chapitre présente le développement d'une nouvelle méthodologie pour purifier sélectivement des peptides qui ont été modifiés par des sondes pouvant former des métabolites réactifs. Cette méthodologie a pour but de permettre l'identification des protéines microsomales modifiées par ces sondes lors d'incubations *in vitro*. Les résultats obtenus feront partie d'une publication à être soumise à une date ultérieure.

Sous la supervision de la professeure Lekha Sleno, mes responsabilités lors de ce projet incluaient: d'effectuer toutes les expériences, les analyses LC-MS/MS et le traitement de données. Tze Chieh Shiao, grâce à la collaboration avec le laboratoire du professeur René Roy, a effectué toutes les synthèses des produits non disponibles commercialement.

5.1 INTRODUCTION

There is presently a lack of information regarding the identity of proteins targeted by reactive metabolites. It has been postulated that reactive metabolites of different structures modify different proteins, which could explain the varying toxic effects that are triggered by these species. As was discussed in the introduction, methods so far have either lacked the sensitivity required to sequence the peptides modified by reactive metabolites or have used probes that were not structurally related to compounds known to form these species. This chapter discusses a methodology, based on click chemistry, which will allow selective purification of peptides from digested proteins that are covalently modified by reactive metabolites in microsomal incubations.

The general purpose for which we want to selectively purify peptides modified by reactive metabolites is evidently to eliminate the presence of those originating from unmodified protein in the incubated sample. These unmodified peptides are present in relatively high concentrations and thus impede our ability to analyze modified peptides by LC-MS/MS. The resulting increase in sensitivity by removing matrix effects (ion suppression) from background peptides is necessary to detect and properly sequence modified peptides by mass spectrometry, thus pinpointing the site of modification.

The main problem with previous work having reported the selective purification of modified protein is their use of probes that aren't structurally similar to compounds relevant to toxicity. Furthermore, the electrophilic functionalities of these probes are not generated via metabolism. In order to gain information relating the structure of drugs to their downstream toxicities, probes must be designed to be structurally similar to drugs known to form reactive metabolites. This not just important to obtain

more relevant protein identifications from *in vitro* liver microsomal incubations, but electrophilic probes generated by metabolism also have the potential to be used to identify relevant protein targets from *in vivo* samples.

Click chemistry was first introduced by Sharpless' group and essentially refers to any reaction that uses simple building blocks with specific functional groups which efficiently react together in a predictable manner (Kolb *et. al.*, 2001). Click chemistry has gained widespread popularity in several areas of research (Iha *et. al.*, 2009; Meldal and Tornoe, 2008) and the copper-catalyzed azide-alkyne Huisgen cycloaddition reaction (CuAAC) is the most commonly used reaction fitting these criteria (Moses and Moorhouse, 2007). The reliability, specificity and biocompatibility of this reaction render it a viable avenue for the purpose of purification from complex biological mixtures (van Dijk, 2009) and it has been applied to the modification of protein and peptides (Ahmad Fuaad, 2013). The general scheme of the CuAAC reaction is shown in Figure 5.1. One of the reasons this reaction is well suited for bioconjugation is the absence of alkyne and azide functional groups in biological matrices, ensuring the specificity required when selectively targeting molecules in complex biological matrices.

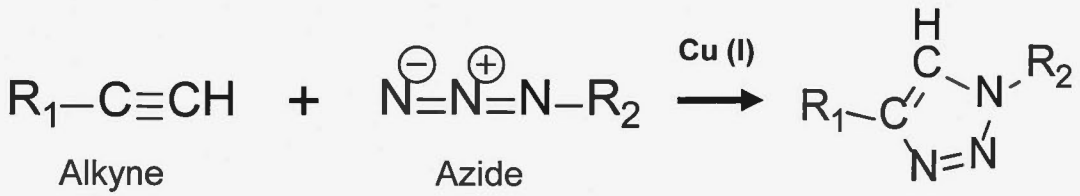

Figure 5.1. The Copper catalyzed azide-alkyne cycloaddition (CuAAC) reaction.

In order to implement the CuAAC reaction in a sample preparation procedure that will be able to purify peptides modified by reactive metabolites, we first need to design probes that contain either an alkyne or azide moiety. As we have stated, we want probes that are not only structurally similar to drugs, but also form analogous reactive metabolites to the model drugs. Since the alkyne moiety is less bulky and less polar than the azide, it was incorporated into two newly conceived probes (Figure 5.2). The first of these is an acetaminophen analog and the second contains a methylenedioxybenzene moiety, representing a very well characterized precursor of reactive metabolites from several related compounds (Kalgutkar *et. al.*, 2005). For both these probes, the alkyne was added in a region of the molecule where it will not interfere with the formation of the reactive metabolite nor binding to the target nucleophile. A third probe, ethinyl estradiol, is an alkyne-containing commercial drug used for birth control and is known to form reactive intermediates (Bolt and Kappus, 1974).

The next step was to devise a purification strategy using an azide-based purification agent. First, we have added an azide group onto a biotin-containing molecule. Biotin's specific and high affinity towards avidin and some of its analogous proteins is very well documented. It is therefore widely used in biochemistry laboratories in order to affinity purify a wide range of molecules from biological matrices. In fact, while the "biotin-N_3" molecule presented here is custom synthesized, closely related structures are commercially available. The use of click chemistry for subsequent purification of target molecules in complex mixtures has been demonstrated previously (Hong *et al.*, 2009). The second purification agent is a resin containing an azide group and featuring a linker region with a disulfide bond. This way, following the CuAAC reaction with the target alkyne, the solid-phase resin can be thoroughly washed to remove any molecules not covalently linked to the resin. Subsequently, the alkyne can easily be released by the cleavage of the disulfide bond present in the linker region with the addition of a reducing agent, such as dithioreitol (DTT). Figure

5.2 shows the chemical structures of the different molecules to be used in our click-based purification strategy for detecting and identifying protein targets of reactive metabolites.

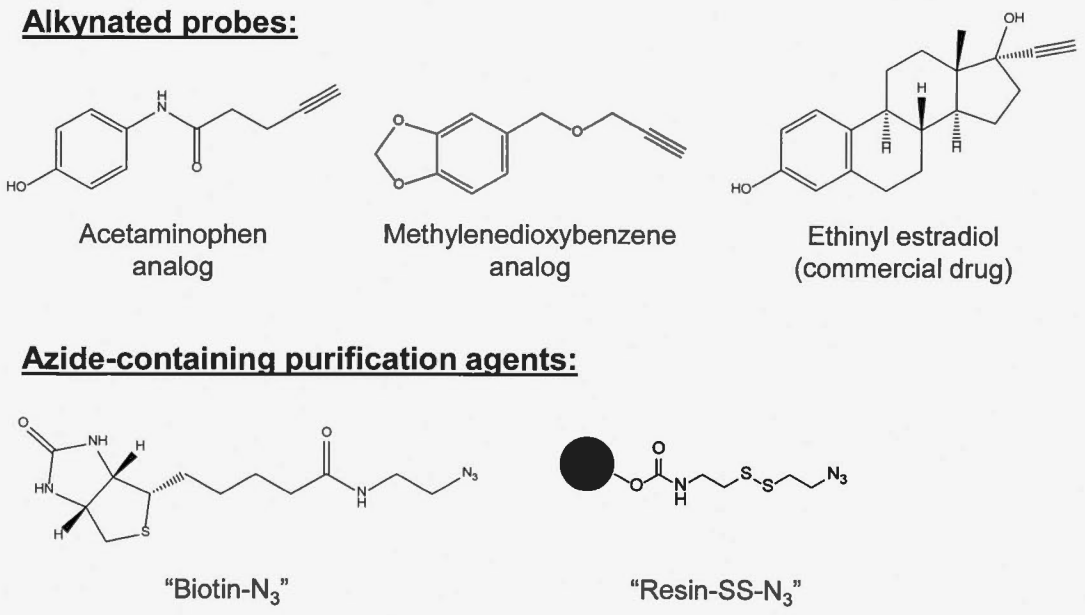

Figure 5.2. Chemical structures of probes and purification agents.

With these chemical tools in hand, we can test the feasibility of the approach as it is applied to the identification of reactive metabolite protein targets in microsomal incubations. An overall scheme summarizing the envisioned strategy is illustrated in Figure 5.3. In the proposed strategy, the purification of modified peptides is performed after digestion of the entire microsomal protein fraction following *in vitro* incubations of alkyne-containing drug analogs. Another viable strategy would be to perform the click chemistry-based purification prior to digestion. The advantage of this alternative strategy is the higher statistical confidence for the identification of

targeted proteins by automated proteomic data analysis software, since each protein will likely have multiple peptides sequenced. There are two main disadvantages in performing the purification step at the protein level. The first is that the click chemistry reaction can be kinetically (and sterically) hindered by size and conformation of the individual target proteins, with the possibility that the environments of the modifications on different protein targets will bias the efficiency of the reaction. The second disadvantage relates to the detection and sequencing of the peptide containing the modification. Purifying proteins, while increasing the chances of obtaining confident protein identification, lowers the chances of sequencing the actual site of modification. The amount of unmodified peptide in our processed sample will still be much greater than the amount of modified peptides. By purifying the modified peptides directly, we increase their relative concentration and thus increase the chances of acquiring high quality MS/MS spectra. Pinpointing the site of modification validates the protein as a covalent target, without which we cannot truly confirm that we have identified a modified protein.

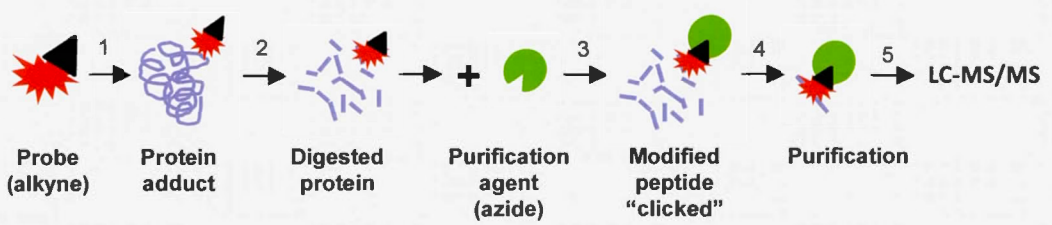

1. Microsomal incubation
2. Digestion of microsomal protein
3. Click chemistry reaction (CuAAC)
4. Affinity purification or resin-based purification
5. Peptide sequencing and identification of targeted microsomal proteins

Figure 5.3. Proposed strategy to identify microsomal protein targets of reactive metabolites.

The results presented herein are meant to prove the feasibility of this proposed strategy in three steps. First, the conditions of the CuAAC reaction for peptides containing an alkyne group reacting with "biotin-N_3" were optimized. Subsequently, the fragmentation patterns of peptides containing a click chemistry modification were studied, to ensure that these peptides can be sequenced by tandem mass spectrometry. Then, the feasibility of performing click chemistry efficiently in a protein digest and subsequently sequencing the resulting products is demonstrated. Finally, our alkyne-containing probes are tested for their ability to generate the anticipated reactive metabolites and related glutathione adducts in microsomal incubations, and assess that our optimized conditions are able to efficiently conjugate these glutathione adducts from a complex microsomal incubation.

5.2 EXPERIMENTAL

5.2.1 MATERIALS

Bovine serum albumin (BSA), ammonium bicarbonate, iodoacetamide (IAM), methanol, aminoguanidine, name TBTA, ethinyl estradiol, sodium ascorbate, copper sulfate, ammonium hydroxide, phosphoric acid, β-nicotinamide adenine dinucleotide 2′-phosphate reduced tetrasodium salt (β-NADPH), reduced L-glutathione (GSH), DMSO, sodium carbonate, formic acid (ultra-pure), potassium phosphate (monobasic), potassium hydroxide and dithiothreitol (DTT) were obtained from Sigma-Aldrich (Oakville, ON). Rat liver microsomes were purchased from BD Biosciences (Mississauga, ON) or Bioreclamation LLC (Baltimore, MD). HPLC grade acetonitrile (ACN) and potassium chloride were purchased from Caledon (Georgetown, ON). Acetone was obtained from Fisher Scientific (Ottawa, ON) and nanopure water was prepared from a Millipore Synergy® UV system (Billerica, MA).

The following compounds were generously provided by the medicinal chemistry and organic synthesis laboratory of Prof. René Roy at UQÀM (custom synthesized by Tze Chieh Shiao):

Custom peptides: QACAFK, QNCAFK, QACDFK, QQCPFDEHVK; Custom alkynes: acetaminophen analog, methylenedioxybenzene analog, Iodoacetamide analog "IPM", and *N*-ethyl maleimide analog "NPM"; Custom azides: "resin-SS-N_3", "resin-SS-N_3" analog (2-(2-Azido-ethyl-disulfide)), biotin analog "biotin N3"; as well as the ligand, THPTA (3 [tris(3-hydroxypropyltriazolylmethyl)amine).

5.2.2 COPPER ASSISTED AZIDE-ALKYNE CYCLOADDITION (CUAAC) REACTION

A series of experiments were performed in order to optimize the conditions of the CuAAC reaction between peptides containing an alkyne moiety and azides that can act as purifying agents in different matrices. The following section discusses the important aspects of this reaction with regards to our experimental requirements. The final optimized CuAAC conditions used are presented in Figure 5.5 (see results). Briefly, the sample containing the alkynated peptides are solubilized in buffer (100 mM HEPES, pH 7.5) and an appropriate concentration of azide is added. Aminoguanidine and sodium ascorbate are added at a final concentration of 5 mM. The last thing added to the reaction is a copper/THPTA mixture (pre-incubated together for 30 minutes at room temperature). The tubes are immediately closed and placed in a temperature controlled incubator for 2 h. Typically, the reaction volume is 200 µl and the total percentage of organic solvent did not exceed 10% (azides are solubilized in DMSO).

5.2.3 LIVER MICROSOMAL INCUBATIONS:

Rat liver microsomal incubations (1 mg/mL protein) were performed with 10 µM probe (acetaminophen analog, methylenedioxybenzene analog, or ethinyl estradiol), 1 mM NADPH (absent in controls) and 1 mM GSH (or GSH-Br) for 2 h at 37°C in a phosphate-buffered solution (50 mM, pH 7.4) and a total volume of 250 µL. Samples were then quenched with an equal volume of ice-cold ACN and centrifuged at 13000 rpm for 10 min. Supernatant was evaporated to dryness using a model RC10.10 centrifuge concentrator (Jouan, Winchester, VA, USA) and reconstituted in 250 µL water for subsequent purification by solid phase extraction on Oasis HLB cartridges (1cc, 30 mg) with methanol elution (1 ml), or directly in 10% acetonitrile for injection by LC-MS/MS.

5.2.4 PEPTIDE PREPARATION

Appropriate concentrations of custom peptide or BSA were solubilized in 100 mM ammonium bicarbonate buffer pH 8.5, treated with DTT (at double the concentration of free thiols in the sample) and placed in a thermomixer (Eppendorf, Mississauga, ON) for 15 min at 37°C. IPM, NPM or IAM (the latter in the case of BSA digests used as background matrix) was added at three times the concentration of DTT. Samples with IPM or IAM were incubated at 37°C for 45 minutes in the dark, while NPM-containing sample were left to react at room temperature for 45 minutes.

Custom peptides modified with alkyne were then purified by HLB solid phase extraction in order to remove DTT and excess alkylating agent. BSA samples were digested overnight with trypsin (1:40 enzyme-to-protein ratio) for 18 h at 37 °C

before SPE. Samples were then reconstituted in appropriate solvents and concentrations to perform subsequent tests.

5.2.5 LC-MS/MS ANALYSIS

Samples were separated using a Shimadzu Nexera HPLC system on a solid-core Phenomenex Kinetex® C18 column (150 x 2.1 mm with 2.6 micron particles), at a flow rate of 0.3 ml/min with a water/acetonitrile gradient containing 0.1% formic acid. The gradients varied depending on the analyte (peptides or metabolites) and the sample matrix (click reaction media, complex peptic digests or microsomal incubations), but all incorporated mobile phases starting at 5% ACN (held for 3 min), followed by an increase to 80-95 % in 12-25 minutes. The gradient was then held at the maximum ACN concentration for 3-5 minutes before re-equilibration.

Most MS and MS/MS spectra were collected on a high-resolution hybrid quadrupole-time-of-flight (QqTOF) TripleTOF® 5600 mass spectrometer (AB Sciex, Concord, ON, Canada) equipped with a DuoSpray™ ion source in positive ion mode. The instrument performed a survey TOF-MS acquisition from *m/z* 140–1250 with an accumulation time of 250 ms, followed by MS/MS on the ten most intense ions with +1 to +4 charge states from *m/z* 250–1250 using information-dependent acquisition (IDA) with dynamic background subtraction (DBS). Each MS/MS had an accumulation time of 100 ms and collision energy ranging from 20 to 40 V, depending on the charge state and mass of the product ion. The total cycle time was 1.3 s.

Fragmentation data from custom peptides containing click chemistry modifications were acquired on a 5500 QTRAP in positive TurboIon spray mode (CUR 30, TEM

500, GS1/GS2 50, CAD 6). Collision-induced dissociation was performed on 2+ charge states of each peptide with collision energies of 18 and 25V in MS/MS mode.

5.3 RESULTS AND DISCUSSION

5.3.1 OPTIMIZATION OF CUAAC REACTION

While the CuAAC reaction has frequently been used for various types of bioconjugation reactions, it is imperative to optimize the reaction conditions depending on the application. The optimization of the reaction is not trivial and a detailed and very helpful paper by the Finn group (Presolski *et. al.*, 2011) has previously outlined the major issues arising for this reaction in bioconjugation applications. Before describing the optimization of our finalized reaction conditions, two main areas of greatest concern for optimal results are discussed.

Copper catalyst:

Copper in its +1 oxidation state catalyzes the CuAAC reaction. This is a crucial aspect of the reaction, especially when used for bioconjugation reactions. Sodium ascorbate is added to the reaction mixture, as a reducing agent capable of generating Cu(I) from Cu(II) present in the sulfate salt. After catalyzing the reaction, Cu(I) becomes Cu(II) so the reducing agent is also needed to regenerate Cu(I) in its catalytic cycle. Also, complex biological matrices contain a range of molecules with functional groups that can oxidize Cu(I) back to Cu(II). Disproportionation of Cu(I) also readily occurs in solution. Sodium ascorbate is therefore crucial in sustaining an appropriate concentration of the copper catalyst in the desired oxidation state and is added at high concentrations to the reaction mixture.

Sodium ascorbate alone is not sufficient to ensure that there is a high enough concentration of Cu(I) when performing the reaction in complex biological matrices. Aminoguanidine is often added to samples in order to occupy some of the chemical groups that can oxidize Cu(I), such as amines, in biological samples. Dissolved oxygen is also capable of oxidizing Cu(I) and care must be taken to protect the sample from too much exposure to air. Lastly, and perhaps most importantly, a Cu(I)-chelating ligand is needed in order to stabilize the oxidation state of Cu(I), prevent the formation of by-products and sequester Cu ions to prevent biomolecule damage. The ligand that is routinely used in aqueous bioconjugation reactions is THPTA (see Figure 5.5 for structure).

Substrate concentrations:

We have previously estimated that in a typical microsomal incubation of a drug (10-50 μM), on the order of 1 μM of reactive metabolites are likely formed. While the CuAAC reaction is an efficient and specific process, we must be realistic in our expectations in terms of substrate concentrations and current literature states that 1 μM is within the limitations in performing this reaction for bioconjugation purposes (Presolski *et. al.*, 2011). It is therefore important to determine to what degree we can decrease the concentration of the alkyne-containing peptide and still have an efficient reaction. Furthermore, while we should add an excess of azide to ensure the maximum amount of alkyne has reacted, the concentration of azide must also be minimized when using the "biotin-N_3" due to the high cost of avidin-containing products using for affinity purification. We also want to avoid that affinity purification be dominated by unclicked biotin. This highlights the main advantage associated with the purification strategy using resin azides, since we can, in theory, simply add a large excess of resin-azide to help push the efficiency of the reaction, even if the kinetic barrier is intrinsically higher.

Optimization:

Purified peptide standards containing alkyne groups on modified cysteines were used for optimizing the conjugation reaction of alkynated peptides. A simple and efficient way to introduce an alkyne group as a modification on the cysteine residue was using the alkyne-containing analogs of two common cysteine alkylating agents, iodoacetamide and *N*-ethyl-maleimide (Figure 5.4). These molecules are able to efficiently and quantitatively bind to free cysteine thiols in order to introduce an alkyne group into the modified peptide, allowing known concentrations of modified peptides to be produced for CuAAC reaction tests.

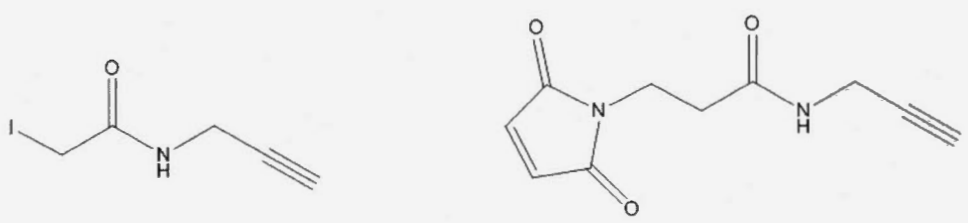

Iodoacetamide (IAM) analog

N-Ethylmaleimide (NEM) analog

Figure 5.4. Structures of cysteine modifiers used to introduce an alkyne moiety on peptides.

The optimized reaction parameters were determined through numerous tests. Each component of the reaction was assessed by comparing the efficiency of the reaction on the custom peptides. These tests were performed both in pure buffer and, since the reaction will eventually be performed following protein digest, in a peptide mixture comprised of 250 μg digested BSA (alkylated with IAM), representing the amount of protein material present in a typical microsomal incubation. The final experimental

conditions (Figure 5.5) have been determined to reproducibly and completely conjugate all tested peptide-alkynes in a background matrix of 250 µg of digested BSA. The criterion for complete reactivity was the absence of a significant peak coming from unreacted alkynated peptide after LC-MS/MS analysis, while of course ensuring that the product of the reaction is present with the highest possible abundance (relative to all tests performed).

Alkyne concentration (modified peptides,100% yield): 2µM
Azide concentration (biotin N_3): 300 µM (or 3x [alkyne])
Copper ($CuSO_4$): 200 µM
THPTA (pre-incubated with $CuSO_4$): 1 mM
Sodium ascorbate: 5 mM
Aminoguanidine: 5 mM
Reaction time: 2h
Temperature: 40 C
Buffer: 100 mM HEPES, pH 7.5
Volume: 200 µl, in 0.5 ml tubes, closed immediately

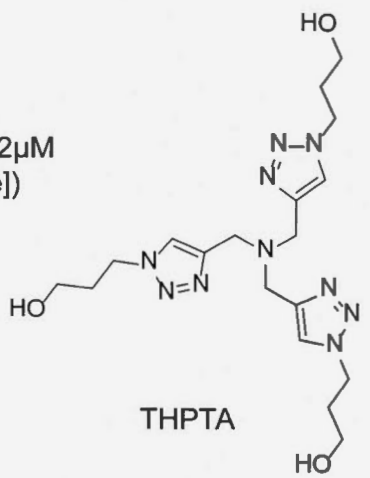

THPTA

Figure 5.5. Optimized click chemistry conditions.

Most of the above optimized parameters fit within the current standard for the reaction in a bioconjugation setting. In order to minimize the exposure to ambient oxygen, 0.5 ml tubes were used and were immediately closed following the addition of the Cu/ligand mixture and this proved to be an important aspect of the procedure. Increasing the concentrations of sodium ascorbate, aminoguanidine, copper or ligand did not prove to produce an increased signal for click products, as was also seen for an increase in reaction time or temperature. Most importantly, the lower limit of

alkyne concentration (2 μM), falls within the expected limits of the reaction. While this concentration may seem not to be low enough for this application, there is some experimental flexibility to increase the concentration of alkyne in the reaction medium. Considering that the reaction is performed in peptide digests, the sample can be easily concentrated prior to bioconjugation as opposed to if bioconjugation were to be performed on undigested target proteins. Furthermore, it is possible to increase the concentration of the probe in incubations. These optimized conditions are therefore primed to be employed to bioconjugate the listed target alkyne-containing probes in microsomal incubation samples.

The glaring omission in this section is any discussion pertaining to the click reaction performed with "resin-SS-N_3", since preliminary tests showed that the CuAAC reaction was not very efficient with this purification agent in its current form. This is likely a result of the polystyrene-based polymer of the designed resin that does not swell very well in aqueous media and consequently prevents the reaction from occurring efficiently. Second generation "resin-SS-N_3" are currently being designed for future testing.

5.3.2 FRAGMENTATION OF MODIFIED PEPTIDES

Once the CuAAC reaction optimized, the fragmentation of the click-modified peptides was studied. As it has been mentioned earlier, it is essential that these peptides be sequenced to be able to determine the identity of its protein of origin. We also need to confirm the presence and location of the modification.

Initial fragmentation tests were performed on all custom peptides, modified with IPM and NPM and then subsequently "clicked" with "biotin-N_3" and (2-(2-Azido-ethyl-disulfide)). This means there were four modification possibilities for each peptide. As

shown in Figure 5.6, 2-(2-Azido-ethyl-disulfide) is an azide designed to mimic the modification that would arise after purification with "resin-SS-N_3" and subsequent cleavage with DTT. The two different alkylating agents were important to have in order to test if the structure of the reactive metabolite modification would influence the fragmentation of the peptide. Also, the custom peptide sequences not only mimic tryptic peptides (with C-terminal lysine), but they mostly only differ from each other by the amino acids adjacent to the cysteine residue, to verify if those positions influence the fragmentation of the modified peptides.

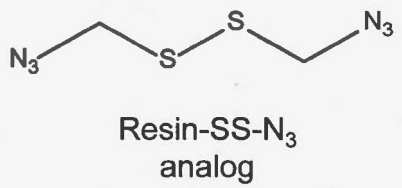

Resin-SS-N_3
analog

Figure 5.6. Structure of 2-(2-Azido-ethyl-disulfide).

In all of the modified peptides, the major y- and b-ions (from the cleavage of amide bond in peptide backbone) were detected allowing the peptide to be sequenced and the location of the modification to be found. Figure 5.7 and 5.8 illustrate two typical peptide MS/MS spectra, one for a peptide containing an IPM-"biotin-N_3" modification, the other with the NPM/resin-SS-N_3 modification.

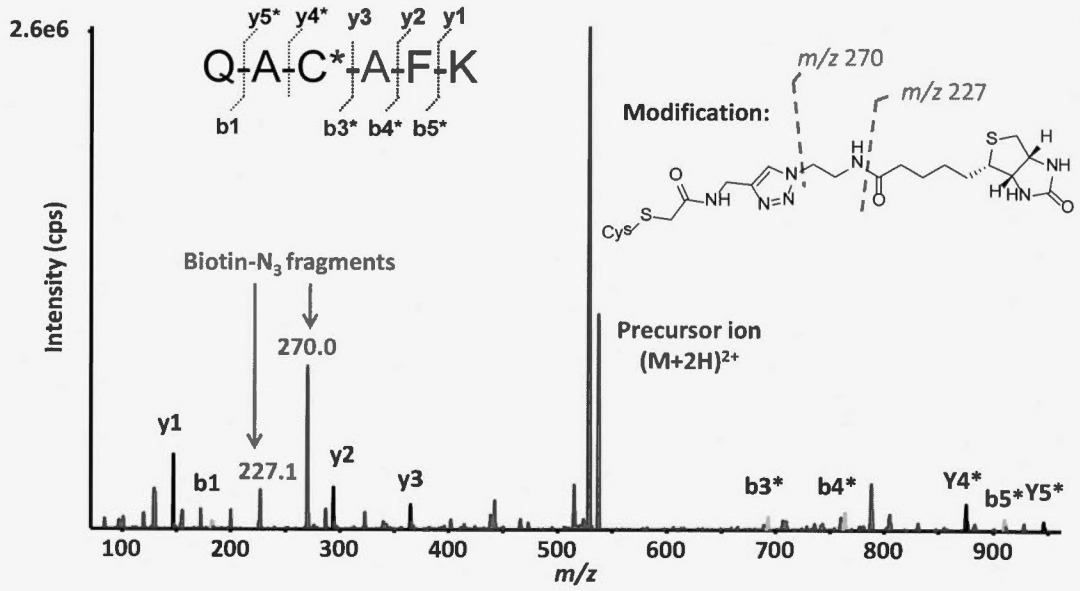

Figure 5.7. MS/MS spectrum of a typical custom peptide (QACAFK) with an IPM/biotin-N_3 modification.

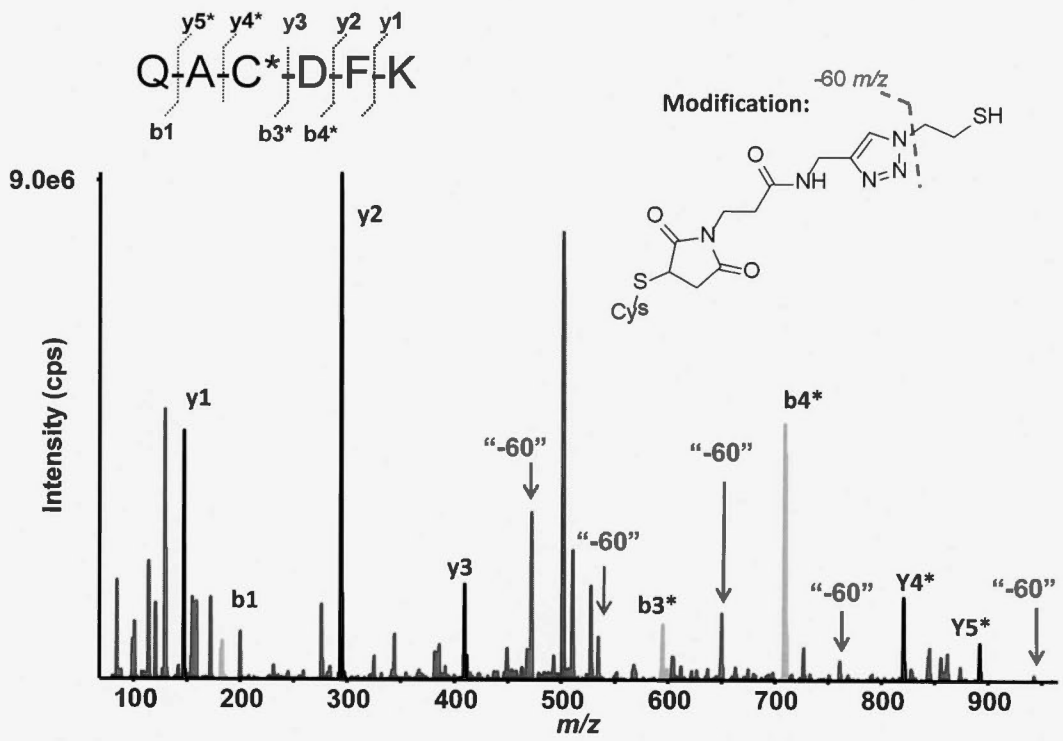

Figure 5.8. Typical MS/MS spectrum of a custom peptide (QACNFK) with an NPM/resin-SS-N_3 modification.

These spectra not only clearly show the presence of y- and b-ions needed for peptide sequencing by MS/MS, but also show that each modification provides diagnostic peaks helping confirm the presence of the specific modification. The triazole ring induces fragmentation adjacent to the N at the 1' position of the ring, resulting in the appearance of a sensitive diagnostic ion of *m/z* 270 for the modifications containing "biotin-N_3" and a series of neutral losses of 60 Da for modifications containing the resin-SS-N_3-like modification. In the case of "biotin-N_3", the abundant diagnostic ions (there is another one at *m/z* 227 resulting from the cleavage of the peptide bond

in its linker region), do not only indicate the presence of the "biotin-N_3" but could also be exploited to implement data-dependent acquisition strategies in future analyses of complex samples to increase the likelihood that the automated method would trigger the acquisition of MS/MS spectra for modified peptides of interest. The other noteworthy feature in the spectra from the peptides containing "biotin-N_3" is they tend to require higher collision energies than their "un-clicked" counterparts. As seen in Figure 5.7, the peaks corresponding to the precursor ion (and of the precursor-NH_3) are by far the two largest peaks in the spectrum. Acquiring MS/MS data using greater collision energy could increase the overall sensitivity of ions for sequencing purposes. The diagnostic neutral losses of 60 Da on the other hand could be a disadvantage since these losses complicate the spectra, potentially posing a problem for automated proteomics software.

Next, an experiment was designed to test both the optimized reaction conditions on a tryptic digest and the sequencing ability of the resulting modifications by LC-MS/MS. To do this, a digest of IPM-modified BSA was employed and the CuAAC reaction was performed at a concentration of 10 μM alkyne. Assuming complete digestion, each individual tryptic peptide containing a cysteine residue (and thus an alkyne) has a maximal concentration of 285 nM. These samples were then analyzed to verify if the click reaction was efficient and clicked tryptic peptides could be sequenced. The ten most abundant cysteine-containing peptides were chosen for data analysis, testing a large diversity of peptide sequences than with custom peptides previously employed.

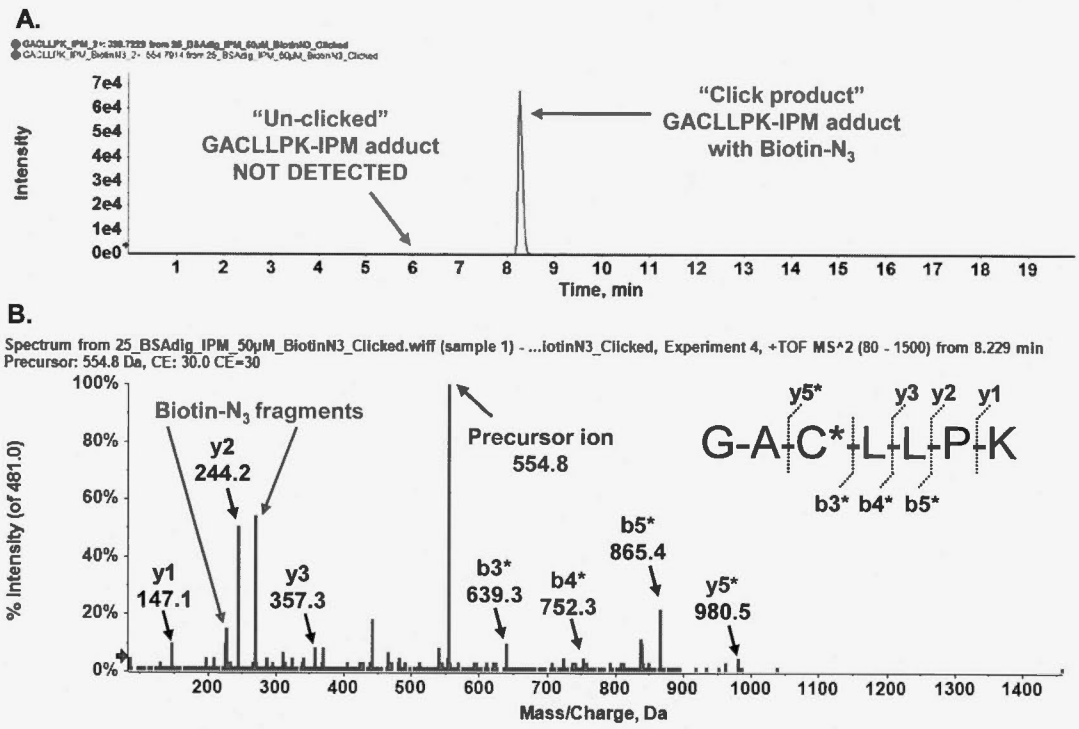

Figure 5.9. Typical IPM-modified BSA tryptic peptide (GACLLPK) in the clicked protein digest: A. Extracted ion chromatogram of the modified peptide and its click product with biotin-N_3. B. MS/MS spectra (CE 30V) of the doubly charged click product (GACLLPK-IPM-biotin-N_3)

The click reaction was proven to be efficient under these conditions for all monitored peptides. At the same time, each of the peptides was sequenced using MS/MS spectra automatically triggered by the acquisition software in data-dependent mode. Figure 5.9 shows the results from a typical tryptic BSA peptide. It clearly demonstrates, that, under the optimized conditions, we are able to conjugate and sequence peptides from a real digest.

5.3.3 DRUG ANALOGS AS PROBES

Our drug analogs were designed to contain alkyne moieties that would least hinder the formation and reactivity of their predicted reactive metabolites. In order to prove the usefulness of these probes, the formation of these reactive metabolites was demonstrated in microsomal incubations. The three alkyne-containing drugs (analogs) were incubated with glutathione as a trapping agent to detect the formation of reactive metabolites. In all three cases, the formation of the predicted reactive metabolites was demonstrated, as shown in Figure 5.10.

This experiment proves that, using these alkyne-containing molecules, metabolism-dependent reactive metabolites can be produced that are structurally and reactively similar to those formed by real model precursor drugs. These reactive metabolites will be able to bind free protein thiols without losing the alkyne moiety during metabolism, rendering them accessible to conjugation via click chemistry.

The ability to perform the optimized click reaction on these GSH-probe adducts was then investigated. Alkyne-containing drugs were incubated at 10 μM, and the sample was diluted to adjust the concentration of alkyne in the click reaction to 2 μM. In this way, the reaction was tested for its efficiency in a media derived from a microsomal incubation at the lower limit of concentrations determined in a tryptic digest. Glutathione being a tripeptide makes it an ideal surrogate for a modified digested peptide. This test was performed with the acetaminophen alkyne analog and the results are shown in Figure 5.11.

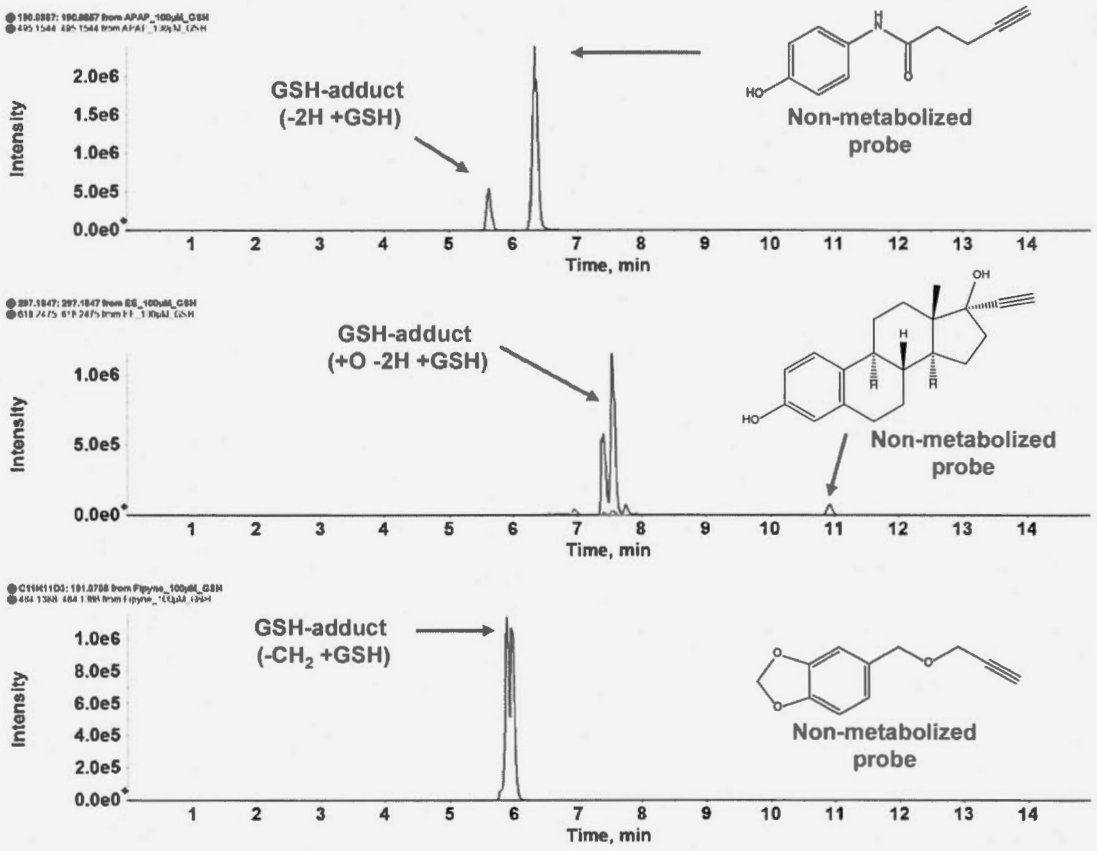

Figure 5.10. Glutathione adducts formed by alkynated probes following *in vitro* incubation with rat liver microsomes.

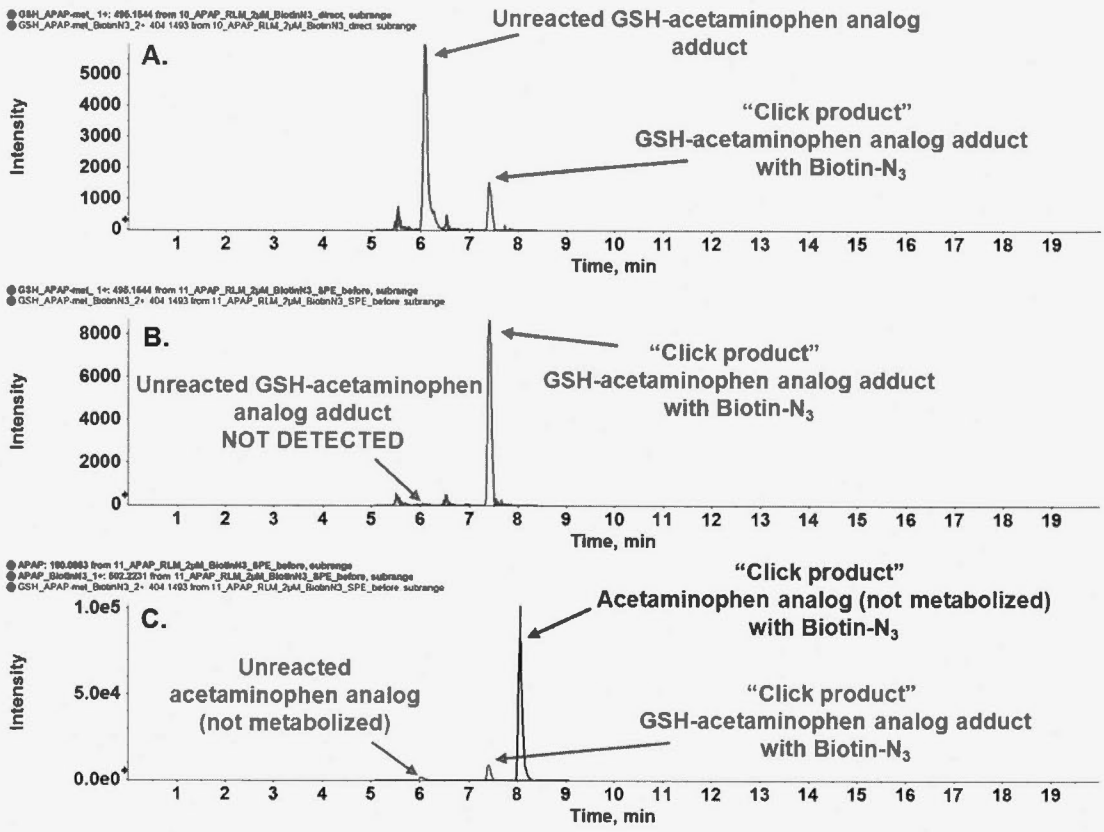

Figure 5.11. Efficiency of the optimized CuAAC reaction with the GSH-acetaminophen analog (probe), formed in microsomal incubations, as substrate (A. without SPE cleanup; B. reaction performed after SPE cleanup; C. reaction after SPE cleanup showing non-metabolized click products).

We can see in Figure 5.11A that the first attempt to perform the CuAAC reaction with the probe's GSH adducts did not work very well. While there were some products formed, the reaction was not very efficient in this matrix at tested (low) concentrations. To verify if the click reaction was affected by the complexity of the matrix, a reverse-phase SPE cleanup of the same sample was performed. Figure 5.11B shows that this simple cleanup step was sufficient to rid the matrix of

interferences. It is important to note that SPE cleanup was also performed for each of the digests previously tested as background for the reaction.

5.4 CONCLUSIONS AND ONGOING WORK

The tests described in this chapter have proven the feasibility of this novel approach to be able to identify protein targets from biologically-relevant samples. First, we have established CuAAC reaction parameters allowing us to conjugate target peptides according to the proposed strategy at relevant concentrations. Subsequently, we have proven that peptides containing these modifications can be sequenced and the site of modification be pinpointed. And last, we demonstrated that the alkyne-containing drugs could form the expected reactive metabolites and that their GSH adducts could be conjugated using the optimized click chemistry reaction.

Ongoing work will now focus on adapting this strategy into an established proteomics workflow proven to be able to identify a large number of proteins from microsomes. One such method has recently been submitted for publication by our group. This method has identified the highest number of proteins within a 1% false discovery rate (FDR) for human, rat and mouse microsomes with high sequence coverage (23-30%). Figure 5.12 shows a scheme outlining the major steps of this proteomics procedure and the steps that will be adapted in the method. Once the method is tailored to this specific application, the proteomics experiment will be performed to identify proteins covalently modified by the alkyne-containing model drugs.

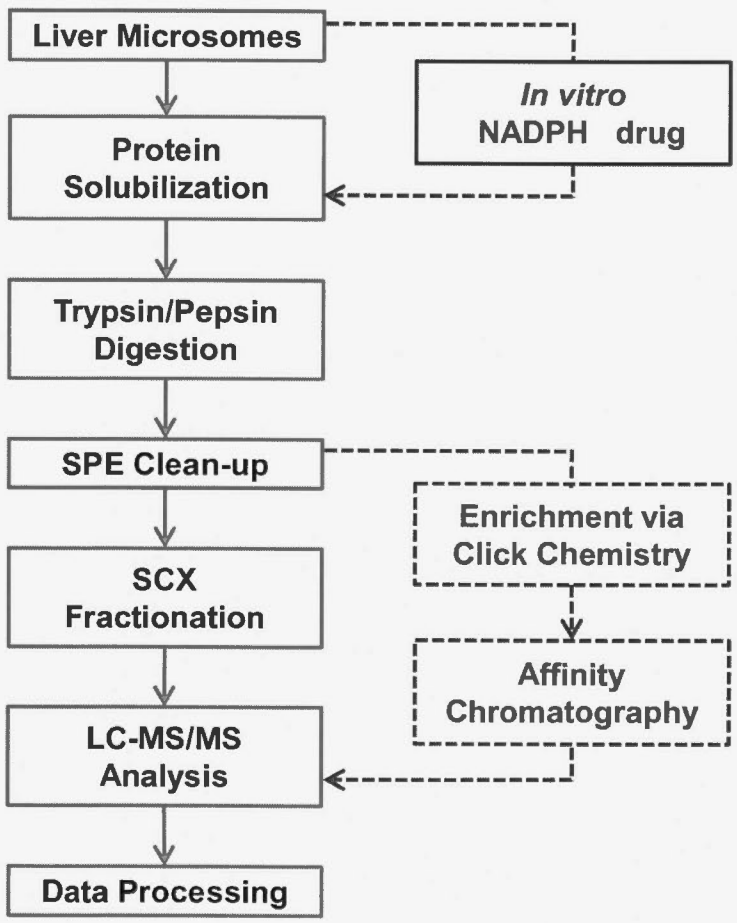

Figure 5.12. Adaptation of an established proteomics method together with the use with our click chemistry based purification for the analysis of microsomal protein targets of reactive drug metabolite (dashed lines represent steps to be incorporated).

CHAPITRE VI

ARTICLE SCIENTIFIQUE: "DETERMINATION OF ISOTOPIC LABELING OF PROTEINS BY PRECURSOR ION SCANNING LIQUID CHROMATOGRAPHY/TANDEM MASS SPECTROMETRY OF DERIVATIZED AMINO ACIDS APPLIED TO NUCLEAR MAGNETIC RESONANCE STUDIES"

André LeBlanc[1], Alexandre A. Arnold[1], Bertrand Genard[2], Jean-Bruno Nadalini[2], Marc-Olivier Séguin Heine[1], Isabelle Marcotte[1], Réjean Tremblay[2], Lekha Sleno[1]*

[1]Université du Québec à Montréal, Chemistry Department, Montréal, QC, Canada
[2]Université du Québec à Rimouski, Institut des sciences de la mer de Rimouski (ISMER), Rimouski, QC, Canada
*Université du Québec à Montréal, Pharmaqam, Chemistry Department, P.O. Box 8888, Downtown Station, Montréal, Québec, Canada H3C 3P8

Article published in:
Rapid Communications in Mass Spectrometry 2012, 26, 1165-1174.

Received: September 11, 2011
Accepted: February 16, 2012

Cet article présente une méthodologie pour mesurer le taux d'incorporation de ^{13}C dans des protéines par LC-MS/MS. Cette méthode est plus performante et plus sensible que ceux qui existaient dans la littérature et elle a été conçue pour soutenir des études structurales de protéines effectuée par RMN. Nous démontrons l'utilité de cette méthode en mesurant le taux d'incorporation de ^{13}C dans les protéines d'algues et de byssus de moules.

Sous la supervision de la professeure Lekha Sleno, je fus responsable de la conception de la méthode analytique et la rédaction du manuscrit, ainsi que de la plupart des manipulations, expérimentations et analyses de données. Le laboratoire du professeur Réjean Tremblay (Bertrand Genard et Jean-Bruno Nadalini) fut responsable de la culture et du prélèvement des échantillons biologiques. Le laboratoire de la professeure Isabelle Marcotte (Alexandre Arnold et Marc-Olivier Séguin-Heine), qui fut responsable de la partie biologie structurale (RMN) du projet, a participé à la manipulation et à la préparation des échantillons biologiques. Alexandre Arnold a aussi contribué à la rédaction de l'article.

6.1 ABSTRACT

Rationale:

A method has been developed for the quantitation of isotopic labeling of proteins using liquid chromatography/tandem mass spectrometry (LC/MS/MS) for the application of protein nuclear magnetic resonance (NMR) studies. NMR relies on specific isotopic nuclei, such as ^{13}C and ^{15}N, for detection and, therefore, isotopic labeling is an important sample preparation step prior to in-depth structural characterization of proteins. The goal of this study was to develop a robust quantitative assay for assessing isotopic labeling in proteins while retaining information on the extent of labeling for individual amino acids.

Methods:

Complete digestion of proteins by acid hydrolysis was followed by derivatization of free amino acids with 6-aminoquinolyl *N*-hydroxysuccinimidyl carbamate (AQC) forming derivatives having identical MS/MS fragmentation behavior. Precursor ion scanning on a hybrid quadrupole-linear ion trap platform was used for amino acid analysis and determining isotopic labeling of proteins.

Results:

Using a set of isotope-labeled amino acid standards mixed with their unlabeled counterparts, the method was validated for accurately measuring % isotopic contribution. We then applied the method for determining the ^{13}C isotopic content of algal proteins during a feeding study using $^{13}C_6$-glucose- or ^{13}C-bicarbonate-supplemented culture media as well as the level of labeling in mussel byssal threads obtained after feeding with labeled algae.

Conclusions:

This method is ideally suited for assessing the extent of protein labeling prior to NMR studies, where the isotopic labeling is a determining factor in the quality of resulting protein spectra, and can be applied to a multitude of different biological samples.

6.2 INTRODUCTION

Protein fibers such as silk, collagen or mussel byssal threads are complex biopolymers which have unique mechanical properties exquisitely tuned to the tasks that they perform (Gosline *et al.*, 2013; Arnold & Marcotte, 2009).These macroscopic properties are a consequence of the structure of these proteins at a molecular level. It is thus desirable to unravel their structure in order to produce bio-inspired synthetic materials, which can be achieved using solid-state nuclear magnetic resonance (SS-NMR). The major drawback of NMR is its lack of sensitivity, a weakness which can be offset by isotopic labeling. This strategy is routinely used in the study of large soluble proteins and becomes a compulsory step in the study of insoluble proteins such as silk or mussel byssal threads by high-resolution SS-NMR of carbon or nitrogen nuclei. The natural abundances of the NMR-active isotopes of these nuclei (^{13}C and ^{15}N) are only 1.1 and 0.37%, respectively, thus leading to very weak NMR signals. Isotopic enrichment not only directly increases the signal-to-noise ratio of the NMR spectrum; it has also a much more marked effect on the number of NMR acquisitions needed for a similar quality spectrum. A 10-fold increase in isotopic enrichment, for example, is thus equivalent to a 100-fold increase in the number of averaged acquisitions. This reduction in acquisition time becomes a critical step when performing the two-dimensional NMR experiments required for the structural study of proteins. For these types of experiments, a 10-fold increase in isotopic labeling

will reduce the total experimental time to a couple of days and the experiments thus become feasible.

In the case of silks or byssal threads, animals are fed a labeled diet to incorporate stable isotopes into the protein fibers. In order to optimize the fiber labeling, the efficiency and kinetics of the transfer between labeled food to the secreted fibers must first be determined. Experimentally, these two parameters (efficiency and kinetics) appear to vary with the organism species, type of food and environmental conditions (Osanai *et al.,* 2000; Hess *et al.,* 2002). We have seen that, in the case of mussels, the most efficient and less costly strategy consists in producing labeled microalgae which will subsequently be fed to the mussels (unpublished data). Consequently, a method for determining the isotopic labeling of total protein mass is required. To be useful for protein NMR studies, the method should be amenable to the measurement of ^{13}C or ^{15}N enrichment and allow labeling levels to be distinguished between different amino acids as well as be able to discriminate between partial and total labeling. Indeed, partially labeled amino acids can yield ambiguous NMR patterns which can lead to wrong assignments and thus render an accurate NMR analysis impossible.
Several techniques exist that can measure isotopic enrichment of molecules, including isotope ratio mass spectrometry (IRMS), gas chromatography/mass spectrometry (GC/MS) and, most recently, liquid chromatography/mass spectrometry (LC/MS). The choice of analytical method for measuring isotope enrichment is highly dependent on the needs of the experiment. In this study, in order to obtain an accurate estimate of isotopic labeling of amino acids from algal and byssal protein extracts, the main priorities for the analytical method were speed, cost effectiveness and the flexibility to determine either ^{13}C or ^{15}N enrichment. IRMS experiments yield very accurate results for isotope measurements; however, they do not allow any structural information to be extracted from the data since all molecules are transformed into combustion products prior to entering the ion source, also necessitating highly specialized instrumentation (Hellerstein & Neese, 1999) and, furthermore, would not

be easily amenable for simultaneous determination of ^{15}N enrichment. GC/MS is a common technique used for isotope analysis and has often been applied to the study of amino acid isotopic enrichment (Shen *et al.,* 2009; Patterson *et al.,* 1997; Molero *et al.,* 2011; Jennings & Matthews, 2005). Most GC/MS analyses use time-consuming derivatization steps in order to transform analytes into volatile species and resulting electron ionization (EI) spectra are often very difficult to interpret when many isotopomers are present at once (Antoniewicz *et al.,* 2007). LC/MS for isotope analysis of amino acids has previously been reported, demonstrating the power and applicability of this technique (van Eijk *et al.,* 1999; van Eijk *et al.,* 2007; Goshe & Anderson, 1995). LC/MS is also amenable to the evaluation of the extent of labeling within a given amino acid (Godin *et al.,* 2007).Previous methods have relied on full scan or single ion monitoring detection. In this study, we have developed an LC/MS/MS-based method for determining isotopic labeling of proteins following acid hydrolysis and rapid amino acid derivatization. A related method has been described by Hess *et al.* (2002) for the determination of isotopic enrichment in silk proteins by derivatization of hydrolyzed amino acids with Nα-(2,4-dinitro-5-fluorophenyl)-L-alaninamide (FDAA) and single quadrupole MS analysis, with results being shown for four amino acids (Ala, Gly, Pro, Glu). The present study, using a selective precursor ion scan for detecting 6-aminoquinolyl *N*-hydroxysuccinimidyl carbamate (AQC)-derivatized amino acids, presents data from a majority of protein amino acids and is shown for determining isotopic enrichment of both algal proteins and mussel byssus thread samples. The method allows the evaluation of feeding protocols of both the microalgae and mussels, for further structural investigation of suitably labeled mussel byssal threads by NMR.

6.3 EXPERIMENTAL

6.3.1 MATERIALS

Alanine, arginine, aspartic acid, asparagine, glutamic acid, cysteine, glutamine, glycine, histidine, isoleucine, lysine (HCl salt), methionine, phenylalanine, proline, serine, threonine, tryptophan, tyrosine and valine, $^{13}C_9{}^{15}N$-tyrosine, $^{13}C_6$(ring-labeled)-phenylalanine, $^{13}C_5{}^{15}N$-methionine, $^{13}C_5{}^{15}N_2$-glutamine, glucose, $^{13}C_6$-glucose, di(*N*-succinimidyl) carbonate and formic acid (ultrapure) were all obtained from Sigma-Aldrich (Oakville, ON, Canada). Sodium [^{13}C]-bicarbonate was purchased from Cambridge Isotope Laboratories (Cambridge, MA, USA). Concentrated hydrochloric acid was supplied by Fisher Scientific (Ottawa, ON, Canada). Sodium tetraborate decahydrate and 6-aminoquinoline were purchased from Alfa Aesar (Ward Hill, MA, USA). HPLC grade methanol and acetonitrile were obtained from Caledon Laboratories Ltd. (Georgetown, ON, Canada). Ultrapure water was supplied by a Synergy purification system (Millipore, Billerica, Massachusetts, USA).

6.3.2 PRODUCTION OF ^{13}C-LABELED MICROALGAE

Glucose diet:

Enrichment of microalgae with isotope-labeled glucose was performed using Amphora sp. obtained from the Centre for Culture of Marine phytoplankton (CCMP) at Bigelow Laboratory for Ocean Sciences (West Boothbay Harbor, ME, USA). Algae were cultured in seawater enriched with f/2 medium at pH 8 and temperature 20.6 ± 0.4°C, under lighting supplied by fluorescent grow lights (intensity of 191.6 ± 9.9 μE/m2s). Seawater was filtered and sterilized prior to use. A 10 mL

volume of the microalgae solution was used to inoculate a 250 mL Erlenmeyer flask filled with f/2 culture media supplemented with 5 g/L glucose (50% mixture of unlabeled and $^{13}C_6$ labeled glucose). Triplicate cultures were maintained for 19 days and cell concentrations were measured each day with a Z2 Coulter counter fitted with a 70-µm orifice tube (Beckman Coulter Canada, Mississauga, ON, Canada). Stationary phase growth was achieved at day 19 and the triplicate cultures had a mean concentration of $1.38 \pm 0.24 \times 106$ cells/mL. Sample aliquots were removed every 2 days from day 1 to day 19, lyophilized and stored (at 4°C) prior to analysis.

Sodium bicarbonate diet

Microalgae (Nannochloropsisocculata) were batch-cultured at 20°C and under continuous illumination during 10 days in f/2 seawater medium (Guillard, 1975) supplemented with 25 mM sodium [^{13}C]-bicarbonate. f/2 medium was transferred into four glass bottles (250 mL) then autoclaved with specific seawater setting to avoid salt precipitation. After the addition of labeled sodium bicarbonate, the culture system was sealed and the medium was purged with nitrogen gas to eliminate atmospheric CO_2. The culture system was built to ensure the elimination of oxygen produced by algae and avoid gas exchange with the ambient atmosphere. Culture bottles were inoculated with 10 mL of a growing culture (±20 cells/mL) using sterile syringes. Sample aliquots were taken after the 10-day culture period, lyophilized and stored (at 4°C) prior to analysis.

Production of ^{13}C-labeled mussel byssus:

Mytilus edulis were fed with ^{13}C-labeled Nannochloropsisocculata microalgae (from bicarbonate-labeling experiment) for 2 days in a 40 L tank filled with UV-treated oxygenated seawater. Water temperature was maintained at 18°C with a salinity ratio of 26. Every 12 h, 250 mL of ^{13}C-labeled microalgae culture was added to the seawater. Subsequently, mussels were placed on a vertical polyvinyl chloride (PVC)

rod using cyanoacrylate glue suspended 10 mm above a PVC plate for byssus production. Mussels were submerged in an experimental flume (Redjah *et al.*, 2010) and submitted to a current velocity of 12 cm/s to stimulate byssus production. Byssi were sampled every second day for analysis.

6.3.3 PROTEIN HYDROLYSIS

Lyophilized microalgae (1–1.5 mg) or mussel byssal thread (0.4–0.6 mg) samples were accurately weighed and dissolved in 1.0 mL of 6 M HCl. The samples were hydrolyzed for 24 h at 110°C, using a VWR Digital Heatblock (VWR International, Mississauga, ON, Canada). Sample tubes were opened and the acid was evaporated, rinsed with 1 mL water, and further evaporated using a SpeedVac concentrator (Fisher Scientific, Ottawa, ON, Canada) before reconstituting the sample in a final volume of 500 µL of water.

6.3.4 STANDARD PREPARATION

Standard mixtures of 0, 1, 2, 3, 4, 5, 10, 20, 40, 50, 60, 80, 90, 95, 96, 97, 98, 99 and 100% (labeled/unlabeled concentrations) of glutamine, methionine, phenylalanine and tyrosine were prepared at a total (labeled + unlabeled) concentration of 1 µM for each amino acid in water

6.3.5 DERIVATIZATION AND LC/MS ANALYSIS

The reconstituted algal and byssal hydrolysates were centrifuged at 13000 rpm for 30 s to sediment particulates prior to derivatization and diluted 10-fold in water. Amino acids were derivatized in a rapid reaction with 6-aminoquinolyl *N*-hydroxy-succinimidylcarbamate (AQC) (see Fig. 1). AQC was synthesized according to the literature (Cohen & Michaud, 1993) in a one-step procedure combining di(*N*-succinimidyl) carbonate and 6-aminoquinoline. Amino acids were derivatized by adding 10 µL of a saturated solution of AQC (approximately 3 mg/mL) dissolved in anhydrous acetonitrile to a mixture of 20 µL amino acid standard or protein hydrolysate and 70 µL of borate buffer (25 mM borate, pH 8.8).

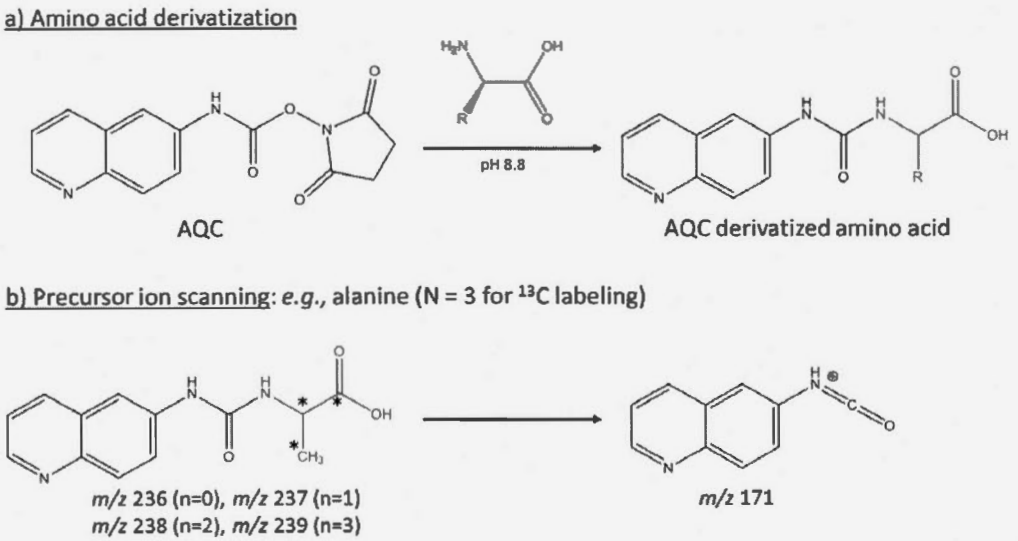

Figure 6.1. AQC derivatization reaction of amino acids (a) and example of extracted precursor ions in the case of a ^{13}C-labeling experiment for monitoring alanine (b).

All samples (1 μL injections) were separated on a Zorbax Eclipse Plus C18 column (2.1 × 100 mm, 1.8 μm) using a Shimadzu Prominence HPLC system (including two LC20AD-XR pumps with in-line degasser, a SIL20AC autosampler, and a CTO20A column compartment) with the following gradient: 5% B with a 2 min hold, up to 70% B at 15 min, 95% B at 15.5 min held until 20 min before re-equilibration, where mobile phases A and B were water and methanol (both containing 0.1% formic acid), respectively, at a flow rate of 0.2 mL/min and a column temperature of 50°C. Mass spectrometric analysis was performed on a QTRAP 5500 hybrid triple quadrupole-linear ion trap (AB Sciex, Concord, ON, Canada) in positive ion mode. The TurboIonSpray® source was operated with an ionspray voltage of 5000 V at 450°C. The curtain gas was maintained at 35 psi and GS1 and GS2 gases were held at 55 and 60 psi, respectively. The declustering potential (DP) and exit potential (EP) were set to 120 and 10 V, respectively. A precursor ion scan of the fragment ion at *m/z* 171.1 was performed with collision energy (CE) of 30V and at a scan rate of 200 Da/s with a 0.1 Da step size between *m/z* 235 and 500. The collision cell exit potential (CXP) was maintained at 13 V. The offset values in the resolution tables for both quadrupoles were adjusted to obtain baseline resolution between consecutive ^{13}C and/or ^{15}N isotope peaks, reflecting slightly higher than unit resolution. All raw data was processed with Analyst® software (version 1.5.1) and MultiQuant™ (version 2.0.2) software for signal integration.

6.3.6 DATA ANALYSIS

Extracted ion chromatograms (EICs) were integrated from precursor ion scan data using a mass selection window of ±0.4 *m/z* relative to the theoretical *m/z* value for each isotopomer precursor ion. The area measured for each isotopomer was divided by the sum of areas for all possible isotopomers (up to fully labeled) of a given amino

acid. The resulting ratio was expressed as a percentage in order to obtain a measure of the relative contribution from each isotopomer to the total amount of amino acid, as shown in the following equation:

$$\%\ contribution\ of\ isotopomer\ (c) = \left(\frac{A_{M_n}}{\sum_{n=0}^{N} A_{M_n}}\right) \times\ 100\%$$

where A represents the area of the EIC peak, M_n is the isotopomer from amino acid 'M' with 'n' labeled atoms, and N is the maximum number of labeled atoms for amino acid 'M'.

From this data, the total labeling percentage was calculated by weighting each isotopomer according to the number of labeled atoms they contain, then dividing by the maximum number of labeled atoms, which corresponds to the atom percent (AP) labeled, as shown below:

$$labeled\ AP\ (of\ amino\ acid\ M) = \frac{\sum_{n=1}^{N}(C_{M_n})n}{N}$$

For example, in a ^{13}C-labeling experiment, the isotopomer masses of AQC-derivatized alanine are shown in Fig. 1. If the extracted precursor ion at *m/z* 260 (n = 0) were twice the size of the peak area for fully labeled alanine (n = 3) at *m/z* 263, and no other isotopomer peak was detected, then the total label atom percent (AP) would be calculated as 33%, since exactly one-third of the total pool of alanine carbons would be ^{13}C-labeled.

6.4 RESULTS AND DISCUSSION

6.4.1 CALCULATION OF % ISOTOPE LABELING

Amino acid separation by reversed-phase chromatography normally requires derivatization due to the polar nature of the analytes. This poses an interesting problem for amino acid isotopomer analysis by reversed-phase LC/MS since the resulting derivatized amino acids will have an altered isotope pattern compared to the free amino acids, thus complicating data analysis. Our derivatization method using AQC, a common reagent used for reversed-phase amino acid analysis and designed for fluorescence detection (Cohen & Michaud, 1993), permits the use of a selective precursor ion scanning method that addresses this problem. The fragmentation of AQC-derivatized amino acids yields a prominent, and thus highly sensitive, product ion at *m/z* 171 that results from the loss of the AQC moiety (Mitrea *et al.,* 2010). Since the ion at *m/z* 171 is the loss of the entire monoisotopic derivatization agent, the isotopic pattern detected from the precursor ion scan corresponding to the AQC-derivatized amino acids is dictated exclusively by the free amino acids. Moreover, the precursor ion scan adds a level of selectivity that non-MS/MS methods, such as single ion monitoring, do not provide. The possibility of mass interference during the analysis of all isotopomers for multiple amino acids from a relatively complex biological sample is a legitimate concern. Fortunately, the precursor ion scan selectively detects AQC-derivatized free amine-containing molecules. Furthermore, the AQC-derivatization reaction is a one-step process that can be performed directly in the injection vial and is complete within a few minutes. In short, AQC derivatization is ideal for isotopomer analysis of amino acids since it is a very fast and easy reaction that allows for separation of amino acids by reversed-phase HPLC and the use of a selective and sensitive precursor ion scanning method that does not include any isotope contribution from the derivatizing agent.

The remaining concern in the development of a method for accurate and reproducible measurement of amino acid isotope enrichment was cross-isotope spectral interference. Quadrupoles are most commonly operated at unit resolution which does not provide baseline separation of spectral peaks separated by a difference of 1 Da. For our method, both filtering quadrupoles (Q1 and Q3) were tuned for increased resolution in order to obtain baseline separation of neighboring isotopomers separated by 1 Da, as well as to assure that there would be no isotope pattern skewing due to a contribution from non-monoisotopic (AQC) fragment ions. Setting the instrument parameters for increased resolution in both quadrupoles does decrease its sensitivity; however, this is generally not a problem for these types of applications since, typically, a few milligrams of dried protein extract are easily available which represents a large excess considering the sensitivity of modern day mass spectrometry. To further insure that there would be no interference when calculating the relative areas of isotope peaks of each amino acid, the mass window used for each EIC was carefully chosen to avoid any contribution from neighboring isotopomers. By choosing mass windows of ± 0.4 *m/z* relative to the theoretical *m/z* value for the isotopomer of interest, we cover nearly the entire spectral width of each peak while avoiding any contribution from its neighbors.

The calculation of the percentage of isotope label for a given amino acid is based on the ratio of the EIC peak area of each isotopomer relative to the sum of all isotopomer signals. The quantitative information is therefore extracted from a chromatographic peak rather than from a spectral peak, removing any possibility of skewed results due to chromatographic shifts from isotopically labeled ions. In order to calculate the total isotopic contribution, the areas corresponding to each isotopomer are weighted according to the number of labeled atoms they contain, resulting in an absolute percentage of labeling, or atom percent (AP). The data can then be treated according to the needs of the experiment, for example a correction factor can be applied to

account for natural abundance, thus yielding a % enrichment value. Isotopomers can also be analyzed individually, since the data from each is available, preserving the opportunity for determining the distribution of labels incorporated in any amino acid for a given experiment.

6.4.2 METHOD VALIDATION USING ISOTOPE-LABELED STANDARDS

In order to test our method of measuring isotopic enrichment, amino acid standards prepared at varying unlabeled to labeled ratios were tested. The standards were prepared by mixing four unlabeled amino acids (phenylalanine, methionine, glutamine and tyrosine) with their corresponding fully ^{13}C and ^{15}N-labeled counterparts (with the exception of phenylalanine, which was $^{13}C_6$ only) in precise ratios. It is difficult to prepare standards that will perfectly reflect biological samples, which will contain various degrees of isotope labeling, since commercially available standards are manufactured to be isotopically uniform. These standards suit our purpose of validating the method by testing our ability to correctly determine isotope ratios and to calculate a percentage of isotope enrichment from these ratios. As an example of the results obtained with these standards, Fig. 2 shows the mass spectra from different standard mixtures of phenylalanine. The spectra clearly show the typical baseline resolution obtained between isotopomers using our method. In the case of the standard mixtures, the total percentage of labeled atoms was corrected for the natural isotopic abundance for each amino acid by adjusting the targeted percentage based on the theoretical isotope distributions of the standard mixtures and the isotopic purity of the labeled amino acids. The results show excellent linearity and consistent results for all standard amino acids (Figure 6.3 and Table 6.1). The precision of the method is excellent, with all standard samples injected having a coefficient of variance (CV) within 20%. The accuracy of the method is also very

good, with all standard samples having a calculated AP within ±2.5% and a percent accuracy within ±20% of the expected theoretical value, including the vast majority (89.5%) of the samples being within ±10% of the expected value. In order to obtain these standard curves, a final concentration of 200 nM derivatized amino acid standard representing between 29 and 36 pg of each pre-derivatized amino acid (from the four standard tested) were injected onto the column. The performance and sensitivity of the method is clearly suitable for the application described since we would always be starting with an initial protein sample of at least 0.1 mg prior to hydrolysis.

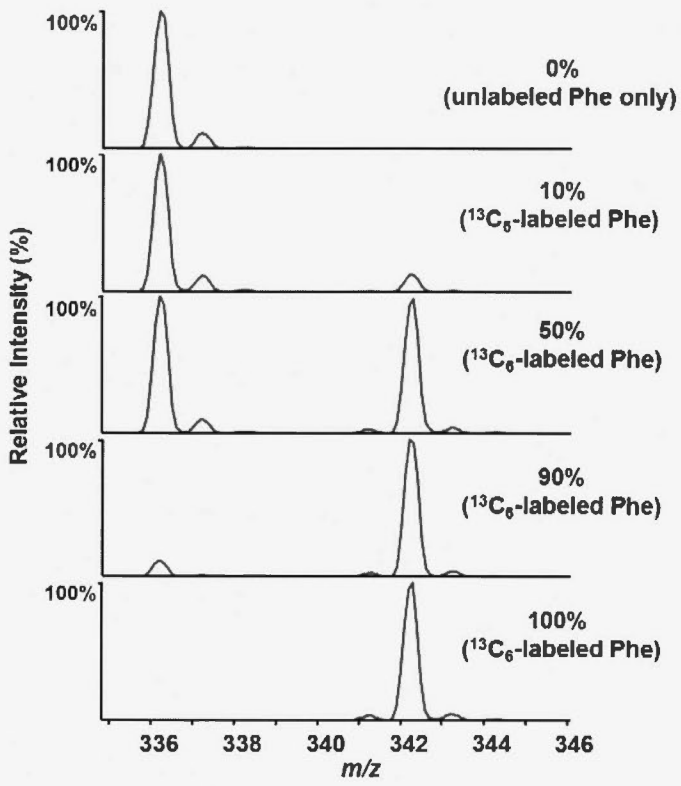

Figure 6.2. Mass spectra (from *m/z* 335 to 346) from different standard mixtures of ring-labeled ($^{13}C_6$) phenylalanine.

6.4.3 AMINO ACID ANALYSIS AND PROTEIN HYDROLYSIS

In order to obtain a good measurement of the degree of isotopic enrichment in proteins, we have opted for one of the simplest and most commonly used methods: acid hydrolysis using concentrated hydrochloric acid. Like most other hydrolysis methods, this one does not permit the analysis of all amino acids. By combining different hydrolysis methods, it is possible to recover every amino acid and it is important to note that our derivatization and LC/MS methods can be adapted to be compatible with any hydrolysis method.

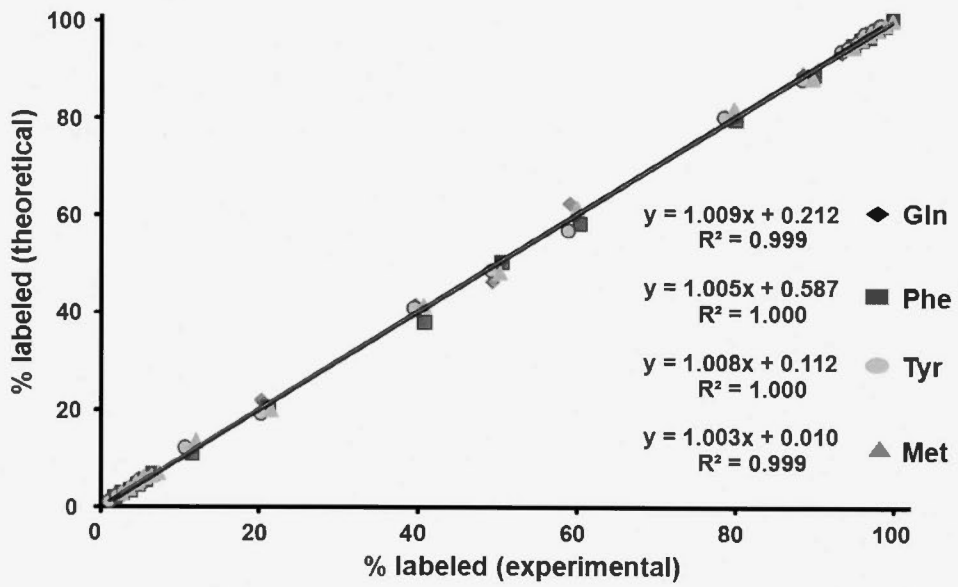

Figure 6.3. Calibration curves of standard amino acids (Gln, Phe, Tyr, Met) at different labeling percentage mixtures.

There are six amino acids that we cannot directly measure using our combination of acid hydrolysis and LC/MS method, as shown in Table 2. Cysteine and tryptophan are known to be destroyed by acid hydrolysis and asparagine and glutamine are deamidated to their carboxylic acid counterparts, aspartic acid and glutamic acid, respectively (Fountoulakis & Lahm, 1998). Even though we cannot directly analyze asparagine or glutamine, all of their ^{13}C-labeling information is incorporated into the data obtained from aspartic acid and glutamic acid. This complicates the individual analysis of these four amino acids and renders the measurement of side-chain ^{15}N-labeling for asparagine and glutamine impossible when using acid hydrolysis. It is best to use other hydrolysis methods (Guillard, 1975) if the precise labeling information for these amino acids is required. Two more amino acids, histidine and arginine, are not sensitive enough to be analyzed using our method, mainly due to the highly polar nature of their AQC derivatives, and therefore very early elution of these derivatives using an acidic mobile phase. If these amino acids are specifically of interest, simply using a more basic mobile phase, such as ammonium acetate, would increase their retention on a C18 column, thus increasing their sensitivity. The formic acid mobile phase, however, was chosen as the best choice since, overall, we obtain very good resolution and sensitivity of a majority of the amino acid derivatives.

Representative chromatograms of overlaid monoisotopic EICs from a mixture of all 20 standard amino acids (without hydrolysis), each at a concentration of 0.5 μM, and a hydrolyzed algal protein sample (from an initial amount of 1 mg lyophilized algae) are illustrated in Fig. 4. Using the precursor ion scanning method from *m/z* 235–500, we did not observe peaks in the standard mix for cysteine, arginine and histidine, since most of the ion intensities for these amino acid AQC derivatives are doubly charged and therefore below the mass range detected (see Table 2). However, if cysteine is protected to remove the free thiol group prior to protein hydrolysis, the corresponding protected AQC derivative will be measurable with the same precursor

ion scanning method as described here. Basic amino acids, such as lysine, arginine and histidine, since they are doubly charged will not have complete resolution between isotopomers, and therefore will not be taken into account in the final assay for protein hydrolysates. One alternative for measuring the isotopic contributions for these two amino acids, as well as lysine, is to use a mobile phase that is less acidic and therefore would more likely form the 1+ charge state. The acidic mobile phase is much more sensitive for the detection of AQC derivatives of amino acids and therefore was chosen for this study.

Table 6.1. Atom percent labeling for mixtures of unlabeled and labeled amino acids

% labeled std	Gln			Phe			Met			Tyr		
	Calc% (Theo)	%Δ	%CV	Calc% (Theo)	%Δ	%CV	Calc% (Theo)	%Δ	%CV	Calc% (Theo)	%Δ	%CV
0	1.1 (1.1)	0.9	19.7	1.9 (1.8)	4.1	1.9	2.7 (2.6)	5.0	11.5	1.1 (1.1)	-0.6	3.9
1	1.7 (2.0)	-14.8	11.4	2.8 (2.8)	0.3	8.5	3.7 (3.6)	5.0	14.6	2.2 (2.1)	5.9	6.8
2	2.4 (3.0)	-19.0	13.4	3.3 (3.8)	-10.9	8.2	4.9 (4.5)	8.7	6.2	2.7 (3.0)	-9.4	8.2
3	3.7 (3.9)	-5.6	7.5	4.4 (4.7)	-5.9	8.5	6.1 (5.4)	11.9	16.3	4.0 (4.0)	-0.1	19.9
4	5.8 (4.9)	18.8	18.0	5.4 (5.7)	-5.6	3.5	6.4 (6.4)	0.4	18.6	4.5 (4.9)	-8.4	19.3
5	5.3 (5.9)	-9.7	6.9	6.8 (6.7)	1.8	10.7	6.9 (7.3)	-5.0	13.6	6.0 (5.9)	2.6	17.2
10	12.4 (10.7)	16.0	3.2	10.9 (11.5)	-5.0	2.1	13.5 (12.0)	12.4	4.8	12.1 (10.7)	14.0	14.5
20	21.8 (20.3)	7.6	15.9	20.3 (21.2)	-4.4	12.4	19.9 (21.5)	-7.2	5.8	19.1 (20.2)	-5.4	6.4
40	41.4 (39.6)	4.5	5.0	37.9 (40.7)	-6.8	4.2	41.3 (40.6)	1.8	0.6	40.8 (39.5)	3.5	8.5
50	46.2 (49.3)	-6.3	3.6	50.3 (50.5)	-0.4	1.8	48.2 (50.2)	-4.1	4.5	48.6 (49.1)	-1.1	4.5
60	62.4 (59.0)	5.6	1.3	58.2 (60.3)	-3.4	9.4	61.5 (60.0)	2.5	2.6	56.8 (58.9)	-3.5	2.9
80	80.4 (78.6)	2.3	4.1	79.7 (80.0)	-0.3	0.3	81.9 (79.7)	2.8	3.5	80.2 (78.4)	2.3	1.8
90	89.1 (88.4)	0.8	0.6	88.9 (89.8)	-1.0	0.9	88.2 (89.6)	-1.6	1.5	88.0 (88.3)	-0.3	0.7
95	93.6 (93.3)	0.4	3.1	95.1 (94.8)	0.4	0.4	94.6 (94.7)	0.0	1.7	93.9 (93.2)	0.7	1.1
96	95.1 (94.3)	0.9	1.3	96.2 (95.7)	0.4	0.3	96.4 (95.7)	0.8	1.2	94.7 (94.2)	0.6	0.6
97	96.0 (95.3)	0.8	0.5	96.7 (96.7)	0.0	0.4	97.3 (96.7)	0.6	0.3	95.6 (95.2)	0.4	0.8
98	97.6 (96.2)	1.4	0.3	98.2 (97.7)	0.5	0.1	98.2 (97.7)	0.6	0.2	97.5 (96.2)	1.4	0.4
99	98.5 (97.2)	1.3	0.3	99.0 (98.7)	0.3	0.0	99.2 (98.7)	0.5	0.3	98.3 (97.2)	1.2	0.1

Table 6.2. Amino acid characteristics following protein hydrolysis, AQC derivatization and LC/MS analysis

Amino acid	**# C's**	**# N's**	**MW (g/mol)**	***m/z* (AQC derivative)**	**RT (min)**	**Comment**
His[a]	6	3	155.1	163.6, 326.1	3.3	Low sensitivity (charge/early elution)
Asn	4	2	132.1	303.1	4.9	Acid hydrolyzed to aspartic acid
Arg[a]	6	4	174.1	173.1, 345.2	5.3	Low sensitivity (charge/fragmentation)
Gln	5	2	146.1	317.1	6.4	Acid hydrolyzed to glutamic acid
Ser	3	1	105.0	276.1	6.5	
Gly	2	1	75.0	246.1	6.8	
Asp	4	1	133.0	304.1	7.4	
Glu	5	1	147.1	318.1	7.8	
Thr	4	1	119.1	290.1	8.2	
Ala	3	1	89.0	260.1	8.7	
Pro	5	1	115.1	286.1	9.2	
Lys[ab]	6	2	146.1	244.1, 487.1	10.6	Doubly derivatized and charged
Tyr	9	1	181.1	352.1	11.0	
Cys[ab]	3	1	121.0	231.6, 462.1	11.1	Degraded during acid hydrolysis
Met	5	1	149.1	320.1	11.3	
Val	5	1	117.1	288.1	11.8	
Trp	11	2	204.1	375.1	13.4	Degraded during acid hydrolysis
Ile/Leu	6	1	131.1	302.1	13.5	Co-elution of isobaric species
Phe	9	1	165.1	336.1	13.6	

[a]doubly charged base peak, [b]doubly derivatized amino acid as major species

One advantage of this approach is that baseline resolution is not needed for all amino acids; however, it is crucial that all amino acids with the potential to share isobaric isotopomers are well resolved chromatographically. For hydrolyzed protein samples, our method therefore has the ability to measure ^{13}C isotope enrichment with data originating from 15 of the 20 amino acids, removing the doubly charged derivatives (Lys, His, Arg) and those that are destroyed by acid hydrolysis (Cys, Trp), providing enough coverage to obtain a reliable estimate of the total ^{13}C enrichment of the protein sample.

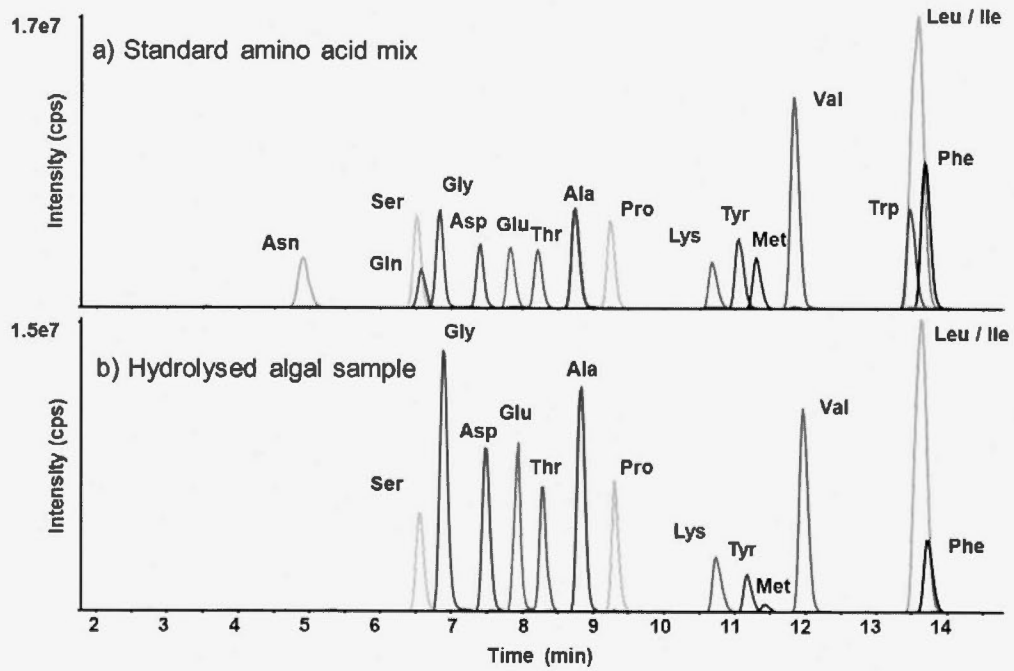

Figure 6.4. Extracted ion chromatograms of monoisotopic peaks for AQC-derivatized amino acid standard mix (at 0.5 μM amino acid concentration) (a) and protein hydrolysate from representative algal sample (b).

6.4.4 ANALYSIS OF ^{13}C ENRICHMENT IN PROTEINS FROM GLUCOSE-FED ALGAE

A cost-effective strategy to obtain labeled byssal threads is to first label algae which will subsequently be used to feed the mussels. In the current study, we have tested two possibilities for labeling of algae: feeding with labeled glucose, as well as growing algae in the presence of labeled salts. Our method was first tested on protein extracts from algae that were fed with isotopically labeled $^{13}C_6$-glucose (50%) for a period of 19 days. Algae were taken from the growth medium every second day for analysis and the total percentage of ^{13}C-labeled carbon atoms was calculated (see Table 6.3). The labeling kinetics is thus established and the optimal time for algae harvesting prior to mussel feeding determined.

The results do not include data for methionine, since it is both one of the lesser sensitive of the amino acids and one of the least abundant in proteins; therefore, the resulting signal obtained from our samples was not sufficient for reliable data to be extracted, resulting in data quantified from 14 amino acids.

In order to compare the mass spectra originating from a standard algal sample with those from the labeled samples, threonine is used as an example in Fig. 5. The mass spectrum of threonine obtained from an algal sample taken on the first day of labeling is, as expected, very similar to that observed from the standard. A difference is clearly seen, however, in the mass spectra between the first (day 1) and last day (day 19) of the feeding experiment. The relative areas of the labeled threonine isotopomers are visibly larger compared to the unlabeled threonine in the day 19 sample, as we can start to see a fully labeled threonine peak starting to emerge. Since the algae were continuously fed ^{13}C-labeled glucose during the experiment, we expect protein extracts to have increasing ^{13}C content throughout the 19 days of sampling. When the

average ^{13}C-labeling percentage of amino acids was calculated, we indeed observed a continuous increase in labeling throughout the sampling period (Fig. 6), reaching a plateau of labeling when the algae entered the stationary phase of growth at day 19.

Table 6.3. % Isotope enrichment in algal samples fed with $^{13}C_6$-glucose over 19 days for individual amino acids

Amino acid	Day 1	Day 3	Day 5	Day 7	Day 9	Day 11	Day 13	Day 15	Day 17	Day 19
Ser	3.9 ±0.3 (9.6)	5.2 ±0.7 (7.7)	6.5 ±0.2 (7.2)	8.1 ±1.4 (4.8)	9.6 ±1.4 (7.6)	10.3 ±0.9 (4.6)	11.8 ±1.8 (4.9)	14.1 ±2.1 (3.1)	15.7 ±1.7 (3.5)	15.2 ±1.3 (3.4)
Gly	4.7 ±0.7 (7.3)	5.5 ±0.8 (5.4)	6.4 ±0.9 (4.5)	7.4 ±1.2 (2.9)	9.3 ±1.6 (4.4)	9.8 ±0.8 (2.3)	11.2 ±1.9 (3.2)	13.5 ±2.1 (3.2)	14.5 ±1.3 (5.8)	14.2 ±1.6 (1.6)
Asp*	3.3 ±0.3 (8.6)	5.0 ±0.9 (6.6)	7.2 ±0.7 (7.1)	8.5 ±1.4 (3.0)	10.2 ±1.5 (4.8)	10.9 ±1.3 (2.8)	12.7 ±2.0 (2.5)	14.4 ±1.5 (3.6)	15.3 ±1.8 (2.6)	15.3 ±1.4 (1.9)
Glu*	2.9 ±0.3 (10.9)	6.0 ±1.1 (5.5)	8.4 ±0.5 (4.3)	9.4 ±1.5 (4.8)	11.0 ±1.9 (1.1)	11.4 ±1.3 (1.4)	13.4 ±2.2 (2.2)	15.1 ±2.3 (2.8)	16.0 ±2.2 (1.7)	16.2 ±1.0 (1.1)
Thr	2.0 ±0.2 (12.6)	3.2 ±0.3 (11.2)	5.0 ±0.7 (4.2)	6.2 ±1.0 (3.8)	7.8 ±1.3 (1.6)	8.3 ±0.8 (4.9)	9.8 ±1.7 (1.5)	11.1 ±1.5 (3.8)	11.7 ±1.3 (3.2)	11.9 ±1.2 (3.0)
Ala	5.5 ±0.3 (13.2)	13.2 ±4.0 (3.1)	17.4 ±4.0 (2.3)	15.6 ±3.8 (1.2)	11.9 ±1.7 (4.0)	13.4 ±1.8 (3.1)	14.2 ±2.4 (7.5)	16.2 ±2.1 (2.8)	17.5 ±2.0 (3.9)	17.4 ±1.4 (4.1)
Pro	2.4 ±0.2 (11.3)	3.3 ±0.6 (15.3)	4.7 ±0.9 (8.9)	5.7 ±0.9 (2.8)	7.0 ±1.0 (6.9)	7.7 ±0.9 (1.4)	8.7 ±1.6 (2.1)	9.1 ±1.1 (6.5)	10.0 ±1.5 (5.0)	10.0 ±1.6 (3.4)
Tyr	1.6 ±0.3 (17.8)	2.2 ±0.8 (10.6)	3.6 ±0.6 (6.9)	5.6 ±1.2 (6.8)	7.1 ±1.4 (2.8)	8.0 ±1.0 (4.8)	9.2 ±1.4 (8.1)	11.4 ±1.4 (2.4)	12.0 ±1.5 (2.0)	11.8 ±1.2 (3.9)
Val	2.3 ±0.2 (7.4)	3.4 ±0.5 (4.7)	5.2 ±0.7 (2.9)	6.3 ±0.9 (4.3)	7.7 ±1.4 (3.9)	9.0 ±1.0 (2.7)	10.4 ±1.7 (5.6)	12.1 ±1.4 (3.2)	13.1 ±1.5 (1.0)	13.1 ±1.5 (2.3)
Leu/Ile	2.4 ±0.3 (5.1)	3.3 ±0.5 (4.0)	4.7 ±0.7 (3.7)	5.8 ±0.9 (1.4)	7.0 ±1.2 (2.0)	7.9 ±0.9 (3.2)	9.1 ±1.5 (2.1)	10.7 ±1.4 (1.5)	11.7 ±1.5 (0.9)	11.7 ±1.1 (1.3)
Phe	1.9 ±0.5 (11.0)	2.5 ±0.5 (11.7)	3.9 ±0.5 (8.5)	5.1 ±0.8 (4.8)	6.4 ±1.0 (2.7)	7.7 ±1.1 (4.3)	9.4 ±1.9 (5.9)	10.6 ±1.1 (1.0)	11.3 ±1.1 (1.1)	11.0 ±0.9 (1.6)

We can clearly see a nice trend in the overall data even if the percentage change is subtle between samples from consecutive sampling days, demonstrating that the method can reliably differentiate samples which differ by about 2% ^{13}C-labeling (AP). The precision of the method for the analysis of algal samples is clearly consistent with the data from the standard curves. Three samples were taken at each time point (biological replicates) and each one of these samples was injected three times (analytical replicates). The %CV of the analytical replicates was again excellent: all samples were under 20%, including over 90% of samples with %CV under 10% (see Table 6.3). The standard deviations between different biological replicates suggest that the accuracy of our method also reflects the results of our standard curves since 91.8% of the samples are within 2% AP.

An important aspect of this method is that the data pertaining to all isotopes are available, allowing for deeper analysis of the data. We can obtain relevant biological information from this type of analysis, since we can monitor the degree of labeling for each amino acid and the relative abundance of each isotopomer, as opposed to only having access to a total amount of ^{13}C labeling. As previously mentioned, it is very useful for subsequent NMR studies to be able to discriminate partial and total labeling of a given amino acid.

While the glucose-feeding experiment does serve as an excellent example of the applicability of our method, the overall percentage of labeling of the algae is not sufficient to obtain a satisfactory labeling of byssal threads for NMR studies; therefore, we assessed a second method of algal production using labeled inorganic salts as carbon source.

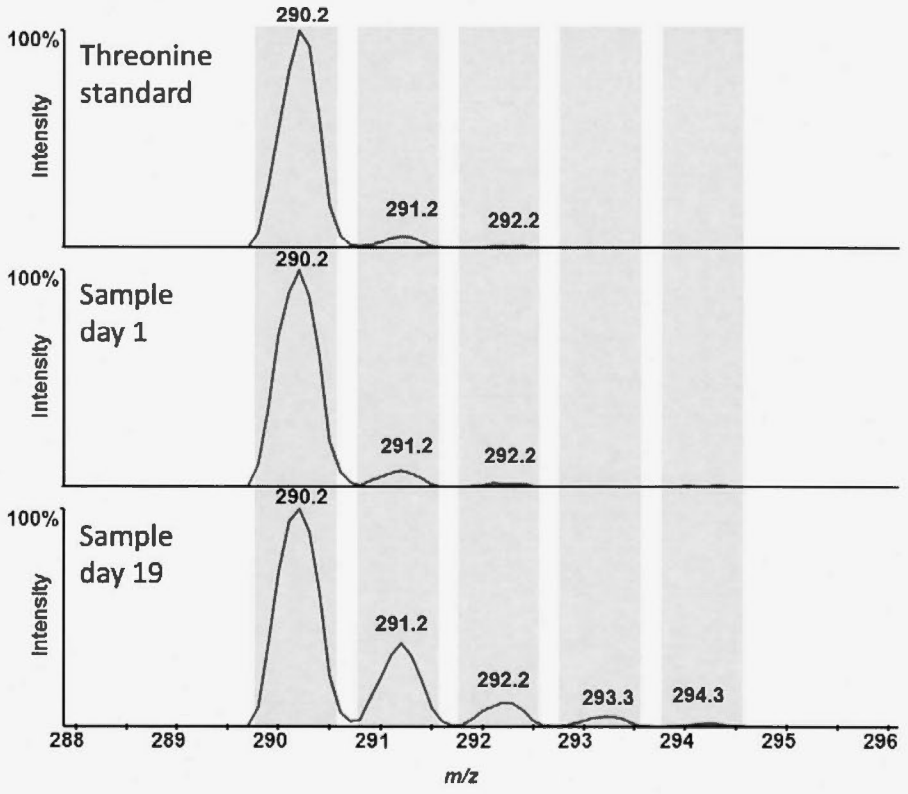

Figure 6.5. Mass spectra (from *m/z* 288 to 296) and integration windows from AQC-derivatized threonine from standard (a), algal sample on day 1 (b), and algal sample day 19 (c).

6.4.5 ANALYSIS OF ^{13}C ENRICHMENT IN PROTEIN FROM SODIUM BICARBONATE-FED ALGAE AND MUSSEL BYSSUS

Sodium bicarbonate is a common carbon source for microalgae and therefore it was expected that a ^{13}C-labeled bicarbonate diet would allow a more efficient incorporation of ^{13}C into algal proteins. In order to maximize labeling efficiency through the labeled salt diet, a culture system was designed to ensure the elimination of oxygen produced by algae and avoid gas exchange with the ambient atmosphere.

Indeed, this experimental approach yields algae with significantly higher ^{13}C labeling than with the previous glucose-feeding experiment, with a ^{13}C labeling of 84.9% (AP). Figure 6.7 shows the extracted ion chromatograms (EICs) corresponding to each of the ^{13}C isotopomers of alanine, comparing the bicarbonate-fed labeled algae to unlabeled (control) algae. The areas of each of these peaks represent the raw data used to calculate the ^{13}C atom percent labeled (AP). The efficiency of this feeding experiment is clearly illustrated since the predominant isotopomer peak from the labeled algae corresponds to the fully labeled ($^{13}C_3$-alanine at *m/z* 263) alanine peak.

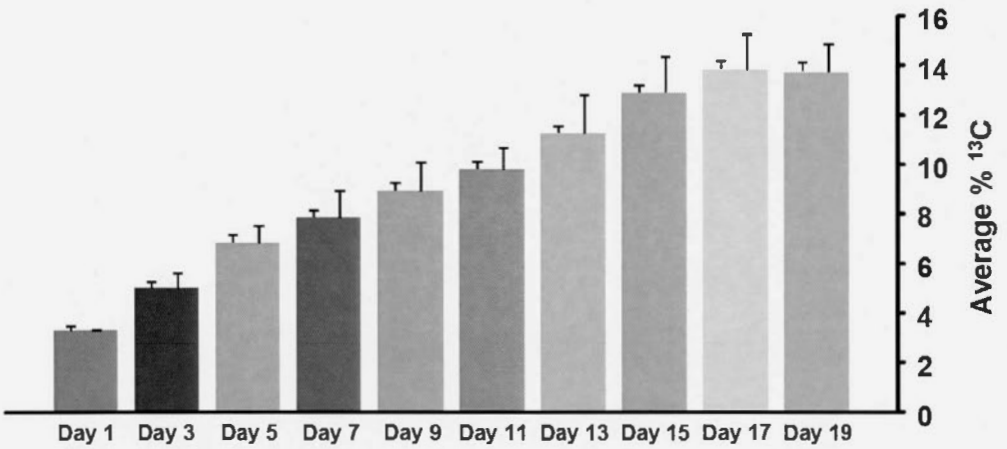

Figure 6.6. Average percentage of ^{13}C labeling in algal protein hydrolysates from time-course $^{13}C_6$-glucose feeding experiment, with error bars showing analytical reproducibility (n = 3) (left) and biological variability (n = 3) (right).

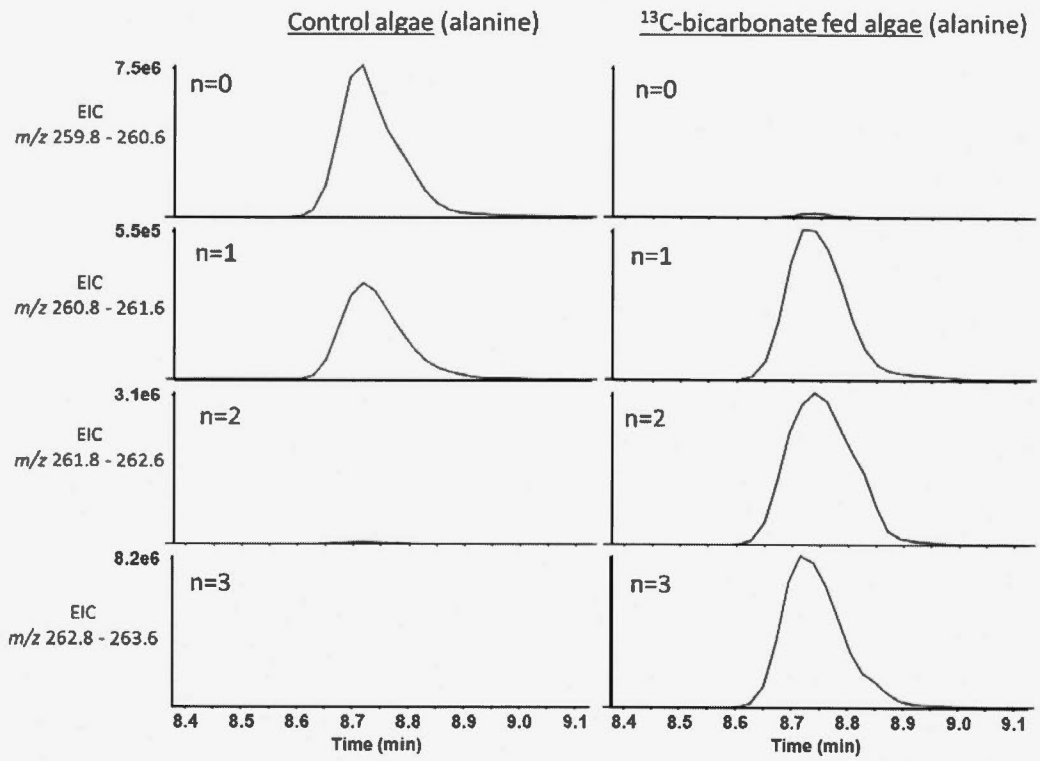

Figure 6.7. Extracted ion chromatograms from precursor ion scanning experiment for alanine ^{13}C isotopomers in unlabeled and ^{13}C-bicarbonate-fed algal samples.

6.5 CONCLUSIONS

We have developed an efficient method for measuring isotopic enrichment of amino acids from protein extracts using a LC/MS/MS platform based on a simple derivatization procedure that is compatible with most protein hydrolysis methods. Furthermore, the use of a precursor ion scan allows us to take advantage of an added level of selectivity not present in non-MS/MS approaches that are more frequently used for this type of isotopomer analysis. The method was validated using standard curves from four different amino acids, obtaining excellent reproducibility and very

good accuracy allowing us to distinguish between samples that differ by 2% (AP) with a very modest amounts of amino acid (≤36 pg of pre-derivatized amino acid) injected onto the column.

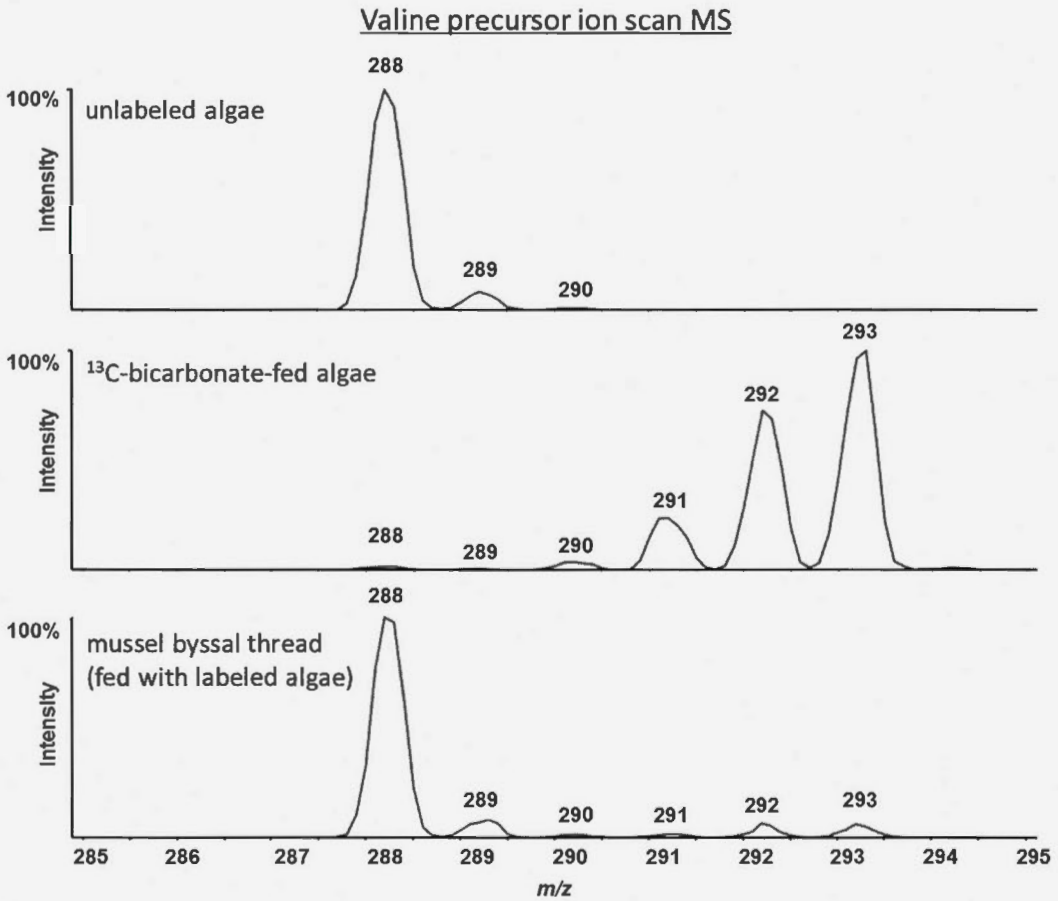

Figure 6.8. Mass spectra (from *m/z* 285 to 295) showing valine isotopomers from ^{13}C-bicarbonate-fed algae and labeled mussel byssus sample.

In short, the performance of the method, its sensitivity and its accessibility render it an ideal approach for assessing protein labeling. Within the context of protein structural studies by NMR, this is especially true since the method is adaptable for the measurement of either ^{13}C or ^{15}N enrichment and allows one to evaluate labeling levels for individual amino acids, while also being able to discriminate between partial and total labeling of a given amino acid.

This new method was used for the measurement of ^{13}C labeling in algal protein and mussel byssus thread proteins, demonstrating that we were able to obtain reliable ^{13}C-labeling data originating from 14 amino acids using the combination of a simple acid hydrolysis method and our analytical approach for two different types of biological samples. The method has allowed us to evaluate two different feeding protocols for microalgae and subsequently monitor the optimization of mussel feeding protocols for selecting suitable mussel byssal threads for further structural investigation.

CONCLUSION

Cinq nouvelles méthodologies ont été présentées dans cette thèse, chacune développée dans le but de fournir de nouvelles connaissances dans leurs domaines d'applications respectifs. Chaque méthode diffère quant à la nature des analytes (petites molécules organiques, peptides et protéines) ainsi qu'aux types d'applications (outil de dépistage pour l'analyse qualitative, l'élucidation de structures détaillées et l'analyse quantitative). Que ce soit pour l'analyse des acides aminés, des peptides ou des métabolites, le fil conducteur de ces méthodologies demeure l'optimisation des étapes de préparation d'échantillons et l'utilisation des techniques de spectrométrie de masse à la fine pointe, dans l'optique de caractériser des molécules importantes d'un point de vue biologique. Selon les défis associés à chaque projet, certains aspects distincts de ces méthodes ont été mis au point pour atteindre nos objectifs, incluant des techniques de préparation d'échantillons, des méthodes instrumentales et des stratégies d'analyse de données. Pour conclure ma thèse, je mettrai en évidence le caractère innovant de chacun des quatre manuscrits publiés présentés et discuterai des perspectives concernant les travaux en cours sur l'identification des cibles protéiques de métabolites réactifs.

Tout d'abord, le chapitre 2 proposait une utilisation de la spectrométrie de masse à haute résolution pour le dépistage de métabolites réactifs ainsi que leurs adduits de glutathion, formés par le métabolisme *in vitro* de l'atrazine et de trois autres pesticides de structures analogues. Le dépistage de métabolites utilise, traditionnellement, l'instrumentation MS/MS à faible résolution pour détecter les métabolites en se fiant sur la similitude structurale qu'ils partagent avec leurs molécules de départ. Cependant, un spectre acquis à haute résolution à l'intérieur d'une gamme de masse appropriée contient, théoriquement, toutes les données nécessaires pour détecter tous

les produits métaboliques compris dans l'échantillon, selon les limites de sensibilité. Ces données acquises de façon impartiales peuvent être réinterrogées à tout moment et les paramètres d'acquisition peuvent être génériquement appliqués pour l'étude d'une multitude de composés. Nous avons également montré que cette stratégie demeure efficace tout en insistant fortement sur l'utilisation d'un ensemble complet d'échantillons contrôles, pour l'analyse de composés dont le métabolisme fut précédemment caractérisé, mais avec des techniques moins sensibles et sophistiquées que les techniques actuellement disponibles. Bien que l'atrazine et ses analogues furent largement étudiés, notre stratégie a permis de mettre en lumière plusieurs nouveaux métabolites en plus d'adduits de glutathion, permettant donc de redéfinir les notions connues de son métabolisme.

L'utilisation de la spectrométrie de masse à haute résolution pour le dépistage d'adduits de glutathion a également été mise en évidence dans le chapitre 3. Un nouvel analogue du glutathion fut utilisé comme agent piégeant, afin d'améliorer les méthodes existantes pour détecter la formation de substances réactives. Ce nouvel agent fut conçu, d'une part pour lui donner à la fois un patron isotopique et un défaut de masse uniques pouvant être exploités, mais également afin de permettre le dépistage efficace des adduits de métabolites réactifs lors du traitement des données provenant du MS à haute résolution. Également, notre méthodologie simplifie la procédure expérimentale, puisqu'elle ne se réfère pas à la fragmentation des adduits. Cet avantage permet ainsi de réduire les faux positifs et les faux négatifs qui surviennent lors de l'utilisation de méthodes traditionnelles pour ce type de d'analyse. Nous avons démontré que notre agent de piégeage peut efficacement et sélectivement détecter les adduits de métabolites réactifs formés par plusieurs composés lors d'incubations microsomales *in vitro*, en utilisant des paramètres d'acquisition génériques et une procédure de traitement de données semi-automatisée.

Dans le même ordre d'idées, une stratégie fut publiée par notre groupe (Mitrea *et al.* 2010) et visait à étudier directement la liaison covalente de médicaments aux protéines via la formation de métabolites réactifs *in vitro*. Cette stratégie inspira le développement d'une méthode afin de connaitre le taux d'incorporation de ^{13}C dans les protéines. Le chapitre 6 décrit cette nouvelle approche appliquée à la quantification du marquage isotopique de protéines. Nous avons conçu une procédure sélective, basée sur une analyse de balayage d'ions précurseurs, afin d'obtenir la répartition isotopique des acides aminés individuels présents dans un échantillon de protéine digérée; ceci en employant un agent de dérivation connu pour l'analyse d'acides aminés. Cette démarche fut consacré à l'analyse de protéines issues des filaments de byssus de moules et des échantillons d'algues, dans le cadre d'études structurales de protéines par RMN. Cette procédure est supérieure à d'autres méthodes existantes pour la quantification de l'incorporation de ^{13}C dans des acides aminés, tout en étant plus sélective.

La publication la plus récente, sujet du chapitre 4, décrit la première analyse quantitative afin de mesurer la concentration absolue de l'adduit acétaminophène-albumine *in vivo*. Ce test, appliqué à un modèle de rat, présente un important potentiel clinique, car la toxicologie engendrée par l'acétaminophène est connue comme étant la première cause d'insuffisance hépatique aiguë en Amérique du Nord. Actuellement, il n'existe aucun indicateur fiable pour prédire l'insuffisance hépatique occasionnée par une surdose d'acétaminophène. La méthode, présentée au chapitre 4, repose sur une nouvelle molécule qui est essentielle à la production d'une courbe standard, conduisant vers une quantification de l'adduit acétaminophène-albumine. Puisque la toxicité de l'acétaminophène dépend de la concentration du médicament parent, et essentiellement de la quantité du métabolite réactif NAPQI générée, il sera d'ores et déjà plus aisé de prévoir l'utilité qu'apportera cette méthode analytique pour évaluer les dommages causés par la liaison covalente des protéines hépatiques. Cette

importante étude est la première analyse permettant la quantification absolue d'une protéine contenant une modification de faible stœchiométrie, basée sur une courbe d'étalonnage interne composée d'une protéine intacte modifiée en utilisant la méthode de dilution isotopique. En modifiant la méthode optimisée pour la quantification de sérum de rat modifié, une procédure semblable appliquée à l'humain est en développement dans notre laboratoire et aura certainement un intérêt clinique important.

Nos travaux actuellement en cours visent à développer une procédure pour identifier les cibles protéiques de métabolites réactifs à l'aide de la purification basée sur la «chimie click». La faisabilité de cette stratégie est décrite dans le chapitre 5. Les travaux à venir se concentreront sur l'incorporation de la stratégie de purification à l'intérieur d'une procédure protéomique efficace et reproductible. Cette méthode démontre un potentiel important quant à l'identification de différentes protéines ciblées par des métabolites réactifs de structures distinctes. Elle serait ainsi utilisée pour démontrer la relation structure-cible entre des métabolites réactifs différant chimiquement, structuralement et de manière toxicologique. Cette relation représentera une étape cruciale à franchir afin de comprendre les mécanismes de la toxicité liée aux métabolites réactifs. Ultimement, l'objectif sera de pouvoir prédire les effets qu'occasionneront de nouveaux médicaments candidats afin d'adapter leur structure en conséquence, ce qui devrait diminuer considérablement l'incidence des effets secondaires imprévisibles. Les retombées les plus importantes de mieux comprendre ces mécanismes de toxicité demeurent probablement le potentiel de découvrir des processus biologiques impliqués dans différents évènements de signalisation.

RÉFÉRENCES

Abel, E. L., Opp, S. M., Verlinde, C. L. M. J., Bammler, T. K., Eaton, D. L. (2004) Characterization of atrazine biotransformation by human and murine glutathione S-transferases. *Toxicol. Sci. 80*, 230-238.

Adams, N. H., Levi, P. E., Hodgson, E. (1990) In vitro studies of the metabolism of atrazine, simazine, and terbutryn in several vertebrate species. *J. Agric. Food Chem. 38*, 1411-1417.

Ahmad Fuaad, A. A., Azmi, F., Skwarczynski, M., Toth, I. (2013) Peptide conjugation via CuAAC 'click' chemistry. *Molecules 18* (11), 13148-13174.

Aldini, G., Regazzoni, L., Orioli, M., Rimoldi, I., Facino, R. M., Carini, M. (2008) A tandem MS precursor-ion scan approach to identify variable covalent modification of albumin Cys34: a new tool for studying vascular carbonylation. *J. Mass Spectrom. 43*, 1470-1481.

Aldini, G., Vistoli, G., Regazzoni, L., Gamberoni, L., Facino, R. M., Yamaguchi, S., Uchida, K., Carini, M. (2008) Albumin is the main nucleophilic target of human plasma: a protective role against pro-atherogenic electrophilic reactive carbonyl species? *Chem. Res. Toxicol. 21*, 824-835.

Alvir, J. M. J., Lieberman, J. A., Safferman, A. Z., Schwimmer, J. L., Schaaf, J. A. (1993) Clozapine-induced agranulocytosis – incidence and risk factors in the United States. *New Engl. J. Med. 329* (3), 162-167.

Antoniewicz, M. R., Kelleher, J. K., Stephanopoulos, G. (2007) Accurate assessment of amino acid mass isotopomer distributions for metabolic flux analysis. *Anal. Chem., 79* (19), 7554-7559.

Arnold, A. A., Marcotte, I. (2009) Studying natural structural protein fibers by solid-state nuclear magnetic resonance. *Concept. Magnetic Res. A 34* (1), 24-47.

Aebersold, R., Mann, M. (2003) Mass spectrometry-based proteomics. *Nature. 422* (6928), 198-207.

Atkin, K., Kendall, F., Gould, D., Freeman, H., Liberman, J., O'Sullivan, D. (1996) Neutropenia and agranulocytosis in patients receiving clozapine in the UK and Ireland. *Br. J. Psychiatry 169* (4), 483-488.

Baillie, T. A., Davis, M. R. (1993) Mass spectrometry in the analysis of glutathione conjugates. *Biol. Mass Spectrom. 22* (6), 319-325.

Bakke, J. E., Larson, J. D., Price, C. E. (1972) Metabolism of atrazine and 2-hydroxyatrazine by the rat. *J. Agric. Food Chem. 20* (3), 602-607.

Barr, D. B., Panuwet, P., Nguyen, J. V., Udunka, S., Needham, L. L. (2007) Assessing exposure to atrazine and its metabolites using biomonitoring. *Environ. Health Perspect. 115*, 1474-1478.

Bartolone, J. B., Sparks, K., Cohen, S. D., Khairallah, E. A. (1987) Immunochemical detection of acetaminophen-bound liver proteins. *Biochem. Pharmacol. 36* (8), 1193-1196.

Bessems, J. G., Vermeulen, N. P. (2001). Paracetamol (acetaminophen)-induced toxicity: molecular and biochemical mechanisms, analogues and protective approaches. *CRC Cr. Rev. Toxicol. 31* (1), 55-138.

Bessems, J. G., Te Koppele, J. M., Van Dijk, P. A., Van Stee, L. L., Commandeur, J. N., Vermeulen, N. P. (1996) Rat liver microsomal cytochrome P450-dependent oxidation of 3,5-disubstituted analogues of paracetamol. *Xenobiotica 26*, 647-666.

Boja, E. S., Rodriguez, H. (2012) Mass spectrometry-based targeted quantitative proteomics: achieving sensitive and reproducible detection of proteins. *Proteomics 8*, 1093-1110.

Bolt, H. M., Kappus, H. (1974) Irreversible binding of ethynyl-estradiol metabolites to protein and nucleic acids as catalyzed by rat liver microsomes and mushroom tyrosinase. *J. Steroid Biochem. 5* (2), 179-184.

Bompani, R., Scali, G. (1986) Fipexide, an effective cognition activator in the elderly: A placebo-controlled, double-blind clinical trial. *Curr. Med. Res. Opin. 10* (2), 99-106.

Brun, V., Masselon, C., Garin, J., Dupuis, A. (2009) Isotope dilution strategies for absolute quantitative proteomics. *J. Proteom. 72*, 740-749.

Buchholz, D., Fultz, E., Haack, K. W., Vogel, J. S., Gilman, S. D., Gee, S. J., Hammock, B. D., Hui, X., Wester, R. C., Maibach, H. I. (1999) HPLC-accelerator MS measurement of atrazine metabolites in human urine after dermal exposure. *Anal. Chem. 71*, 3519-3525.

Cho, M., Jedrychowski, R., Hammock, B., Buckpitt, A. (1994) Reactive naphthalene metabolite binding to hemoglobin and albumin. *Fundam Appl Toxicol.* 22 (1), 26-33.

Clay, S. A., Dowdy, R. H., Lamb, J. A., Anderson, J. L., Lowery, B., Knighton, R. E., Clay, D. E. (2000) Herbicide movement and dissipation at four midwestern sites. *J. Environ. Sci. Health B 35*, 259-278.

Cohen, S. A., Michaud, D. P. (1993) Synthesis of a fluorescent derivatizing reagent 6-aminoquinolyl-*N*-hydroxysuccinimidyl carbamate, and its application for the analysis of hydrolysate amino acids via high performance liquid chromatography. *Anal. Biochem. 211* (2), 279-287.

Cohen, S. D., Khairallah, E. A. (1997) Selective protein arylation and acetaminophen-induced hepatotoxicity. *Drug Metab. Rev. 29* (1-2), 59-77.

Cooper, R. L., Stoker, T. E., Goldman, J. M., Parrish, M. B., Tyrey, L. (1996) Effect of atrazine on ovarian function in the rat. *Reprod. Toxicol. 10*, 257-264.

Cribb, A. E., Nuss, C. E., Alberts, D. W., Lamphere, D. B., Grant, D. M., Grossman, S. J., Spielberg, S. P. (1996) Covalent binding of sulfamethoxazole reactive metabolites to human and rat liver subcellular fractions assessed by immunochemical detection. *Chem. Res. Toxicol. 9* (2), 500-7.

Dahlin, D. C., Miwa, G. T., Lu, A. Y., Nelson, S. D. (1984) *N*-acetyl-*p*-benzoquinone imine: a cytochrome P-450-mediated oxidation product of acetaminophen. *Proc. Natl. Acad. Sci. 81*, 1327-1331.

Damsten, M. C., Commandeur, J. N. M., Fidder, A., Hulst, A.G., Touw, D., Noort, D., Vermeulen, N. P. E. (2007) Liquid chromatography/tandem mass spectrometry detection of covalent binding of acetaminophen to human serum albumin. *Drug Metab. Dispos. 35*, 1408-1417.

Damsten, M. C., de Vlieger, J. S., Niessen, W. M., Irth, H., Vermeulen, N. P., Commandeur, J. N. (2008) Trimethoprim: novel reactive intermediates and bioactivation pathways by cytochrome p450s. *Chem. Res. Toxicol. 21* (11), 2181-2187.

Das, G., Bailey, M. J., Wickham, J. E. A. (1988) Drug points: Toxic epidermal necrolysis and trimethoprim. *Br. Med. J. (Clin. Res. Ed.) 296*(6636), 1604.

Devi, S. S, Palkar, P. S., Mehendale, H. M. (2007) Measuring covalent binding in hepatotoxicity. *Curr. Protoc. Toxicol. 14.6*, DOI: 10.1002/0471140856.tx1406s32.

Dieckhaus, C. M., Fernández-Metzler, C. L., King, R., Krolikowski, P. H., Baillie, T. A. (2005). Negative ion tandem mass spectrometry for the detection of glutathione conjugates. *Chem. Res. Toxicol. 18* (4), 630-638.

Dingley, K. H., Curtis, K. D., Nowell, S., Felton, J. S., Lang, N. P., Turteltaub, K. W. (1999) DNA and protein adduct formation in the colon and blood of humans after exposure to a dietary-relevant dose of 2-amino-1-methyl-6-phenylimidazo[4,5-b]pyridine. *Cancer Epidem. Biomar. 8*, 507-512.

Domon, B., Aebersold, R. (2006) Mass spectrometry and protein analysis. *Science 312*, 212-217.

Dooley, G. P., Prenni, J. E., Prentiss, P. L., Cranmer, B. K., Andersen, M. E., Tessari, J. D. (2006) Identification of a novel hemoglobin adduct in Sprague Dawley rats exposed to atrazine. *Chem. Res. Toxicol. 19*, 692-700.

Durand, F., Samuel, D., Bernuau, J., Saliba, F., Pariente, E. A., Marion, S., Benhamou, J. P., Bismuth, H. (1992) Fipexide-induced fulminant hepatitis: report of three cases with emergency liver transplantation. *J. Hepatol. 15* (1), 144-146.

Evans, D. C., Watt, A. P., Nicoll-Griffith, D. A., Baillie, T. A. (2004) Drug-protein adducts: an industry perspective on minimizing the potential for drug bioactivation in drug discovery and development. *Chem. Res. Toxicol. 17* (1), 3-16.

Fenn, J. B., Mann, M., Meng, C. K., Wong, S. F., Whitehouse, C. M. (1989) Electrospray ionization for mass spectrometry of large biomolecules. *Science. 246* (4926), 64-71.

Fountoulakis M., Berndt P., Boelsterli U. A., Crameri F., Winter M., Albertini S., Suter L. Two-dimensional database of mouse liver proteins: changes in hepatic protein levels following treatment with acetaminophen or its nontoxic regioisomer 3-acetamidophenol. Electrophoresis. 2000; 21 (11):2148-61.

Fountoulakis, M., Lahm, H. W. (1998) Hydrolysis and amino acid composition analysis of proteins. *J. Chromatogr. A, 826* (2), 109-134.

Gammon, D. W., Aldous, C. N., Carr, W. C., Jr, Sanborn, J. R., Pfeifer, K. F. (2005) A risk assessment of atrazine use in California: human health and ecological aspects. *Pest Manag. Sci. 61*, 331-355.

Gan, J., Harper, T. W., Hsueh, M. M., Qu, Q., Humphreys, W. G. (2005) Dansyl glutathione as a trapping agent for the quantitative estimation and identification of reactive metabolites. *Chem. Res. Toxicol. 18* (5), 896-903.

Gaynor, J. D., Tan, C. S., Drury, C. F., Welacky, T. W., Ng, H. Y. F., Reynolds, W. D. (2002) Runoff and drainage losses of atrazine, metribuzin, and metolachlor in three water management systems. *J. Environ. Qual. 31*, 300-308.

Gerber, S.A., Rush, J., Stemman, O., Kirschner, M.W., Gygi, S.P. (2003) Absolute quantification of proteins and phosphoproteins from cell lysates by tandem MS. *Proc. Natl. Acad. Sci. 100*, 6940-6945.

Godin, J. P., Fay, L. B., Hopfgartner, G. (2007) Liquid chromatography combined with mass spectrometry for ^{13}C isotopic analysis in life science research. *Mass Spectrom. Rev. 26* (6), 751-774.

Gojmerac, T., Kartal, B., Bilandzic, N., Roic, B., Rajkovic-Janje, R. (1996) Seasonal atrazine contamination of drinking water inpig-breeding farm surroundings in agricultural and industrial areas of Croatia. *Bull. Environ. Contam. Toxicol. 56*, 225-230.

Goshe, M. B., Anderson, V. E. (1995) Determination of amino acid isotope ratios by electrospray ionization–mass spectrometry. *Anal. Biochem. 231* (2), 387-392.

Gosline, J., Lillie, M., Carrington, E., Guerette, P., Ortlepp, C., Savage, K. (2002) Elastic proteins: biological roles and mechanical properties. *Philos. T. Roy. Soc. B 357* (1418), 121-132.

Gottlieb, H. E., Kotlyar, V., Nudelman, A. (1997) NMR chemical shifts of common laboratory solvents as trace impurities. *J. Org. Chem. 62* (21), 7512-7515.

Griffin, J. M., Lipscomb, J. C., Pumford, N. R. (1998) Covalent binding of trichloroethylene to proteins in human and rat hepatocytes. *Toxicol. Lett. 95* (3), 173-81.

Guengerich, F.P. (2011) Mechanisms of drug toxicity and relevance to pharmaceutical development. *Drug Metab. Pharmacokinet. 26* (1), 3-14.

Guillard, R. R. L. Culture of Phytoplankton for feeding marine invertebrates. (1975) Dans Culture of marine invertebrate animals (Eds. Smith W. L. et Chanley, M. H.). New York, Plenum Press, pp.29-60.

Guy, C., Blay, N., Rousset, H., Fardeau, V., Ollagnier, M. (1989) Fever caused by fipexide: Evaluation of the national pharmacovigilance survey. *Therapie 45* (5), 429-431.

Halmes, N. C., McMillan, D. C., Oatis, J. E. Jr., Pumford, N. R. (1996) Immunochemical detection of protein adducts in mice treated with trichloroethylene. *Chem. Res. Toxicol. 9* (2), 451-6.

Hawkins, T., Carter, J. M., Romeril K. R., Jackson, S. R., Green, G. J. (1993) Severe Trimethoprim induced neutropenia and thrombocytopenia. *New Zeal. Med. J. 106* (958): 251.

Hayes, T. B., Khoury, V., Narayan, A., Nazir, M., Park, A., Brown, T., Adame, L., Chan, E., Buchholz, D., Stueve, T., Gallipeau, S. (2010) Atrazine induces complete feminization and chemical castration in male African clawed frogs (Xenopus laevis). *Proc. Natl. Acad. Sci. U.S.A. 107*, 4612-4617.

Hellerstein, M. K., Neese, R. A. (1999) Mass isotopomer distribution analysis at eight years: theoretical, analytic, and experimental considerations. *Am. J. Physiol.-Endoc. M. 276* (6), E1146-E1170.

Hess, S., van Beek, J., Pannell, L. K. (2002) Acid hydrolysis of silk fibroins and determination of the enrichment of isotopically labeled amino acids using precolumn derivatization and high-performance liquid chromatography–electrospray ionization–mass spectrometry. *Anal. Biochem. 311* (1), 19-26.

Hinchman, C. A., Ballatori, N. (1994) Glutathione conjugation and conversion to mercapturic acids can occur as an intrahepatic process. *J. Toxicol. Environ. Health A 41* (4), 387-409.

Hinson, J. A., Pumford, N. R., Roberts, D. W. (1995) Mechanisms of acetaminophen toxicity: immunochemical detection of drug-protein adducts. *Drug Metab. Rev. 27*, 73-92.

Hong, V., Presolski, S.I., Ma, C., and Finn, M.G. (2009) Analysis and optimization of copper catalyzed azide-alkyne cycloaddition for bioconjugation. *Angew. Chem. Int. Ed. 48*, 9879-9883.

Hua, W., Bennett, E. R., Letcher, R. J. (2006) Ozone treatment and the depletion of detectable pharmaceuticals and atrazine herbicide in drinking water sourced from the upper Detroit River, Ontario, Canada. *Water Res. 40*, 2259-2266.

Ikehata, K., Duzhak, T. G., Galeva, N. A., Ji, T., Koen, Y. M., Hanzlik, R. P. (2008) Protein targets of reactive metabolites of thiobenzamide in rat liver in vivo. *Chem. Res. Toxicol. 21* (7), 1432-42.

Iha, R. K., Wooley, K. L., Nystrcm, A. M., Burke, D. J., Kade, M. J., Hawker, C. J. (2009) Applications of orthogonal "click" chemistries in the synthesis of functional soft materials. *Chem. Rev. 109*, 5620-5686.

Jaeschke, H., Bajt, M. L. (2010) Mechanisms of acetaminophen hepatotoxicity. Dans Comprehensive Toxicology 2nd edition (Charlene A. McQueen, Ed.) pp. 457-473.

Jollow, D. J., Mitchell, J. R., Potter, W. Z., Davis, D. C., Gillette, J. R., Brodie, B. B. (1973) Acetaminophen-induced hepatic necrosis. II. Role of covalent binding in vivo. *J. Pharmacol. Exp. Ther. 187* (1), 195-202.

Jennings, M. E., Matthews, D. E. (2005) Determination of complex isotopomer patterns in isotopically labeled compounds by mass spectrometry. *Anal. Chem. 77* (19), 6435-6444.

Jia, L., and Liu, X. (2007) The Conduct of Drug Metabolism Studies Considered Good Practice (II): In Vitro Experiments. *Curr. Drug Metab., 8* (8), 822–829.

Jian, W., Yao, M., Zhang, D., Zhu, M. (2009) Rapid detection and characterization of in vitro and urinary *N*-acetyl-L-cysteine conjugates using quadrupole-linear ion trap mass spectrometry and polarity switching. *Chem. Res. Toxicol. 22* (7), 1246-1255.

Jiang, H., Adams, C., Graziano, N., Roberson, A., McGuire, M., Khiari, D. (2006) Occurrence and removal of chloro-S-triazines in water treatment plants. *Environ. Sci. Technol. 40*, 3609–3616.

Jollow, D. J., Mitchell, J. R., Potter, W. Z., Davis, D. C., Gillette, J. R., Brodie, B. B. (1973) Acetaminophen-induced hepatic necrosis. II. Role of covalent binding in vivo. *J. Pharmacol. Exp. Ther. 187*, 195-202.

Joo, H., Choi, K., Hodgson, E. (2010) Human metabolism of atrazine. *Pest. Biochem. Physiol. 98*, 73-79.

Kalgutkar, A. S., Soglia, J. R. (2005) Minimising the potential for metabolic activation in drug discovery. *Expert Opin. Drug Metab. Toxicol. 1* (1), 91-142.

Karas, M., Hillenkamp, F. (1988) Laser desorption ionization of proteins with molecular masses exceeding 10,000 daltons. *Anal. Chem. 60* (20), 2299–301.

Khojasteh, S. C., Hartley, D. P., Ford, K. A., Uppal, H., Oishi, S., Nelson, S. D. (2012) Characterization of rat liver proteins adducted by reactive metabolites of menthofuran. *Chem. Res. Toxicol. 25* (11), 2301-9.

Kiely, T., Donaldson, D., Grube, A. (2004) Pesticides industry sales and usage 2000 and 2001 Market Estimates, Environmental Protection Agency, Washington, D.C.

Kirkpatrick, D. S., Gerber, S. A., Gygi, S. P. (2005) The absolute quantification strategy: a general procedure for the quantification of proteins and post-translational modifications. *Methods 35*, 265-273.

Koen, Y.M., Gogichaeva, N.V., Alterman, M.A., Hanzlik, R.P. (2007) A proteomic analysis of bromobenzene reactive metabolite targets in rat liver cytosol in vivo. *Chem. Res. Toxicol. 20* (3), 511-9.

Kolb, H. C., Finn, M. G., Sharpless, K. B. (2001) Click Chemistry: Diverse Chemical Function from a Few Good Reactions. *Angew. Chem. Int. Ed. Engl. 40* (11), 2004-2021.

Krupp, P., Barnes, P. (1992) Clozapine-associated agranulocytosis: risk and aetiology. *Br. J. Psychiatry Suppl. 17*, 38-40.

Lai, W. G., Zahid, N., Uetrecht, J. P. (1999) Metabolism of trimethoprim to a reactive iminoquinone methide by activated human neutrophils and hepatic microsomes. *J. Pharmacol. Exp. Ther. 291* (1), 292-299.

Lallana, E, Riguera, R, Fernandez-Megia, E (2011) Reliable and efficient procedures for the conjugation of biomolecules through Huisgen azide-alkyne cycloadditions. *Angew. Chem. Int. Ed. Engl. 50* (38), 8794-8804.

Lang, D. H., Rettie, A. E., Bocker, R. H. (1997) Identification of enzymes involved in the metabolism of atrazine, terbuthylazine, ametryne, and terbutryne in human liver microsomes. *Chem. Res. Toxicol. 10*, 1037-1044.

Lang, D., Criegee, D., Grothusen, A., Saalfrank, R. W., Bocker, R. H. (1996) In vitro metabolism of atrazine, terbuthylazine, ametryne, and terbutryne in rats, pigs, and humans. *Drug Metab. Dispos. 24*, 859-865.

Larson, A. M., Polson, J., Fontana, R. J., Davern, T. J., Lalani, E., Hynan, L. S., Reisch, J. S., Schiødt, F. V., Ostapowicz, G., Shakil, A. O., Lee, W. M. (2005) Acetaminophen-induced acute liver failure: results of a United States multicenter, prospective study. *Hepatology 42* (6), 1364-1372.

Lau, E., Lam, M. P. Y., Siu, S. O., Kong, R. P. W., Chan, W. L., Zhou, Z., Huang, J., Lo, C., Chu, I. K. (2011) Strong cation exchange (SCX) based analytical methods for the targeted analysis of protein post-translational modifications. *Mol. BioSyst. 7*, 1399-1408.

Lee, W. M. (2004) Acetaminophen and the U.S. Acute liver failure study group: Lowering the risks of hepatic failure. *Hepatology 40*, 6-9.

Li, A., May, M. P., Bigelow, J. C. (2006) Identification of a metabolite of atrazine, *N*-ethyl-6-methoxy-N'-(1-methylethyl)-1,3,5-triazine-2,4-diamine, upon incubation with rat liver microsomes. *J. Chromatogr. B 836*, 129-132.

Liebler, D. C., Guengerich, F. P. (2005) Elucidating mechanisms of drug-induced toxicity. *Nat. Rev. Drug Discov. 4* (5), 410-20.

Liebler, D. C., Zimmerman, L. J. (2013) Targeted quantitation of proteins by mass spectrometry. *Biochemistry 52*, 3797-3806.

Lim, H. K., Chen, J., Cook, K., Sensenhauser, C., Silva, J., Evans, D. C. (2008). A generic method to detect electrophilic intermediates using isotopic pattern triggered data-dependent high-resolution accurate mass spectrometry. *Rapid Commun. Mass Sp. 22*(8), 1295-1311.

Liu, Z. C., Uetrecht, J. P. (1995). Clozapine is oxidized by activated human neutrophils to a reactive nitrenium ion that irreversibly binds to the cells. *J. Pharmacol. Exp. Ther. 275* (3), 1476-1483.

Lucas, A. D., Jones, A. D., Goodrow, M. H., Saiz, S. G., Blewett, C., Seiber, J. N., Hammock, B. D. (1993) Determination of atrazine metabolites in human urine: Development of a biomarker of exposure. *Chem. Res. Toxicol. 6*, 107-116.

Ma, S., Subramanian, R. (2006) Detecting and characterizing reactive metabolites by liquid chromatography/tandem mass spectrometry. *J. Mass Spectrom. 41* (9), 1121-1139.

Ma, S., Zhu, M. (2009) Recent advances in applications of liquid chromatography–tandem mass spectrometry to the analysis of reactive drug metabolites. *Chem.-Biol. Interact. 179* (1), 25-37.

Madsen, K. G., Olsen, J., Skonberg, C., Hansen, S. H., Jurva, U. (2007) Development and evaluation of an electrochemical method for studying reactive phase-I metabolites: correlation to in vitro drug metabolism. *Chem. Res. Toxicol. 5*, 821-831.

Maggs, J. L., Williams, D., Pirmohamed, M., Park, B. K. (1995) The metabolic formation of reactive intermediates from clozapine, a drug associated with agranulocytosis in man. *J. Pharmacol. Exp. Ther. 275* (3), 1463-1475.

Mann, M., Hendrickson, R. C., Pandey, A. (2001) Analysis of proteins and proteomes by mass spectrometry. *Annu Rev Biochem. 70*, 437-73.

McGill, M. R., Lebofsky, M., Norris, H.-R. K., Slawson, M. H., Bajt, M. L., Xie, Y., Williams, C. D., Wilkins, D. G., Rollins, D. E., Jaeschke, H. (2013) Plasma and liver acetaminophen-protein adduct levels in mice after acetaminophen treatment: dose-response, mechanisms, and clinical implications. *Toxicol. Appl. Pharm. 269*, 240-249.

McMullin, T. S., Andersen, M. E., Nagahara, A., Lund, T. D., Pak, T., Handa, R. J., Hanneman, W. H. (2004) Evidence that atrazine and diaminochlorotriazine inhibit the estrogen/progesterone induced surge of luteinizing hormone in female Sprague-Dawley rats without changing estrogen receptor action. *Toxicol. Sci. 79*, 278-286.

McMullin, T., Brzezicki, J., Cranmer, B., Tessari, J., Andersen, M. (2003) Pharmacokinetic modeling of disposition and time-course studies with [^{14}C] atrazine. *J. Toxicol. Environ. Health A 66*, 941-964.

Meldal, M., Tornoe, C.W. (2008) Cu-catalyzed azide-alkyne cycloaddition. *Chem. Rev. 108*, 2952-3015.

Meng, X., Howarth, A., Earnshaw, C. J., Jenkins, R. E., French, N. S., Back, D. J., Naisbitt, D. J., Park, B. K. (2013) Detection of drug bioactivation in vivo: mechanism of nevirapine-albumin conjugate formation in patients. *Chem. Res. Toxicol. 26*, 575-583.

Mitchell, J. R., Jollow, D. J., Potter, W. Z., Davis, D. C., Gillette, J. R., Brodie, B. B. (1973) Acetaminophen-induced hepatic necrosis. I. Role of drug metabolism. *J. Pharmacol. Exp. Ther. 187*, 185-194.

Mitrea, N., LeBlanc, A., St-Onge, M., Sleno, L. (2010) Assessing covalent binding of reactive drug metabolites by complete protein digestion and LC-MS analysis. *Bioanalysis 2* (7), 1211-1221.

Molero, G., Aranjuelo, I., Teixidor, P., Araus, J. L., Nogués, S. (2011) Measurement of ^{13}C and ^{15}N isotope labeling by gas chromatography/combustion/isotope ratio mass spectrometry to study amino acid fluxes in a plant–microbe symbiotic association. *Rapid Commun. Mass Spectrom. 25* (5), 599-607.

Moses, J. E., Moorhouse, A. D. (2007) The growing applications of click chemistry. *Chem. Soc. Rev. 36* (8), 1249-1262.

Nelson, H., Lin, J., Frankenberry, M. (2001) Drinking water exposure assessment for atrazine and various chloro-triazine and hydroxy-triazine degradates. Environmental Protection Agency, Washington, D.C.

Noort, D., Fidder, A., Degenhardt-Langelaan, C. E. A. M., Hulst, A. G. (2008) Retrospective detection of sulfur mustard exposure by mass spectrometric analysis of adducts to albumin and hemoglobin: an in vivo study. *J. Anal. Toxicol. 32*, 25-30.

Osanai, M., Okudaira, M., Naito, J., Demura, M., Asakura, T. (2000). Biosynthesis of L-alanine, a major amino acid of fibroin in Samia cynthia ricini. *Insect Biochem. Molec. 30* (3), 225-232.

Panuwet, P., Nguyen, J. V., Kuklenyik, P., Udunka, S., Needham, L. L., Barr, D. B. (2008) Quantification of atrazine and its metabolites in urine by on-line solid-phase extraction-high-performance liquid chromatography-tandem mass spectrometry. *Anal. Bioanal. Chem. 391*, 1931-1939.

Patterson, B. W., Zhang, X. J., Chen, Y., Klein, S., Wolfe, R. R. (1997) Measurement of very low stable isotope enrichments by gas chromatography/mass spectrometry: application to measurement of muscle protein synthesis. *Metabolism 46* (8), 943-948.

Peng, L., Turesky, R.J. (2011) Mass spectrometric characterization of 2-amino-1-methyl-6-phenylimidazo [4,5-b]pyridine *N*-oxidized metabolites bound at Cys34 of human serum albumin. *Chem. Res. Toxicol. 24*, 2004-2017.

Pirmohamed, M., Madden, S., Park, B. K. (1996) Idiosyncratic drug reactions. Metabolic bioactivation as a pathogenic mechanism. *Clin. Pharmacokinet. 31* (3), 215-30.

Pohl, L.R. (1993) An immunochemical approach of identifying and characterizing protein targets of toxic reactive metabolites. *Chem. Res. Toxicol. 6* (6), 786-93.

Potter, W. Z, Davis, D. C., Mitchell, J. R., Jollow, D. J., Gillette, J. R., Brodie, B. B. (1973) Acetaminophen-induced hepatic necrosis. 3. Cytochrome P-450-mediated covalent binding in vitro. *J. Pharmacol. Exp. Ther. 187*, 203-210.

Potter, W. Z., Thorgeirsson, S. S., Jollow, D. J., Mitchell, J. R. (1974) Acetaminophen-induced hepatic necrosis V. Correlation of hepatic necrosis, covalent binding and glutathione depletion in hamsters. *Pharmacology 12* (3), 129-143.

Prescott, L. F. (2000) Paracetamol: past, present, and future. *Am. J. Ther. 7* (2), 143-148.

Presolski, S. I., Hong, V. P., Finn, M. G. (2011) Copper-Catalyzed Azide–Alkyne Click Chemistry for Bioconjugation. *Curr. Protoc. Chem. Biol. 3* (4), 153-162.

Pumford, N. R., Hinson, J. A., Potter, D. W., Rowland, K. L., Benson, R. W., Roberts, D. W. (1989) Immunochemical quantitation of 3-(cystein-S-yl)acetaminophen adducts in serum and liver proteins of acetaminophen-treated mice. *J. Pharmacol. Exp. Ther. 248*, 190-196.

Pumford, N. R., Hinson, J. A., Wayne Benson, R., Roberts, D. W. (1990) Immunoblot analysis of protein containing 3-(cystein-S-yl) acetaminophen adducts in serum and subcellular liver fractions from acetaminophen-treated mice. *Toxicol. Appl. Pharm. 104* (3), 521-532.

Redjah, I., Olivier, F., Tremblay, R., Myrand, B., Pernet, F., Neumeier, U., Chevarie, L. (2010) The importance of turbulent kinetic energy on transport of juvenile clams (Mya arenaria). *Aquaculture 307* (1), 20-28.

Rendic, S. (2002) Summary of information on human CYP enzymes: human P450 metabolism data. *Drug Metab. Rev. 34* (1-2), 83-448.

Rolandi, E., Franceschini, R., Marabini, A., Messina, V., Bongera, P., Barreca, T. (1984) Pituitary secretion after administration of a new cerebroactive drug, fipexide. *Brit. J. Clin. Pharmaco. 18* (2), 236-239.

Ross, M. K., Filipov, N. M. (2006) Determination of atrazine and its metabolites in mouse urine and plasma by LC-MS analysis. *Anal. Biochem. 351*, 161-173.

Ross, M. K., Jones, T. L., Filipov, N. M. (2009) Disposition of the herbicide 2-chloro-4-(ethylamino)-6-(isopropylamino)-s-triazine (atrazine) and its major metabolites in mice: A liquid chromatography/ mass spectrometry analysis of urine, plasma, and tissue levels. *Drug Metab. Dispos. 37*, 776-786.

Rousu, T., Pelkonen, O., Tolonen, A. (2009) Rapid detection and characterization of reactive drug metabolites in vitro using several isotope-labeled trapping agents and ultra-performance liquid chromatography/time-of-flight mass spectrometry. *Rapid Commun. Mass Sp. 23* (6), 843-855.

Shen, T., Shen, W., Xiong, Y., Liu, H., Zheng, H., Zhou, H.,Rui, B., Liu, J., Wu, J., Shi, Y. (2009) Increasing the accuracy of mass isotopomer analysis through calibration curves constructed using biologically synthesized compounds. *J. Mass Spectrom. 44* (7), 1066-1080.

Sheweita, S.A. (2000) Drug-metabolizing enzymes: mechanisms and functions. *Curr. Drug Metab. 1* (2), 107-32.

Shi, Y., Bajrami, B., Yao, X. (2009) Passive and active fragment ion mass defect labeling: distinct proteomics potential of iodine-based reagents. *Anal. Chem. 81* (15), 6438-6448.

Shin, N. Y., Liu, Q., Stamer, S. L., Liebler, D. C. (2007) Protein targets of reactive electrophiles in human liver microsomes. *Chem. Res. Toxicol. 20* (6), 859-67.

Singh, M., Sandhir, R., Kiran, R. (2010) Oxidative stress induced by atrazine in rat erythrocytes: Mitigating effect of vitamin E. *Toxicol. Mech. Methods 20*, 119-126.

Sivilotti, M. L. A., Yarema, M. C., Juurlink, D. N., Good, A. M., Johnson, D. W. (2005) A risk quantification instrument for acute acetaminophen overdose patients treated with N acetylcysteine. *Ann. Emerg. Med. 46*, 263-271.

Sleno, L., Staack, R. F., Varesio, E., Hopfgartner, G. (2007) Investigating the in vitro metabolism of fipexide: characterization of reactive metabolites using liquid chromatography/mass spectrometry. *Rapid Commun. Mass Sp. 21* (14), 2301-2311.

Sleno, L., Varesio, E., Hopfgartner, G. (2007) Determining protein adducts of fipexide: mass spectrometry based assay for confirming the involvement of its reactive metabolite in covalent binding. *Rapid Commun. Mass Sp. 21* (24), 4149-4157.

Soglia, J. R., Contillo, L. G., Kalgutkar, A. S., Zhao, S., Hop, C. E., Boyd, J. G., Cole, M. J. (2006) A semiquantitative method for the determination of reactive metabolite conjugate levels in vitro utilizing liquid chromatography-tandem mass spectrometry and novel quaternary ammonium glutathione analogues. *Chem. Res. Toxicol. 19* (3), 480-490.

Soglia, J. R., Harriman, S. P., Zhao, S., Barberia, J., Cole, M. J., Boyd, J. G., Contillo, L. G. (2004) The development of a higher throughput reactive intermediate screening assay incorporating micro-bore liquid chromatography–micro-electrospray ionization–tandem mass spectrometry and glutathione ethyl ester as an in vitro conjugating agent. *J. .Pharmaceut. Biomed. 36* (1), 105-116.

Solomon, K. R., Carr, J. A., Du Preez, L. H., Giesy, J. P., Kendall, R. J., Smith, E. E., Van Der Kraak, G. J. (2008) Effects of atrazine on fish, amphibians, and aquatic reptiles: A critical review. *Crit. Rev. Toxicol. 38*, 721-772.

Switzar, L., Kwast, L. M., Lingeman, H., Giera, M., Pieters, R. H. H., Niessen, W. M. A. (2013) Identification and quantification of drug-albumin adducts in serum samples from a drug exposure study in mice. *J. Chromatogr. B 917-918*, 53-61.

Tanaka, K., Waki, H., Ido, Y., Akita, S., Yoshida, Y., Yoshida, T., Matsuo, T. (1988) Protein and Polymer Analyses up to *m/z* 100 000 by Laser Ionization Time-of flight Mass Spectrometry. *Rapid Commun. Mass Spectrom. 2* (20): 151–3.

Tillitt, D. E., Papoulias, D. M., Whyte, J. J., Richter, C. A. (2010) Atrazine reduces reproduction in fathead minnow (Pimephales promelas). *Aquat. Toxicol. 99*, 149–159.

Tzouros, M., Pähler, A. (2009) A targeted proteomics approach to the identification of peptides modified by reactive metabolites. *Chem. Res. Toxicol. 22* (5), 853-62.

U.S. Environmental Protection Agency (2009) Atrazine science reevaluation: Potential health impacts, October 7, 2009, EPA-HQ-OPP- 2009-0759-0003.

Ueda, M., Imai, T., Takizawa, T., Onodera, H., Mitsumori, K., Matsui, T., Hirose, M. (2005) Possible enhancing effects of atrazine on growth of 7,12-dimethylbenz(a)anthracene-induced mammary tumors in ovariectomized Sprague Dawley rats. *Cancer Sci. 96*, 19-25.

Uetrecht, J. (2007) Idiosyncratic drug reactions: Past, present, and future. *Chem. Res. Toxicol. 21* (1), 84–92.

Van Dijk, M., Rijkers, D. T. S., Liskamp, R. M. J., Van Nostrum, C. F., Hennink, W. E. (2009) Synthesis and applications of biomedical and pharmaceutical polymers via click chemistry methodologies. *Bioconjug. Chem. 20* (11), 2001-2016.

Van Eijk, H. M. H., Rooyakkers, D. R., Soeters, P. B., Deutz, N. E. (1999) Determination of amino acid isotope enrichment using liquid chromatography–mass spectrometry. *Anal. Biochem. 271* (1), 8-17.

Van Eijk, H. M. H., Rooyakkers, D. R., Wagenmakers, J. M., Soeters, P. B., Deutz, N. E. (1997) Isolation and quantitation of isotopically labeled amino acids from biological samples. *J. Chromatog. B 691* (2), 287-296.

Van Eijk, H. M., Suylen, D. P. L., Dejong, C. H. C., Luiking, Y. C., Deutz, N. E. P. (2007) Measurement of amino acid isotope enrichment by liquid chromatography mass spectroscopy after derivatization with 9-fluorenylmethylchloroformate. *J Chromatog. B 856* (1), 48-56.

Van't Klooster, G. A., Kolker, H. J., Woutersen-Van Nijnanten, F., Noordhoek, J., Van Miert, A. S. (1992) Determination of trimethoprim and its oxidative metabolites in cell culture media and microsomal incubation mixtures by high-performance liquid chromatography. *J. Chromatog. B 579* (2), 355-360.

Walther, T. C., Mann, M. (2010) Mass spectrometry-based proteomics in cell biology. *J. Cell Biol. 190* (4), 491-500.

Wen, B., Ma, L., Nelson, S. D., Zhu, M. (2008) High-throughput screening and characterization of reactive metabolites using polarity switching of hybrid triple quadrupole linear ion trap mass spectrometry. *Anal. Chem. 80* (5), 1788-1799.

Wetzel, L. T., Luempert, L. G., Breckenridge, C. B., Tisdel, M. O., Stevens, J. T., Thakur, A. K., Extrom, P. J., Eldridge, J. C. (1994) Chronic effects of atrazine on estrus and mammary tumor formation in female Sprague-Dawley and Fischer 344 rats. *J. Toxicol. Environ. Health 43*, 169-182.

Williams, D. P., Pirmohamed, M., Naisbitt, D. J., Maggs, J. L., Park, B. K. (1997) Neutrophil cytotoxicity of the chemically reactive metabolite (s) of clozapine: possible role in agranulocytosis. *J. Pharmacol. Exp. Ther. 283* (3), 1375-1382.

Wokolo, C. N., Byrne, L., Misch, K. J. (1988) Toxic epidermal necrolysis occurring during treatment with trimethoprim alone. *Brit. Med. J. 296* (6627), 970.

Wong, H. L., Liebler, D. C. (2008) Mitochondrial protein targets of thiol-reactive electrophiles. *Chem. Res. Toxicol. 21* (4), 796-804.

Yan, Z., Maher, N., Torres, R., Caldwell, G. W., Huebert, N. (2005) Rapid detection and characterization of minor reactive metabolites using stable-isotope trapping in combination with tandem mass spectrometry. *Rapid Commun. Mass Sp. 19* (22), 3322-3330.

Zamek-Gliszczynski, M. J., Hoffmaster, K. A., Nezasa, K. I., Tallman, M. N., Brouwer, K. L. (2006) Integration of hepatic drug transporters and phase II metabolizing enzymes: mechanisms of hepatic excretion of sulfate, glucuronide, and glutathione metabolites. *Eur. J. Pharm. Sci. 27* (5), 447-486.

Zhang, H., Yang, Y. (2008) An algorithm for thorough background subtraction from high resolution LC/MS data: application for detection of glutathione-trapped reactive metabolites. *J. Mass Spectrom. 43* (9), 1181-1190.

Zhang, H., Zhang, D., Ray, K., Zhu, M. (2009) Mass defect filter technique and its applications to drug metabolite identification by high-resolution mass spectrometry. *J. Mass Spectrom. 44* (7), 999-1016.

Zhang, J., Tian, Q., Yung Chan, S., Chuen Li, S., Zhou, S., Duan, W., Zhu, Y. Z. (2005). Metabolism and transport of oxazaphosphorines and the clinical implications. *Drug Metab. Rev. 37* (4), 611-703.

Zhou, S., Chan, E., Duan, W., Huang, M., Chen, Y. Z. (2005) Drug bioactivation, covalent binding to target proteins and toxicity relevance. *Drug Metab. Rev. 37* (1), 41-213.

Zhou, Z., Jin, M., Ding, J., Zhou, Y., Zheng, J., Chen, H. (2007) Rapid detection of atrazine and its metabolites in raw urine by extractive electrospray ionization mass spectrometry. *Metabolomics 3*, 101-104.

Zhu, M., Ma, L., Zhang, H., Humphreys, W. G. (2007) Detection and structural characterization of glutathione-trapped reactive metabolites using liquid chromatography-high-resolution mass spectrometry and mass defect filtering. *Anal. Chem. 79* (21), 8333-8341.